UNITED NATIONS UNIVERSITY
GEOTHERMAL TRAINING PROGRAMME
Orkustofnun, Grensásvegur 9,
IS-108 Reykjavík, Iceland

Reports 2008
Number 1

GEOTHERMAL RESOURCE ASSESSMENT THROUGH WELL TESTING AND PRODUCTION RESPONSE MODELLING

MSc thesis
Department of Mechanical and Industrial Engineering
University of Iceland

by

Daher Elmi Houssein
Centre d´Etudes et de Recherches Scientifique de Djibouti – CERD
P.O. Box 486
Djibouti
REPUBLIQUE DE DJIBOUTI
daherelmihoussein@yahoo.fr

United Nations University
Geothermal Training Programme
Reykjavík, Iceland
Published in December 2008

ISBN 978-9979-68-247-9
ISSN 1670-7427

This MSc thesis has also been published in April 2008 by the
Faculty of Engineering – Department of Mechanical and Industrial Engineering,
University of Iceland

INTRODUCTION

The Geothermal Training Programme of the United Nations University (UNU) has operated in Iceland since 1979 with six month annual courses for professionals from developing countries. The aim is to assist developing countries with significant geothermal potential to build up groups of specialists that cover most aspects of geothermal exploration and development. During 1979-2008, 402 scientists and engineers from 43 countries have completed the six month courses. They have come from Asia (44%), Africa (26%), Central America (15%), and Central and Eastern Europe (15%). There is a steady flow of requests from all over the world for the six month training and we can only meet a portion of the requests. Most of the trainees are awarded UNU Fellowships financed by the UNU and the Government of Iceland.

Candidates for the six month specialized training must have at least a BSc degree and a minimum of one year practical experience in geothermal work in their home countries prior to the training. Many of our trainees have already completed their MSc or PhD degrees when they come to Iceland, but several excellent students have made requests to come again to Iceland for a higher academic degree. In 1999, it was decided to start admitting UNU Fellows to continue their studies and study for MSc degrees in geothermal science or engineering in co-operation with the University of Iceland. An agreement to this effect was signed with the University of Iceland. The six month studies at the UNU Geothermal Training Programme form a part of the graduate programme. Six UNU-GTP MSc Fellows completed their MSc degree in 2008, the biggest group to date.

It is a pleasure to introduce the eleventh UNU Fellow to complete the MSc studies at the University of Iceland under the co-operation agreement. Mr. Daher Elmi Houssein, BSc and MSc in Physics and Chemistry, of Centre d'Etudes et de Reserches Scientifiques de Djibouti - CERD, completed the six month specialized training in Reservoir Engineering at the UNU Geothermal Training Programme in October 2005. His research report was entitled "Analysis of geothermal well test data from the Asal Rift area, Republic of Djibouti". A year later, in September 2006, he came back to Iceland for MSc studies in Reservoir Engineering at the Department of Mechanical and Industrial Engineering, within the Faculty of Engineering of the University of Iceland. In April 2008, he defended his MSc thesis presented here, entitled "Geothermal resource assessment through well testing and production response modelling". His studies in Iceland were financed by a fellowship from the Government of Iceland through the UNU Geothermal Training Programme. We congratulate Mr. Daher Elmi on his achievements and wish him all the best for the future. We thank the Department of Mechanical and Industrial Engineering of the University of Iceland for the co-operation, and his supervisors for the dedication.

Finally, I would like to mention that Daher's MSc thesis with the figures in colour is available for downloading on our website at page *www.unugtp.is/yearbook/2008.*

With warmest wishes from Iceland,

Ingvar B. Fridleifsson, director
United Nations University
Geothermal Training Programme

ACKNOWLEDGEMENTS

I would like to express my gratitude to Dr. Ingvar B. Fridleifsson, Director of the UNU-GTP and to Dr. Jalludin Mohamed, General Director at CERD, for giving me the opportunity to complete this M.Sc. programme. I wish to thank my supervisors, Dr. Gudni Axelsson, head of the Physics Department at ISOR (Iceland GeoSurvey) and visiting professor at the University of Iceland (UI) and Dr. Ólafur Pétur Pálsson, professor at UI, for their continuous supervision and valuable discussions during my work. Reykjavik Energy is acknowledged for allowing me to use and publish data from the Hellisheidi and Nesjavellir fields. I also appreciate the assistance of Dr. Einar Gunnlaugsson, head of Research at Reykjavik Energy throughout the work. The work on this thesis was sponsored by the Government of Iceland through the United Nation University Geothermal Training Programme.

Thanks to Reykjavik Energy to allow me to use the date from the Hellisheidi geothermal systems. My appreciation goes also to Mr. Lúdvík S. Georgsson, Ms. Thórhildur Ísberg and Ms. Dorthe H. Holm for their different helps. I would like to thank all MSc UNU-GTP Fellows for their friendship and fellow feeling.

I appreciate the warmth and friendship that existed between me and the staff at Orkustofnun and with the teachers I interacted during my study at the University of Iceland.

ABSTRACT

Assessment of the properties and capacity of geothermal resources involves various kinds of tests, data interpretation, monitoring and modelling. This ranges from the analysis of data collected during testing of single wells to the simulation of the response of geothermal reservoirs to utilization for years or even decades. This work presents a comprehensive review of the theoretical background and methodology used in analysing well-test, temperature- and pressure logging data from geothermal wells as well as a review of methods used for geothermal reservoir pressure response modelling. These methods are, consequently, applied to data from the Hellisheidi and Nesjavellir fields in the Hengill volcanic region of SW-Iceland. The purpose of well test analysis is to identify the type of reservoir involved and to determine the parameters of the reservoir quantitatively. Data from two Hellisheidi wells, HE-06 and HE-20, have been analyzed by applications of modern well-test analysis techniques such as derivative analysis and computer software simulation. Wellbore simulator analysis of discharge test data from the wells was used to estimate the productivity index (PI) for each well and the results compared with the injectivity indices (II) obtained from injection tests. The results were compared with results from three other high-temperature geothermal fields, one in Iceland and two in Japan. The production capacity of geothermal reservoirs can be assessed most accurately by modelling the long-term production response of the reservoir. This is demonstrated by the simulation of a 17-year (1989-2006) long pressure-decline data series from the Nesjavellir field. Both the lumped parameter modelling (LPM) and continuous time stochastic modelling (CTSM) methods are used and their results compared.

TABLE OF CONTENTS

Page

LIST OF FIGURES

Page

LIST OF TABLES

1. INTRODUCTION

Geothermal resources provide more than half of the energy utilized in Iceland (Ragnarsson, 2000 and 2005) and have the potential of contributing significantly to the energy economy of many countries of the world. A good example is Djibouti, the author's home-country, where geothermal development is in its infancy, however. The drilling of geothermal wells is expensive, not to mention the construction of power-plants and the associated pipe-line network and electric transmission lines (Teodoriu and Falcone, 2008). The drilling of geothermal wells is also risky and the results often inconsistent, due to the complex and poorly known nature of the geothermal systems, which are located at great depth. Therefore, it is essential to utilize the time span after the drilling of a well is completed until it is connected to a power plant for comprehensive testing and detailed data collection. This is ultimately aimed at assessing the power production potential of individual wells as well as the geothermal reservoir as a whole. After exploitation of a geothermal reservoir starts data collection through monitoring continues to be essential as this will continue to add to the understanding of the reservoir and its behaviour. Such monitoring also enables continuous upgrading of the production potential estimate for the geothermal reservoir in question, i.e. through modelling. In addition to allocating an adequate drilling budget, it is, therefore, essential to allocate adequate resources, much smaller of course, to well testing and well test analysis. The same applies to including a budget for monitoring and modelling in the long-term operation budget of a geothermal reservoir.

Well testing is a technique which allows the petroleum/geothermal engineer, to determine reservoir properties, such as permeability, porosity, the drainage volume of the reservoir, static pressure and, in general, to characterize or describe the reservoir-well system in order to indicate well damage or stimulation, fracturing or not of the well, the existence of faults or flow barriers, the approximate shape of the drainage area of the reservoir or the change of the reservoir lithological properties (Earlougher, 1977; Horne, 1995). During a well test, the response of a reservoir to changing production (or injection) conditions is monitored. Well test interpretation is therefore an inverse problem in that model parameters are inferred by analyzing model response to a given input (Earlougher, 1977; Horne, 1995). During production and injection test it is measured respectively the productivity index PI and injectivity index II by monitored the temperatures profiles at the same time.

Mathematical modelling and numerical simulation have become standard techniques in the evaluation of geothermal reservoirs. They are used to assess the generating capacity of a geothermal field, to design production and reinjection operations, and to assist in various reservoir management decisions. Geothermal reservoir simulation is based on the physics of fluid flow and heat transfer, on quantitative information about geothermal reservoir properties, and on the thermodynamics and thermophysical properties of reservoir fluids, chiefly water (Bodvarsson et al., 1986). Detailed numerical modelling of geothermal reservoirs is time consuming, costly and requires large amounts of field data. Lumped parameter modelling is a cost effective alternative and provides information on the global hydrological characteristics of the geothermal reservoir (Axelsson, 1989).

Intense drilling activity has been ongoing in the Hengill geothermal region during the last few years. In April 2008, when this is written, 44 wells had been drilled in the Hellisheidi field with up to 3 large drill rigs being active there at once. Because of this intense activity, time has not allowed comprehensive analysis of well-test, temperature logging and production testing data from these wells. To-date 27 wells have been drilled in the Nesjavellir field, where a combined heat and power plant has been in operation since 1990. The production capacity of the power plant has increased from 60 MW_{th} in 1998 to 90 MW_{th} and 120 MW_{th} in 2005 (Ragnarsson, 2005). This has caused a continuously increasing pressure decline in the geothermal reservoir, which has been monitored carefully. The pressure monitoring data is ideal for simple modelling and reservoir pressure forecasting, which can supplement the numerical modelling conducted for the Nesjavellir field to-date. In this report well-testing, temperature-logging and production testing data from two Hellisheidi wells, HE-6 and HE-20, is subjected to comprehensive analysis. In addition pressure monitoring data from the Nesjavellir field is used as the basis of simple pressure-response modelling.

This MSc-project has the following multiple purposes:

(1) To present a comprehensive review of the methodology used in analysing well-test, temperature- and pressure logging data from geothermal wells. The review is intended to be a kind of manual for such work.
(2) To review the theoretical background of the relevant analysis-methods.
(3) To review methods of geothermal reservoir modelling with emphasis on simple methods of pressure response simulation, this can complement more complex numerical modelling methods.
(4) Comprehensive analysis of well test, temperature- and pressure as well as flow test data from two recently drilled Hellisheidi geothermal production wells.
(5) To compare the injectivity- and productivity-indices, respectively, of the two wells and analyse the possible difference between them.
(6) Simulation of long-term pressure-response data from the Nesjavellir field with the LPM and the CTSM methods with a comparison of the two methods.
(7) Comparison of the results of (6), regarding the production potential of the Nesjavellir system, with the results of more complex and detailed numerical modelling.
(8) Recommendations for the Hengill region applicable to other high-temperature regions of the world such as the authors home country, Djibouti, where a geothermal drilling program is in the preparation phases.

Methods published in the oil and gas literature (Earlougher, 1977) have been adapted for analyzing data from geothermal reservoirs, assuming uniform initial steam saturation. A comprehensive well test analysis was made in Iceland in 1986 (Bodvarsson and Cox, 1986).

Reservoir models have been an integral part of reservoir assessment and management in the Hengill area since 1986. Initially the modelling effort focused on the Nesjavellir site. This preliminary model study resulted in a generating capacity estimate of 300 MW thermal for 30 years without re-injection, and that 400 MW thermal could only be sustained by injection (Bodvarsson et al., 1990). Several recalibrations were carried out in 1992, 1998 and 2000 for a final planning of 120 MW electrical and 300 MW thermal units (Bjornsson et al., 2003).

In this thesis, a brief outline of the geological characteristics of the Hengill geothermal system is given to clarify the reader about the nature of the field. The main emphasis of this report is on a well test, well bore and production history simulation theories and some examples of their applications. For well flow testing it is focus on injection test and also using a well test modelling software developed at ISOR to compare the hydrological parameters estimated. A wellbore simulator called HOLA was used for wellbore simulation. From this last computation, the value of *PI* was estimated and compared with *II* by including some other data obtained in three geothermal high temperature fields in Japan. LPM and CTSM methods are set up based on available long-term monitoring data from well 15 at Nesjavellir. Consequently, an assessment of the production potential of the geothermal system is carried out.

2. THEORETICAL BACKGROUND ON WELL TESTING AND RESERVOIR EVALUATION

2.1 Well and reservoir assessment procedures

In a hydrological well test, such as for a geothermal well, the pressure response of a given well and reservoir, due to production or injection, is monitored. Well testing is conducted in order to evaluate the conditions of a well, its flow capacity and reservoir properties. The most important properties are permeability-thickness and formation storage coefficient of the reservoir. These are not evaluated directly from the data. The data has to be interpreted on the basis of the most appropriate model, resulting in average values. In addition the properties are model dependent.

After a successful drilling programme, typical high-enthalpy well assessment in Iceland is undertaken through: single- or multi-step injection tests, pressure build-up tests and interference tests in order to estimate the main physical proprieties of the reservoir around the well like the permeability-thickness and storage coefficient, by assuming some values for porosity and compressibility of the basalt rock, as well as well parameters such as injectivity index and skin factor. In this study a well test simulator program was used to simulate data from such tests and to compare the results with 'classic methods' like semilog, log-log and type curves methods. After this the well is closed in order to allow it to warm-up and reach the steady state formation temperature (often 3-4 months). During and after the well testing, the temperature and pressure profiles of the well are logged and from those information the phase conditions of fluid, the real formation temperature, the flow paths and the main feed zones can be obtained. However caution must be used when interpreting logs as measurements are not made directly in the reservoir but in the well where internal flows and boiling can cause disturbances and give misleading results, even though the well is shut-in. When a well is not flowing, the aquifers (feed zones) usually warm up more slowly after drilling, than impermeable rock, (Stefansson and Steingrimsson, 1990).

After warm-up a well is discharged to estimate the production potential of the well. If the temperature and pressure conditions of the well are logged during discharge the logs can be simulated by a wellbore simulator. In this study the HOLA computer wellbore simulation program. Based on wellbore simulation results the productivity index of the well can be estimated and then compared with the injectivity index previously estimated. Several important flow parameters are monitored during discharge testing: water and steam flow, temperature or enthalpy of the fluid discharged, non condensable gas content, dissolved solid content, wellhead pressure, depth to the water level in pumped wells, the pressure drop from the reservoir into the well during discharge. During long term testing and utilization the parameters described above should be measured at regular intervals.

These parameters can be used in a simple reservoir models for matching and predicting changes in one reservoir parameter caused by the production of the system like a LPM or CTSM methods. This simple modelling is helpful and can give good prediction comparing to a detailed numerical modelling which needs a lot of information from geochemistry, geophysics, geology and enough wells drilled that can be representative of the geothermal system area.

2.1.1 The pressure diffusion equation

The basic equation of well testing theory is the pressure diffusion equation. It is used to calculate the pressure (P) in the reservoir at a certain distance (r) from a production well producing at given rate (q) as a function of time (t). The most commonly used solution of the pressure diffusion equation is the so-called Theis solution or the line source solution (Earlougher, 1977; Horne, 1995).

The three governing laws that are used in deriving the pressure diffusion equation are the following (Earlougher, 1977; Horne, 1995):

Conservation of mass inside a given control volume:

Mass flow in - Mass flow out = Rate of change of mass within the control volume

Conservation of momentum, expressed by Darcy's law:

$$q = 2\pi rh\frac{k}{\mu}\frac{\delta P}{\delta r} \tag{2.1}$$

where q = Volumetric flow rate (m^3/s)
h = Reservoir thickness (m)
k = Formation permeability (m^2)
P = Reservoir pressure (Pa)
r = Radial distance (m)
μ = Dynamic viscosity of fluid (Pa.s)

Equation of state of the fluid:

$$c = \frac{1}{\rho}\left(\frac{\delta\rho}{\delta P}\right)_T \tag{2.2}$$

where c = Compressibility of fluid (Pa^{-1})
ρ = Density of fluid (kg/m^3)
T = Temperature (°C)

Initially the following simplifying assumptions are used:

- The flow is considered isothermal
- The reservoir is considered homogeneous and isotropic
- The producing well penetrates the entire formation thickness
- The formation is completely saturated with a single fluid

By combining the three equations above and using the above assumptions, the pressure diffusion equation is given by:

$$\frac{\delta}{\delta r}\left(\frac{r\delta P(r,t)}{\delta r}\right) = \frac{\mu C_t}{k}\frac{\delta P(r,t)}{\delta t} \tag{2.3}$$

where C_t = Total compressibility of rock and water (Pa^{-1}).

In 1935, Theis (Earlougher, 1977; Horne, 1995) proposed an integral solution for this equation with:

Initial condition:

$P(r, t) = P_i$ for $t = 0$ $r > 0$

Boundary conditions:

i) $P(r, t) = P_i$ for $r \to \infty$ $t > 0$

ii) $q = 2\pi rh\frac{k}{\mu}\frac{\delta P}{\delta r}$ for $r \to 0$ $t > 0$

The solution to the radial diffusion equation with these boundary and initial conditions is given by:

$$P(r,t) = P_i + \frac{q\mu}{4\pi kh} Ei\left(\frac{-\mu C_t r^2}{4kt}\right) \tag{2.4}$$

where $Ei(-x) = -\int_x^{\infty} \frac{e^{-u}}{u} du$ is the exponential integral function

If $t > 100\ \frac{\mu C_t r^2}{4k}$ the exponential integral function can be expanded by a convergent series and thus, the Theis solution, for a pumping well with skin gives the total pressure change as:

$$\Delta P_t = -\frac{2.303 q\mu}{4\pi hk}\left[\log\left(\frac{\mu C_t r_w^{\ 2}}{4kt}\right) + \frac{0.5772 - 2s}{2.303}\right] \tag{2.5}$$

where s = skin factor

Skin is an additional pressure change to the normal pressure change in the near vicinity of the well due to production. A negative factor indicates that the well is in good communication with the reservoir.

2.1.2 Semi-logarithmic well test analysis

A plot of the Theis solution for ΔP vs. log t gives a semi-log straight line with a slope m per log cycle response for the infinite acting radial flow period of a well, and is referred to as semi-log analysis (Earlougher, 1977; Horne, 1995).

$$m = \frac{2.303 q\mu}{4\pi kh} \text{ (Pa/log cycle)} \tag{2.6}$$

The skin-factor is given by:

$$s = 1.151 * \left[\frac{\Delta P}{m} - \log\left(\frac{k}{\phi\mu C_t r_w^{\ 2}}\right) - \log(t) - 0.351\right] \tag{2.7}$$

The semi-log analysis is based on the interpretation of the semi-log straight line response that represents the infinite acting radial flow behaviour of the well. However, an actual wellbore has finite volume, and it becomes necessary to determine the duration of the wellbore storage effect or the time at which the semi-log straight line begins.

The wellbore storage effect can be identified by an unit slope relationship when the data is plotted on a log (ΔP) vs. log (t) graph. After about 1½ log cycle from the end of the unit slope line, the semilog straight line is expected to start (Earlougher, 1977; Horne, 1995).

As time proceeds, the response is characteristic of conditions further and further away from the wellbore. At very late time, the pressure response is affected by the influence of reservoir boundaries, but prior to those late times the pressure response does not "see" the reservoir boundaries, and the reservoir acts as if it were infinite in extent. This intermediate time response, between the early wellbore-dominated response and the late time boundary-dominated response, is known as the infinite acting period (Earlougher, 1977; Horne, 1995).

2.1.3 Type curve methods

Well test analysis often makes use of dimensionless variables. The importance of dimensionless variables is that they simplify the reservoir models by embodying the reservoir parameters (such as *k*), thereby reducing the total number of unknowns. They have the additional advantage of providing model solutions that are independent of any particular unit system. It is an inherent assumption in the definition that permeability, viscosity, compressibility, porosity, and thickness are all constants. The following dimensionless parameters are defined:

$P_D = \frac{2\pi kh}{q\mu}\Delta P$ - Dimensionless pressure change

$t_D = \frac{kt}{C_t \mu r_w^{\,2}}$ - Dimensionless time

$r_D = r / r_w$ - Dimensionless radial distance from the active well

Even though the reservoir parameters have already been estimated, there are several advantages in performing a type curve match. Whereas the semilog method and unit slope log-log line used only portions of the data, a type curve match uses the entire data set. This helps ensure consistency over the whole range of time, and also provides a mechanism to make use of the transition data which lies between the individual response periods (Earlougher, 1977; Horne, 1995).

In a log-log type curve, it is known that the P_D versus t_D curves (the reservoir model) will have exactly the same shape as the P_i - P_{wf} versus Δt data (the measurements during the well test) (Earlougher, 1977; Horne, 1995).

Generally, the procedure for type curve analysis can be outlined as follows (Earlougher, 1977; Horne, 1995):

- The data is plotted as log ΔP vs. log Δt on the same scale as that of the type curve;
- The curves are then moved, one over the other, by keeping the vertical and horizontal grid lines parallel, until the best match is found;
- The best match is chosen and the pressure and time values are read from fixed points on graphs, ΔP_M and P_{DM} as well as Δt_M and t_{DM};
- For an infinite acting system, the transmissivity, *T*, is evaluated from:

$$T = \frac{kh}{\mu} = \frac{q}{2\pi}\left(\frac{P_D}{\Delta P}\right)_M \tag{2.8}$$

- And the storage coefficient *S*, is calculated as:

$$S = C_t h = \frac{kh}{\mu r_w^{\,2}}\left(\frac{\Delta t}{t_D}\right)_M \tag{2.9}$$

2.1.4 Multirate drawdown tests - Odeh and Jones´s method

A multiple-rate test involves measuring the pressure response to a step-wise changing flow rate at a fixed depth in a well (Earlougher, 1977; Horne, 1995). The approximate solution for such a test is:

$$\frac{P_i - P_{wf}(t)}{q_N} = \frac{2.303\mu}{4\pi kh}\sum_{j=1}^{N}\left[\frac{(q_j - q_{j-1})}{q_N}\log(t - t_{j-1})\right] + b' \tag{2.10}$$

where P_i = initial pressure (Pa)
$P_{wf}(t)$ = flowing pressure well at time t (Pa)
N = number of flow rates
q_j = flow step between t_{j-1} and t_j (m^3/s)
t_j = time at the flow rate q_j (s)

A plot of $\frac{P_i - P_{wf}(t)}{q_N}$ vs. $\sum_{j=1}^{N}\left[\frac{(q_j - q_{j-1})}{q_N}\log(t - t_{j-1})\right]$ should show a straight line with slope m´:

$$m' = \frac{2.303\mu}{4\pi kh} \quad (\text{Pa}/(\text{m}^3/\text{s})) \tag{2.11}$$

2.1.5 Build-up test - Horner method

Pressure build-up testing requires shutting in a production well. The effect of these two flow rates can be represented by a well which is produced for a time t_p, at rate q, and then shut in for a running time Δt (Earlougher, 1977; Horne, 1995). Thus (same approximation as before):

$$\Delta P_{ws} = \frac{2.303 q\mu}{4\pi kh}\log\left(\frac{t_p + \Delta t}{\Delta t}\right) \tag{2.12}$$

ΔP_{ws} = pressure change after time t_p (Pa)

A plot of ΔP_{ws} vs. $\log\left(\frac{t_p + \Delta t}{\Delta t}\right)$ should follow a straight line with slope m when the reservoir behaves as infinite and the semi-log approximation applies.

$$m = \frac{2.303 q\mu}{4\pi kh} \tag{2.13}$$

If we have applied a series of N different flow rates prior to shut-in, the well shut-in pressure assuming infinite acting (semilog) behaviour can be written:

$$\Delta P_{ws} = m'\sum_{j=1}^{N}\frac{q_j}{q_N}\log\left(\frac{t_N - t_{i-1} + \Delta t}{t_N - t_j + \Delta t}\right) \tag{2.14}$$

q_N = last rate the well flowed at before being shut.

Thus a plot of ΔP_{ws} vs. $\sum_{j=1}^{N}\frac{q_j}{q_N}\log\left(\frac{t_N - t_{i-1} + \Delta t}{t_N - t_j + \Delta t}\right)$ should show the slope m' as in Equation 2.11.

2.1.6 Fractures

The fracture has much greater permeability than the formation it penetrates; hence it influences the pressure response of a well test significantly (Horne, 1995). Due to the linear flow in the fracture, different flow regimes can be observed at different times (Figure 1).

At early time, there is linear flow within the fracture and linear flow into the fracture from the formation (Figure 1a). The combination of these two linear flows gives rise to the bilinear flow

period. Following the bilinear flow period, there is a tendency towards linear flow (Figure 1b) (Horne, 1995).

The effect of fractures can be detected in well testing as follows (Horne, 1995):

- Bi-linear flow: this response is reflected by a straight line pressure response with slope ¼ at an early time on log (ΔP) vs. log (Δt) graph
- Linear flow: this response is reflected by a straight line pressure response with slope ½ at an early time on log (ΔP) vs. log (Δt) graph
- Radial flow: at late times the pressure response may develop into a radial flow response (Theis solution)

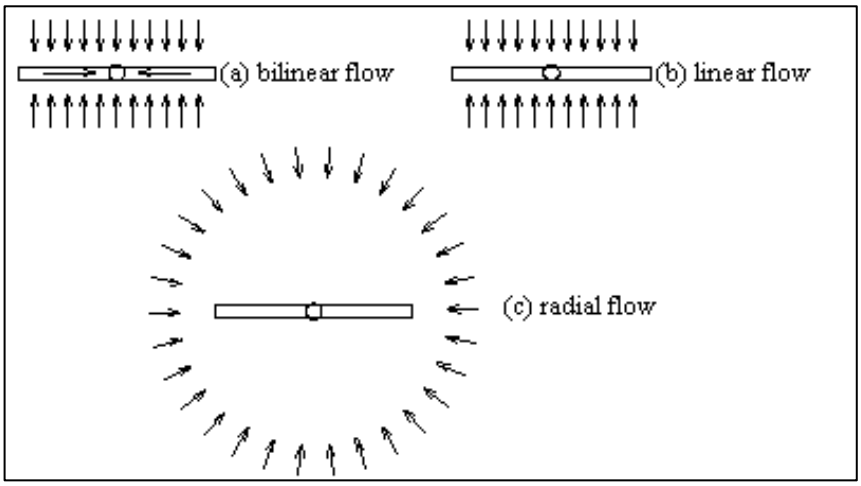

FIGURE 1: Different flow regimes at different times (Horne, 1995)

2.1.7 Interference test

In an interference test, one well is produced and pressure is observed in a different well (or wells). An interference test monitors pressure changes out in the reservoir, at a distance from the original producing well. The advantage of interference testing is that a much greater area of the reservoir is tested, providing estimates of reservoir properties between wells. In addition, the interference response is little affected by the complicating factors of wellbore storage and skin effect that make single well test interpretation more difficult. Furthermore, the nature of the response over distance makes it possible to estimate not only the reservoir transmissivity (kh), but also storativity ($\varphi C_t h$). The disadvantage is that pressure drops can be very small over distance, and are affected by other operational variations in the field at large. Nonetheless, modern electronic gauges are quite capable of registering such small pressure drops (often less than 1 psi over days or even weeks), and thus interference testing is a useful method of proving up new discoveries. In new reservoirs, an interference test is not affected by other production in the field (since there is none) and serves to prove the existence of productive reservoir between the wells (Horne, 1995).

To process interference test data the type-curve matching technique is commonly used with semi-log method and computerized fitting (Earlougher, 1977; Horne, 1995).

There are some other new methods described either by Eppelbaum and Kutasov (2008), by introducing a hydraulic diffusivity of formations (η) or by Néstor and Fernando (2001) by analysis the pressure interference test through the use of the pressure derivative.

2.1.8 Derivative plot

A derivative plot is a useful diagnostic tool for examining the effects of wellbore storage, recharge and barrier boundaries, leakage, delayed gravity response and fracture flow. The technique was introduced in the petroleum industry literature (Bourdet et al., 1983; Bourdet et al., 1989). The derivative plot provides a simultaneous presentation of log ΔP vs. log Δt and log tdP/dt vs. log Δt (Horne, 1995) and consequently provides information on many characteristics in one plot. Examples of various characteristics seen by such plots are presented in Appendix I.

An important aspect of performing derivative analysis is the selection of an appropriate calculation method. Using adjacent points (nearest neighbors) for preliminary derivative analysis will produce a very noisy derivative.

$$t\left(\frac{\partial P}{\partial t}\right)=t_i\left[\frac{(t_i-t_{i-1})\Delta P_{i+1}}{(t_{i+1}-t_i)(t_{i+1}-t_{i-1})}+\frac{(t_{i+1}+t_{i-1}-2t_i)\Delta P_i}{(t_{i+1}-t_i)(t_i-t_{i-1})}-\frac{(t_{i+1}-t_i)\Delta P_{i-1}}{(t_{i+1}-t_{i-1})(t_i-t_{i-1})}\right] \quad (2.15)$$

Where t is the time, P the pressure and the index i-1 and i+1 are concerning to the two adjacent points to i.

To remove noise from the calculations, the Bourdet method uses data points separated by a fixed distance measured in logarithmic time (Horne, 1995).

$$t\left(\frac{\partial P}{\partial t}\right)=\left(\frac{\partial P}{\partial \ln t}\right)=\left[\frac{\ln(t_i/t_{i-1})\Delta P_{i+1}}{\ln(t_{i+1}/t_i)\ln(t_{i+1}/t_{i-1})}+\frac{\ln\left(t_{i+1}*t_{i-1}/t_i^{\,2}\right)\Delta P_i}{\ln(t_{i+1}/t_i)\ln(t_i/t_{i-1})}-\frac{\ln(t_{i+1}/t_i)\Delta P_{i-1}}{\ln(t_{i+1}/t_{i-1})\ln(t_i/t_{i-1})}\right] \quad (2.16)$$

Typically, the separation or differentiation interval required to remove noise ranges between 0.1 and 0.5 of a log cycle. In selecting the differentiation interval, care must be exercised to avoid overly smoothing the data, however. This method is considered the best method.

$$t\left(\frac{\partial P}{\partial t}\right)=\left(\frac{\partial P}{\partial \ln t}\right)=\left[\frac{\ln(t_i/t_{i-k})\Delta P_{i+j}}{\ln(t_{i+j}/t_i)\ln(t_{i+j}/t_{i-k})}+\frac{\ln\left(t_{i+j}*t_{i-k}/t_i^{\,2}\right)\Delta P_i}{\ln(t_{i+j}/t_i)\ln(t_i/t_{i-k})}-\frac{\ln(t_{i+j}/t_i)\Delta P_{i-k}}{\ln(t_{i+j}/t_{i-k})\ln(t_i/t_{i-k})}\right]$$
$$\ln t_{i+j}-\ln t_i\geq 0.2 \quad (2.17)$$
$$\ln t_i-\ln t_{i-k}\geq 0.2$$

2.2 Discharge testing methods

One of the basic tasks of a geothermal reservoir engineer is to measure the fluid flow from a discharging well and its energy content as well as to analyse the flow characteristics of the well. High-enthalpy wells are discharge tested after they have been allowed to heat up after drilling for 2-4 months. The well is opened up and allowed to flow to the atmosphere. Geothermal high-temperature wells are usually discharged into a silencer which also acts as a steam-water separator at atmospheric pressure.

There are two main methods used commonly in Iceland for two phase flow measurements: the lip pressure method and the chemical tracer method.

2.2.1 Lip pressure method

The lip pressure method is based on an empirical formula developed by James (James, 1962). The lip pressure method is not quite as accurate as the separator method (which separates the steam-water

flow into a flow of water and a flow of steam at the pressure of the separator) but is desirable because a minimum of hardware and instrumentation is required to obtain good results.

To use this method, the steam-water mixture is discharged through an appropriately sized pipe into a silencer or some other simple device to separate the steam and water phases at atmospheric pressure. Assuming that we have a fairly large amount of steam/water mixture flowing at sonic velocity through an open-ended pipe to the atmosphere, the absolute pressure at the external end of the pipe is then proportional to the mass flowrate and enthalpy (Figure 2). The flow in geothermal wells is assumed to be isenthalpic (adiabatic). Water flow from the silencer is commonly measured by the weir-box method (Grant et al., 1982).

The formula that Russel James deduced is:

$$\frac{W_t H_t^{1.102}}{A P_{lip}^{0.96}} = 1680 \qquad (2.18)$$

where P_{lip} = lip pressure at the end of the pipe (MPa)
W_t = total mass flow rate (kg/s)
A = cross-section area of the lip (cm^2)
H_t = total fluid enthalpy (kJ/kg)

When the water flow W_w (kg/s) from the atmospheric silencer, measured in the weir-box, and the lip pressure are known, the total fluid enthalpy is given by:

$$\frac{W_w}{A P_{lip}^{0.96}} = Y = \frac{0.74\,(2675 - H_t)}{H_t^{1.102}}$$

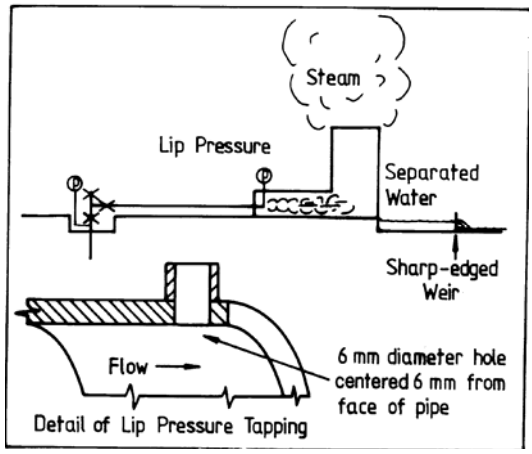

FIGURE 2: Flow measurement by lip pressure and silencer (Grant et al., 1982)

Then H_t is usually determined by iteration from the above equation. This equation can also be solved for H_t between 400 and 2800 kJ/kg as a function of Y with an accuracy of 1.5% by (Grant et al., 1982):

$$H_t = \frac{2675 + 365\,Y}{1 + 3.1\,Y} \qquad (2.20)$$

The water flow W_w is related to the total mass flow by:

$$W_t = \frac{W_w}{1 - X} \qquad (2.21)$$

where $X = \dfrac{H_t - H_w}{H_s - H_w}$

and X = Steam mass fraction as ratio
H_w = Specific enthalpy of water (kJ/kg)
H_s = Specific enthalpy of steam (kJ/kg)

The specific enthalpies for water and steam should be look up in the steam tables for the conditions that the separator is operated at.

As a rule of thumb, total mass output plotted against wellhead pressure (WHP) should give a smooth curve (Figure 3). If not, the calculation or measurements are suspect. For all short-term flow tests, a continuous record of WHP should be made. This is a simple indication of stability of flow conditions.

For a liquid reservoir, the well output (and WHP) may stabilise within minutes of changing the throttle conditions, whereas wells producing from a two-phase reservoir may require days of running at constant throttle conditions before stability is even approached. In some such wells and in dry steam producers, conditions of constant flow at constant throttle may never be obtained, and transient analysis must be made of such flow data (Stefansson and Steingrimsson, 1990).

Disadvantage of this method is if the water flow is high water may be lost through the silencers (not all separated). Then liquid water flow rate measured at the weir-box is too low and by the way the value of enthalpy measured is higher than what we expected.

The maximum discharging pressure MDP if it was not made, it'll be the case of wells HE-06 and HE-20 in chapter 6, there is simple correlation between MDP and discharge enthalpy deduced from Russell-James method by assuming that the reservoir contains liquid water at boiling point for depth and uses a homogenous flow model

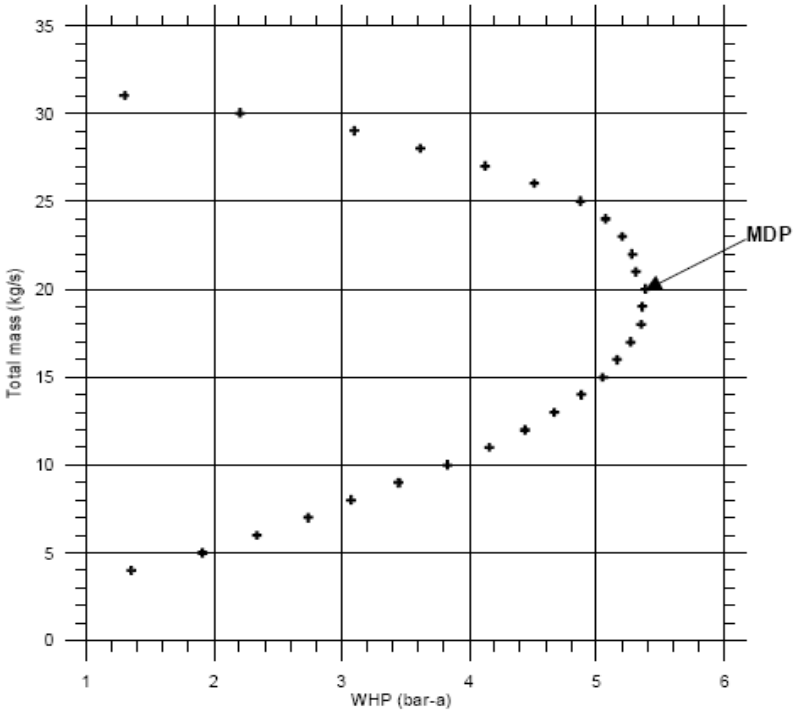

FIGURE 3: A typical output curve of a geothermal well (Grant et al., 1982)

$$T = 100P^{0.283} \tag{2.22}$$

where T is the temperature of the feed water and P the MDP pressure in bar-g.

The classification of geothermal system is based on reservoir fluid state like:

- Liquid dominated system: Hydrostatic pressure gradients. Reservoir temperature generally less than 300°C.
- Vapour dominated systems: Vapour-static pressure gradients. Reservoir temperatures generally around 240°C
- Boiling system: Pressure gradients generally close to hydrostatic. Reservoir temperatures as high as 300-350°C

2.2.2 Chemical tracer

This method is using two different tracers one for the liquid phase and one for the steam phase.

The principle in this method is to measure the dilution when a solution containing a chemical indicator is injected into the well discharge. The solution is injected at a know constant rate an upstream location. Analysis of a downstream sample will then make it possible to determine the well discharge by the formula:

$$Q = q\frac{C_1 - C_2}{C_2 - C_0} \tag{2.23}$$

Where q is the injection rate of the chemical solution and C_0, C_1 and C_2 are respectively the concentrations of the chemical indicator in the well fluid, the solution injected and the downstream sample.

For the steam phase, same principle as for liquid water is applied. Instead of injecting solution into the flow stream, more commonly it has used non-condensible gas (SF_6 diluted in N_2).

2.2.3 Injection tests

Injection testing is in principle a simple variant of discharge flow testing, with the flow reversed. Water is injected into a well and the flow rate recorded along with changes in down-hole pressure or depth to water level. A quasi-stable flow versus pressure curve can be obtained, and transient behaviour measured at changes in flow rate.

Injection is a simple inverse of production if the fluid injected is of the same enthalpy (quality or temperature) as that produced. Generally the fluid injected is water cooler than reservoir temperature then it has different viscosity and compressibility from the reservoir fluid (Grant et al., 1982). The non-isothermal injectivity index obtained from these tests depends on the mobility ratio of the cold region to the hot reservoir and the extent of the cold spot. Sigurdsson et al., (1983) propose a method of estimation of the apparent viscosity which accounts for these effects and relates the non-isothermal injectivity index to the isothermal injectivity index.

During injection tests, the injectivity index (*II*) is often used as a rough estimate of the connectivity of the well to the surrounding reservoir. Here it is given in the units [(L/s)/bar] and it is defined as the change in injection flow rate divided by the change in stabilized reservoir pressure.

$$II = \frac{\Delta Q}{\Delta P} \tag{2.24}$$

Where $\Delta Q = Q_{end\ of\ step} - Q_{beginning\ of\ step}$ and $\Delta P = P_{end\ of\ step} - P_{beginning\ of\ step}$. In Well Tester the pressure values used to calculate *II* are taken from the modelled response (not the actual data collected).

2.3 Wellbore simulation

The simulator HOLA was used to simulate the wellbore conditions (temperature, pressure, etc.) that influence the transport of fluid from the reservoir to the surface. The simulator numerically solves a set of differential equations that describe the steady-state energy, mass and momentum flow in a vertical pipe for single or two-phase flow. The governing steady-state differential equations for mass, momentum and energy fluxes in a vertical well are (Bjornsson et al., 1993):

$$\begin{aligned} &\frac{dW}{dz} = 0 \\ &\frac{dP}{dz} - \left[\left(\frac{dP}{dz}\right)_{fri} + \left(\frac{dP}{dz}\right)_{acc} + \left(\frac{dP}{dz}\right)_{pot}\right] = 0 \\ &\frac{dE_t}{dz} \pm Q = 0 \end{aligned} \tag{2.25}$$

where W = Total mass flow (kg/s),

P = Pressure (Pa),
E_t = Total energy flux in the well (J/s),
z = Depth coordinate (m),
Q = Ambient heat loss over unit distance (W/m).

The plus and minus signs indicate down-flow and up-flow respectively. The pressure gradient is composed of three terms: wall friction, acceleration of fluid and change in gravitational load over depth interval (*dz*).

The governing equation of mass flow between the well and the reservoir, through a given feed-zone, is:

$$W_{feed} = PI\left[\frac{k_{rw}\rho_w}{\mu_w} + \frac{k_{rs}\rho_s}{\mu_s}\right] * \left(P_r - P_{well}\right) \tag{2.26}$$

where W_{feed} = Feedzone flow rate (kg/s),
PI = Productivity index of the feedzone (m^3),
k_r = Relative permeability of the phases (subscripts w for liquid and s for steam),
μ = Dynamic viscosity (Pa.s),
ρ = Density (kg/m^3),
P = Pressure (Pa) subscripts r for reservoir.

Hola programme calculates *PI* at one feed zone by

$$PI = \left(\frac{q_\beta}{P_\beta - P_{wb}}\right)\left(\frac{\mu_\beta}{k_{r\beta}\rho_\beta}\right) \tag{2.27}$$

where PI = Productivity index (m^3)
q_β = Inflow mass rate (kg / m^3) at the feed zone of the phase β (liquid, gas)
P_β = Pressure reservoir (Pa) at the feed zone
P_{wb} = Bottomhole pressure at that depth
μ_β = Viscosity (Pa .s)
$k_{r\beta}$ = Dimensionless relative permeability
ρ_β = Density (kg / m^3)

Here the PI will be calculated by summing all the PI from each feed zone

$$PI = \sum_{j=1}^{N} PI_j = \sum_{j=1}^{N} \frac{Q_j}{\Delta P_j} \tag{2.28}$$

where N is the number of feed zones, Q_j the flow rate through feed-zone *j* (kg / s), and ΔP_j is the difference between the reservoir pressure and down-hole pressure at feed-zone *j* (Grant et al., 1982).

2.4 Simulation of long-term reservoir pressure response

A practical model of the geothermal field is essential for prediction of changes in a geothermal reservoir. To construct the model, a variety of geosciences field data, such as hydrological, gravity, self-potential, geological and geochemical data are necessary.

The application of reservoir engineering begins during the exploration phase of the project with the analysis of the initial geophysical measurement data that indicate a promising geothermal system, and

it continues throughout the operational life of the geothermal resource. It is the reservoir engineer's task to test wells, monitor their output, design new wells, and predict the long-term performance of the reservoir and wells. This design and prediction is accomplished by studying field and operational measurement data and using computer models like Tough2 for a detailed numerical modelling or LPM/CTSM simple methods to project the field operation into the future.

The next subchapters will focus description of the two simple methods and compared.

2.4.1 The LUMPFIT program

Lumped parameter models of hydrological systems such as geothermal systems consist of a few capacitors or tanks that are connected by resistors (Figure 4). The program LUMFIT, which employs a non-linear, iterative, least square procedure, has been used successfully to simulate data on pressure changes in geothermal systems caused by mass extraction and/or mass injection (Axelsson and Arason, 1992). The tanks simulate the storage of different parts of the reservoir in question, whereas the resistors simulate the permeability. A tank in lumped model has the mass storage coefficient κ. The tank response to a load of liquid mass m gives a pressure increase given by $p = m/\kappa$. The mass conductance of a resistor in a lumped model is σ when it transfers $q = \sigma\Delta p$ units of liquid mass per unit time at the impressed pressure differential Δp. The pressures in the tank simulate the pressures in different parts of the reservoir, whereas production from the reservoir is simulated by withdrawal of water from only one of the tanks (Axelsson, 1989).

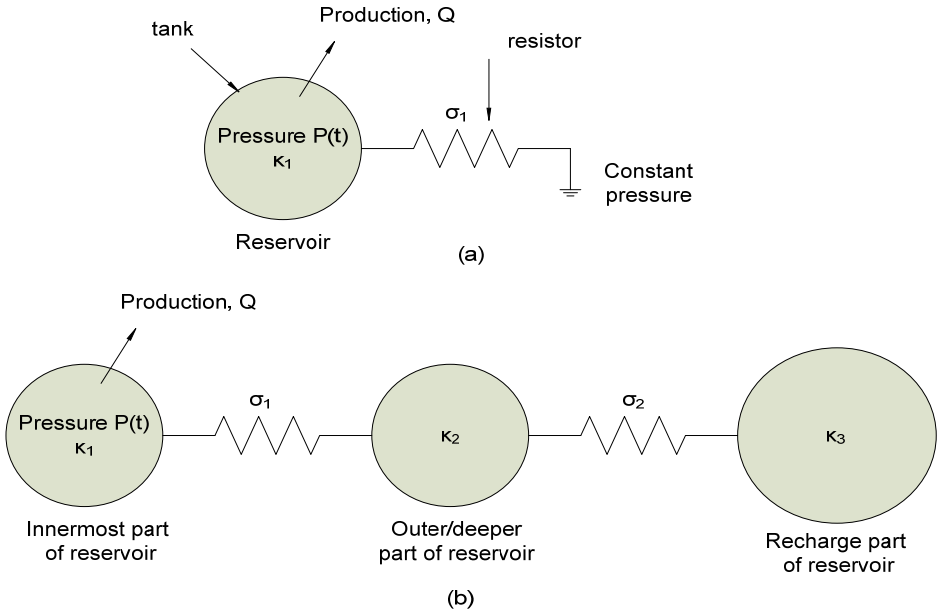

FIGURE 4: Examples of lumped models of hydrological reservoirs: (a) one tank open model (b) three tank closed model

Lumped models can be either open or closed. Open models are connected by a resistor to an infinitely large imaginary reservoir, which maintains a constant pressure. On the other hand, closed lumped models are isolated from any external reservoir. Actual reservoirs can most generally be represented and simulated by two- or three-tank closed or open lumped parameter models (Axelsson, 1989). The pressure response, ΔP, of a single-tank open model for a production, $Q(t)$ assuming a step response, since time $t = 0$ is given by the following equation (Axelsson, 1989):

$$\Delta P(t_i) = -\left(\frac{Q(t_i)}{\sigma_1}\right)\left(1 - e^{-\frac{\sigma_1 * t_i}{\kappa_1}}\right) \tag{2.29}$$

The pressure response of a more general open model with N tanks, to $Q(t)$ assuming a step response, since time $t = 0$, is given by

$$\Delta P(t_i) = -\sum_{j=1}^{N} Q(t_i)\frac{A_j}{L_j}\left(1 - e^{-L_j * t_i}\right) \tag{2.30}$$

The pressure response of an equivalent *N*-tank closed model is given by the equation

$$\Delta P(t_i) = -\sum_{j=1}^{N-1} Q(t_i)\frac{A_j}{L_j}\left(1 - e^{-L_j * t_i}\right) + Q(t_i) * B * t_i \tag{2.31}$$

The coefficients A_j, L_j and B are functions of the storage coefficients of the tanks (κ_j) and the conductance coefficients of resistors (σ_j) of the model, and can be estimated by the LUMPFIT program by using a non-linear iterative least squares techniques inverse modelling described by Axelsson (1989).

Lumped parameter models can in general be considered as distributed parameter models with a very coarse spatial discretization. The LUMPFIT approach, however, tackles the modelling as an inverse problem, which requires much less time and operator intervention than direct or forward modelling. Reservoir modelling by using LUMPFIT is therefore highly cost effective and has been shown to yield quite acceptably accurate results (Axelsson et al., 2005a).

Capacitance or storage, in a liquid-dominated geothermal system can result from two types of capacitive effects (Axelsson, 1989). The capacitance may be on one hand be controlled by liquid/formation compressibility. In that case the capacitance in a lumped model is given by Axelsson (1989):

$$\kappa = V\rho C_t \tag{2.32}$$

where V is the volume of that part of the reservoir in question the capacitor simulates, ρ the liquid density and C_t the total compressibility.

In other hand the capacitance can be controlled by the mobility of a free surface (Axelsson, 1989), then:

$$\kappa = A\phi / g \tag{2.33}$$

where A = Area of the reservoir;
φ = Porosity; and
g = The gravity.

2.4.2 Continuous Time Stochastic Modelling - CTSM

CTSM is a computer program for performing Continuous Time Stochastic Modelling (http://www2.imm.dtu.dk/~ctsm/). The program has been developed at Informatics and Mathematical Modelling (IMM) at the Technical University of Denmark (DTU). Continuous Time Stochastic Modelling means semi-physical modelling of dynamic systems based on stochastic differential equations. Stochastic differential equations contain a diffusion term to account for random effects, but are otherwise structurally similar to ordinary differential equations. This means that conventional modelling principles can be applied to set up the model.

Statistical methods are used for identification and estimation of continuous time state space models of geothermal reservoirs (Jonsson, 1990). Here the reservoir is again modelled as a number of tanks coupled in series (Figure 5) by based on the same principles as have been used by Axelsson (1989).

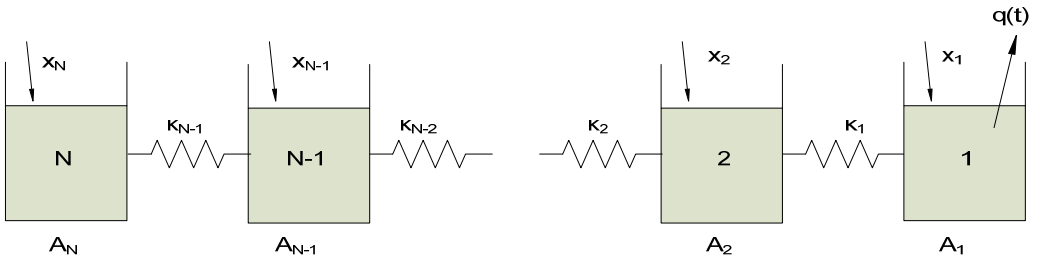

FIGURE 5: A schematic diagram of the thank setup used in Kalman model

The differential equation for the water level in tank number *i* is then given by:

$$\dot{x}_i(t) = \frac{1}{A_i}\left[q_i(t) - q_{i-1}(t)\right] \tag{2.34}$$

And furthermore the flow between tanks *i* and *i+1* is

$$q_i(t) = \frac{x_{i+1}(t) - x_i(t)}{K_i} \tag{2.35}$$

By rearranging the two equations (2.34) and (2.35) gives:

$$\dot{x}_i(t) = \frac{1}{A_i}\left[\frac{1}{K_i}x_{i+1}(t) - \left(\frac{1}{K_i} + \frac{1}{K_{i-1}}\right)x_i(t) + \frac{1}{K_{i-1}}x_{i-1}(t)\right] \tag{2.36}$$

The cross-sectional areas, A_i, i = 1, 2... N, are measured in m^2 and the flow resistance, K_i, i = 1, 2... N, in days/m^2. N is the number of tanks in the model. With $q_0(t) = q(t)$ as the reservoir discharge and thus an input to the model and assuming that $x_N(t) = \bar{x}_N$ is constant, the model is readily expressed on state space form for the Kalman filters. As an example, with tree tanks it becomes:

$$\begin{bmatrix}\dot{x}_1(t)\\ \dot{x}_2(t)\end{bmatrix} = \begin{bmatrix}\frac{-1}{A_1K_1} & \frac{1}{A_1K_1}\\ \frac{1}{A_2K_1} & \frac{-1}{A_2}\left(\frac{1}{K_1} + \frac{1}{K_2}\right)\end{bmatrix}\begin{bmatrix}x_1(t)\\ x_2(t)\end{bmatrix} + \begin{bmatrix}\frac{-1}{A_1} & 0\\ 0 & \frac{1}{A_2K_2}\end{bmatrix}\begin{bmatrix}q(t)\\ \bar{x}_3\end{bmatrix} \tag{2.37}$$

or generally the differential equation on state space form (Jonsson, 1990):

$$dx(t) = \mathbf{B}x(t)dt + \mathbf{C}q(t)dt) \tag{2.38}$$

For N thanks there are 2N-1 parameters to be estimated. Expressing the model for $N > 3$ shows that the matrix $\mathbf{B}$ Eq. (2.32) is tridiagonal and that the matrix $\mathbf{C}$ Eq. (2.32) contains only zeroes apart from the first and last elements, i.e. $\mathbf{C}(1,1)$ and $\mathbf{C}(N\text{-}1,2)$ as in Eq. (2.31).

To allow for variations between the model and the true water level, a noise term is added in Eq. (2.38) and then the model is described by a stochastic differential equation and written as

$$dx(t) = \mathbf{B}x(t)dt + \mathbf{C}q(t)dt + dw(t) \tag{2.39}$$

Where x, q, B and C are defined as before and $w(t)$ is assumed to be a Wienner process with incremental covariance $Q'(t)dt$ (Jonsson, 1990).

The discharge from the reservoir varies with time and the sampling period of the data is not constant. By assuming that q and the model parameters are constant during the sampling interval, i.e, the discharge is constant between sampling instants, the model can be written in discrete time (Åström, 1970; Jonsson, 1990) as:

$$x(t+\Delta t) = \Phi(\Delta t)x(t) + \Gamma(\Delta t)q(t) + w(t+\Delta t) \tag{2.40}$$

or:

$$x(t_i) = \Phi_i x(t_{i-1}) + \Gamma_i q(t_{i-1}) + w(t_i) \tag{2.41}$$

where

$$\Phi_i = \Phi(\Delta t_i) = \Phi(t_i - t_{i-1}) = e^{\Delta t_i B} = I + \Delta t_i B + \frac{(\Delta t_i B)^2}{2} + \ldots = \sum_{i=0}^{\infty} \frac{\Delta t_i{}^i B^i}{i!} \tag{2.42}$$

and

$$\Gamma_i = \Gamma(\Delta t_i) = C\left[\int_0^{\Delta t_i} e^{B^* j}\, dj\right] \tag{2.43}$$

The model measurements is assumed to be:

$$z(t_i) = Dx(t_i) + v(t_i) \tag{2.44}$$

The measurement matrix D in Eq. (2.44) relates the state to the measurement z_k. In practice D might change with each time step or measurement, but here it is assumed constant with only zeroes apart from the first element $D(1,1) = 1$ meaning the output model measurement corresponds to the water of the first tank.

The random variables w_k and v_k represent the process and measurement noise (respectively). They are assumed to be independent (of each other), white, and with normal probability distributions:

$$\begin{aligned} p(w) &\approx N(0, Q) \\ p(v) &\approx N(0, R) \end{aligned} \tag{2.45}$$

Q and R are respectively the process noise covariance and measurement noise covariance matrices.

Kalman filter is used to estimate the states values from the state space form. The filter is very powerful in several aspects: it supports estimations of past, present, and even future states, and it can do so even when the precise nature of the modeled system is unknown (Welch and Bishop, 2006; Jonsson and Palsson, 1992; Jonsdottir et al., 2006).

The parameters A_i and K_i are estimated in continuous time models from discrete measurements as described Jonsson (1990).

The Algorithm for estimation the state of process and parameter is summarized in CTSM software. The model will be consider closed when the flow resistance K_{N-1} between tanks N and $N-1$ is infinite then the term $\frac{1}{K_{N-1}} \xrightarrow{\infty} 0$.

3. THE HENGILL GEOTHERMAL FIELDS

3.1 General information

Hengill is one of the highest mountains in the region east of Reykjavík, Iceland's capital. It is the central volcano of the homonymic Hengill volcanic zone, composed of crater rows and a large fissure swarm. It is located on the eastern part of the Reykjanes Peninsula, South West Iceland (Figures 6 and 7). It is set at the continuation of the Mid-Atlantic ridge (Reykjanes Ridge) at the triple junction of the Reykjanes Peninsula volcanic zone, the Western volcanic zone and the South Iceland Seismic Zone. The Hengill volcanic zone has a 100km long NE-SW axis and is 3 to 16 km wide. It extends from Selvogur in the south to Ármannsfell in the north.

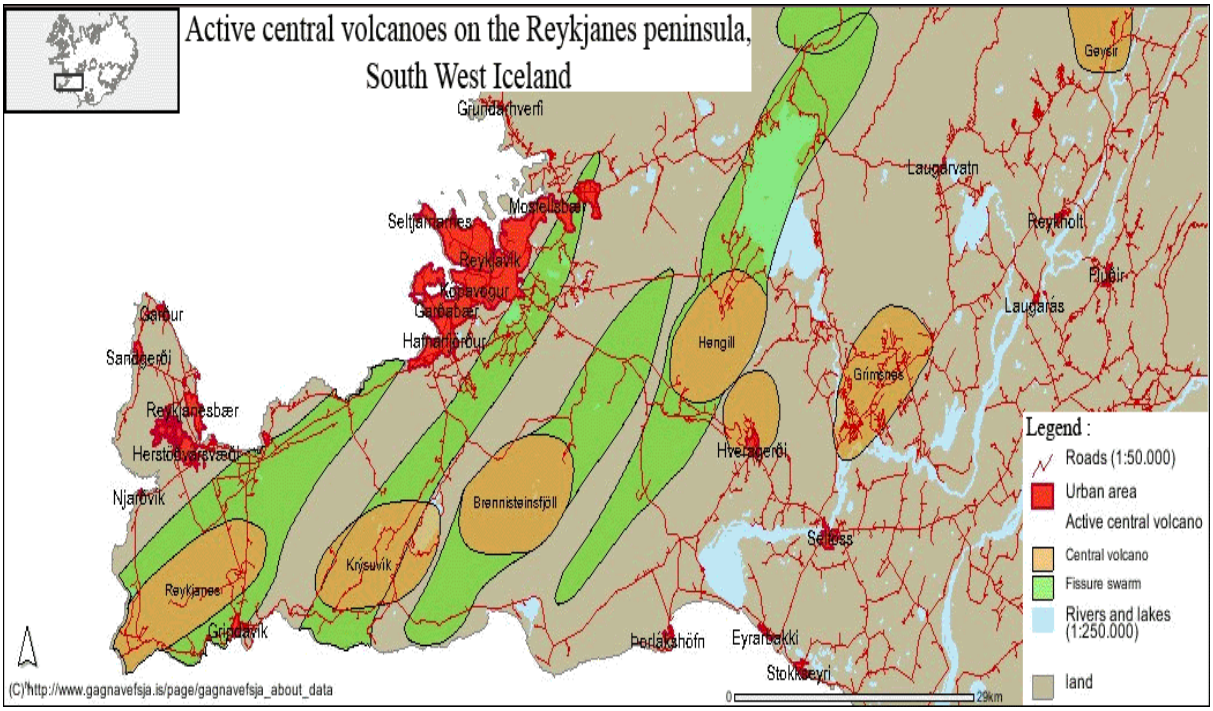

FIGURE 6: Active central volcanoes on the Reykjanes peninsula, South West Iceland (Gislason and Gunnlaugsson, 2003)

The Hengill central volcano covers an area of about 40 km² (Bjornsson et al., 1986). The Hellisheidi geothermal field is located in the South part of Mt Hengill, and some 20 km south of the Nesjavellir high-temperature field (Figure 7). The present well field in Hellisheidi covers some 12 km². The first exploration well was drilled in 1985 at Kolvidarhóll (KhG-1) at the western boundary of the Hellisheidi field. A total of 17 wells had been drilled in Hellisheidi till September 2005, nine of them deviated. Now 44 wells have been drilled there.

Production plans for the Hellisheiði Plant aim at 300 MW electrical generation capacity and 400 MW thermal energy production. Two steam turbines (45 MW each; 90 MW total) have been online from December 2006 and a 33 MWe back pressure turbine from 2007. The plant's purpose is to meet increasing demand for electricity and hot water for space heating in the industrial and domestic sectors of the greater Reykjavík area.

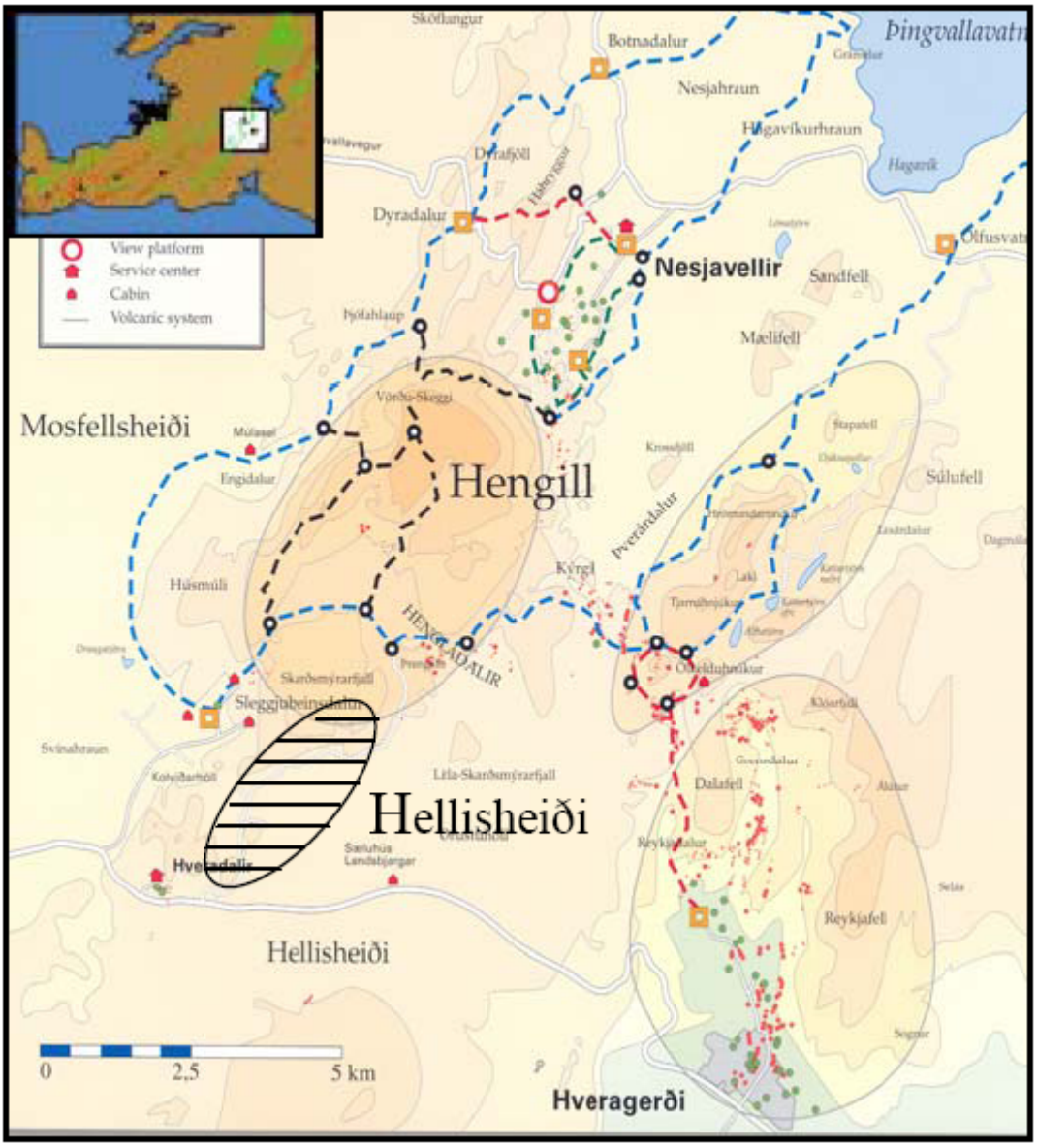

FIGURE 7: Location map of the study areas
(modified from Gislason and Gunnlaugsson, 2003)

3.2 Geology of the Hengill area

The Hengill area, east of Reykjavik, is one of the largest high-temperature areas in Iceland, extending over some 100-110 km². The geothermal activity is believed to be connected to three volcanic systems. The geothermal area in Reykjadalur and Hveragerdi belongs to the oldest system, called the Grensdalur system. Northwest of this is another volcanic system named after Mt. Hrómundartindur, with the last eruption taking place about 10,000 years ago. The geothermal area at Ölkelduháls is connected to this volcanic system. West of these two volcanic systems lies the Hengill volcanic system, with active tectonic and volcanic NE-SW fractures and faults extending from Lake Thingvallavatn to Nesjavellir and further to the southwest through Innstidalur, Kolvidarhóll, Hveradalur (hot spring valley) and Hellisheidi (Saemundsson 1979). A geological map of the southern part of Hengill volcano, in which the Hellisheidi project lies, is shown in Figure 8.

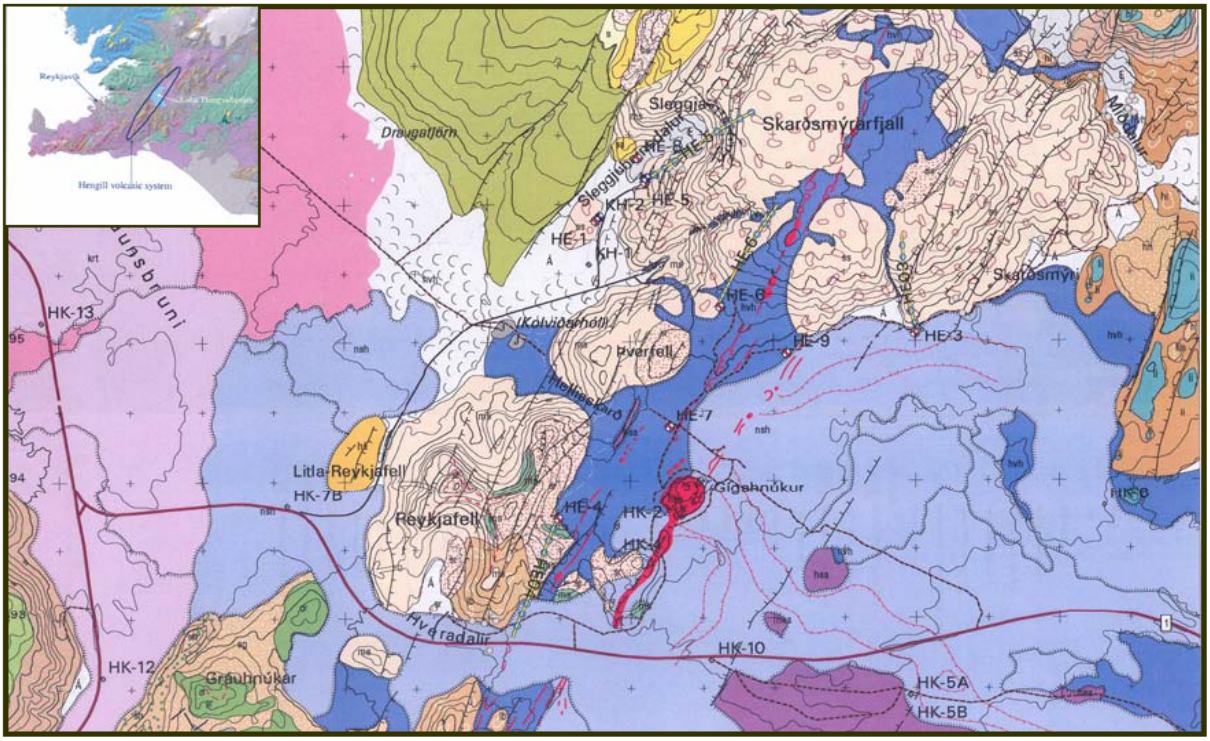

FIGURE 8: Geological map of Hellisheidi area (Saemundsson, 1995), the part shown extends over an area of approx. 9 km × 6 km; wells marked with HE are recently drilled high-temperature wells in the Hellisheidi field (Hartanto, 2005)

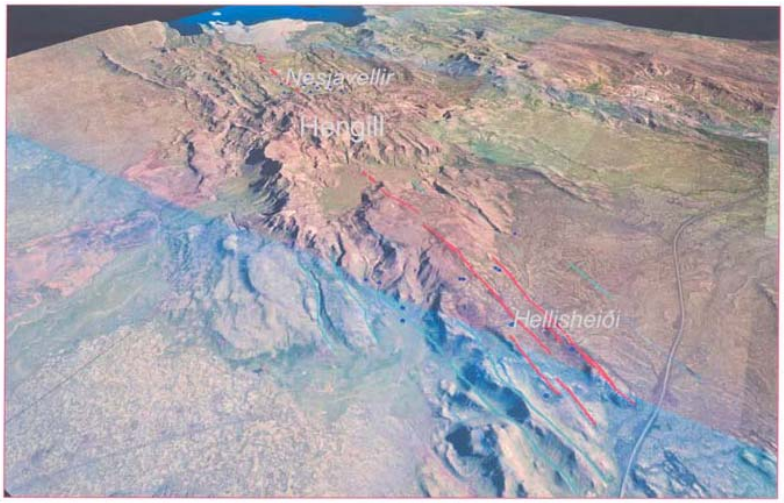

FIGURE 9: Volcanic systems of the Hengill high-temperature area, shown by shaded regions (Gunnlausson and Gislason, 2005)

A tensional stress system has developed in the zone of the active Hengill volcanic system. The tensional stress has opened northeast trending vertical fractures, faulting, graben and geothermal systems that occur along the fissure swarm, which provide highly permeable conditions for fluid flow (Bjornsson et al., 1986), as shown in Figure 9. The fracture network is periodically activated, providing conduits for the episodic eruption of basalt and the intrusion of dikes. Magma moves into the shallow crust at temperatures of the order of 1200°C and supplies heat to the hydrothermal system (Bodvarsson et al., 1990). On the surface the Hengill area is almost entirely built up by volcanic rocks of late Quaternary and Holocene age (Arnason et al., 1967). The rocks are mostly subaerial basaltic flows and hyaloclastites but small amounts of rocks of intermediate and rhyolitic composition occur as well.

The Hengill Mountain itself was mostly built-up in one or two large subglacial eruptions during the last glacial period. New geological data presented in 2002 suggest that the lower part of the mountain may have formed during the 2nd last glacial period (Fridleifsson et al., 2003). The geology of the

Hellisheidi geothermal field is characterized by the presence of two kinds of common hyaloclastite formations and basaltic fissure lavas produced in an active fissure swarm.

Hyaloclastite formations: Subglacial fissure eruptions produce elongated ridges that are 1-5 km wide, up to tens of kilometres long, and a few hundred metres thick. The cores of these ridges consist of permeable pillow lavas, but the flanking hyaloclastite deposits can serve as aquitards. Thus subglacial eruptions are remarkable in that they are able to create both the geothermal reservoir rocks and the caprock in one volcano (Wohltz and Heiken, 1992). Commonly, hyaloclastite formations in Iceland are created by the effect of volcanism under glaciers. The sequence of formation is shown in Figure 10. The most recent volcanism of this type was in Bárdarbunga 1996 in the glacier Vatnajökull, but the most famous episode was formed at the seafloor south of Iceland in 1963-1967, and formed the island Surtsey which belongs to the Vestmannaeyjar archipelago. The morphological structure is named móberg (in Icelandic) or hyaloclastite, and the formation, table mountain (Figure 10). Hyaloclastite formations characterize the environment in the Hengill region and form mountains like Mt. Skardsmýrarfjall, Mt. Reykjafell and Mt. Hengill.

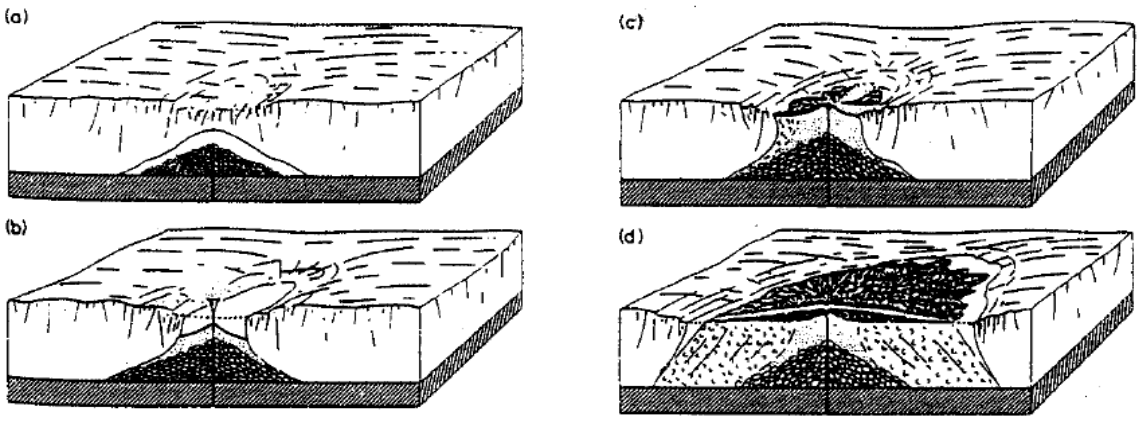

FIGURE 10: Growth of a subglacial, monogenetic volcano; a) a pile of pillow lava forms deep in melt water lake; b) slumping on the flanks of the pillow lava pile produces pillow lava breccia; c) hyaloclastite tuffs are erupted under the shallow water, d) a lava cap propagates across its delta of foreset breccia (Jones, 1969; Saemundsson, 1979)

The fissure swarm: There are two main volcanic fissure-swarms of Holocene age trending NE-SW in the Hengill area that have fed the last volcanic eruptions in the area, extending from Lake Thingvallavatn in the northeast part of the Hengill area (Nesjavellir high-temperature field) to about 20 km southwest of the Hengill mountain (Hellisheidi). The age of the older one is about 5500 years and the younger one is about 2000 years old (Saemundsson, 1967). Lava flows from the fissure swarms are widespread and cover a large part of Hellisheidi. These eruptive fissures and parallel faults are believed to control up- and out-flow of hot water and steam from the centre of the Hengill system. Tectonic activity is episodic and accompanied by rifting and major faulting along the fissure swarm that intersects the Hengill central volcano and magma is injected into the fissure swarm.

3.3 Geophysical surveys of the Hengill area

Extensive resistivity surveys have been conducted in the Hengill region, including the Hellisheidi geothermal field, including Schlumberger and TEM resistivity measurements (Bjornsson et al., 1986; Arnason and Magnússon, 2001). Aeromagnetic and gravity surveys have furthermore been done in the Hengill geothermal area, including Hellisheidi (Bjornsson et al., 1986). The DC resistivity surveys delineated 110 km^2 low-resistivity area at 200 m b.s.l., and the magnetic survey showed a negative and transverse magnetic anomaly coherent with the most thermally active grounds. Transient electro-magnetic soundings (TEM) revised the resistivity map (Figure 11).

The electrical resistivity also provides information on the degree of alteration and therefore hydrothermal activity, including both fossil and recent alteration. A low-resistivity area covering 110 km^2, measured at a depth of 400 m, indicates roughly the extent of the high-temperature fields. All surface manifestations, like fumaroles and altered ground, are within this area (Hersir et al., 1990). The main resistivity feature is a high-resistivity zone (50-500 Ωm) which is observed beneath the low-resistivity layer.

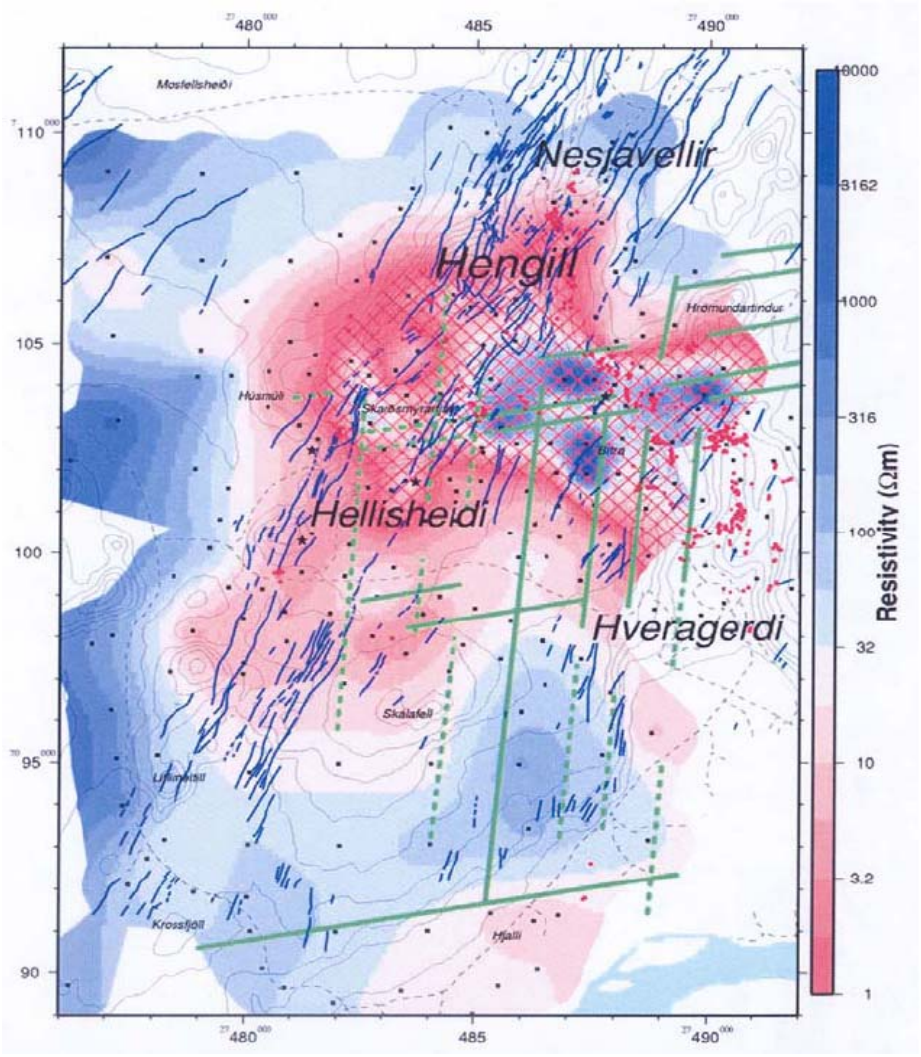

FIGURE 11: Hengill area, resistivity at 100 m b.s.l. according to a recent TEM survey, also showing faults (Arnason and Magnússon, 2001)

A correlation between resistivity, rock temperature and alteration at Nesjavellir (northeast of Hellisheidi) shows high-resistivity values close to the surface which can be attributed to fresh unaltered rocks. The low-resistivity values (1-5 Ωm) are connected with the smectite-zeolite alteration belt at temperatures between 50 and 200°C. But below the low resistivity there is the high-resistivity core or layer, mentioned above, associated with a high-temperature alteration zone. This high-resistivity core is related to the chlorite–epidote zone, located under a chlorite zone, indicating temperatures of more than 240°C (Arnason et al., 2000).

3.4 Conceptual model of the geothermal systems

The Hengill volcanic system lies on the boundary between the North American and European plates. The 2 cm/year rifting of the two plates activates a NNE trending system of normal faults and frequent magma intrusions. The rift zone is permeable, with numerous fumaroles and hot springs on the surface. This system is currently active, whereas its predecessor, the Hveragerdi system, is volcanically extinct but still hosting geothermal resources. Geology, geo-physics, and drilling indicate a total resource area of around 110 km^2 (Gunnlaugsson and Gislason, 2005). In a paper published by Bjornsson et al. (2006) a conceptual model of the Hengill geothermal systems was presented.

Figure 12 presents measured temperatures at 650 m below sea level in the Hengill area. One dominant feature is the elongated temperature high (>240 °C) between the Hellisheidi and Nesjavellir fields. A common upflow zone for both fields has been suggested near the Hengill summit.

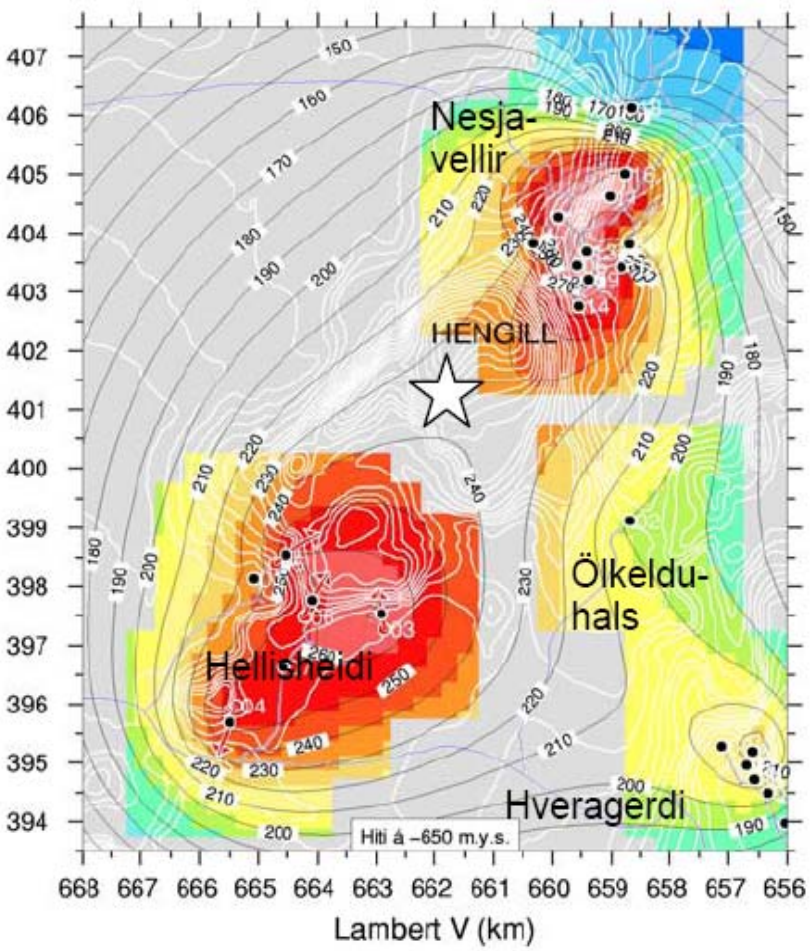

FIGURE 12: Temperature (°C) at 650 m b.s.l in Hengill. Star shows upflow zone for Hellisheiði and Nesjvallir; black dots are wells (Bjornsson et al. 2006)

Figure 13 presents a temperature cross-section drawn between the Hellisheidi and Nesjavellir subfields of the Hengill geothermal system that also demonstrates the main features of the present conceptual model of the whole Hengill system. An up-flow zone of hot fluid is assumed to reside beneath the summit of the Hengill volcano. The ascending fluid is then believed to flow diagonally or laterally into both the Nesjavellir and the Hellisheidi fields. A gradual rise in temperature is observed with depth in Nesjavellir, whereas a temperature reversal with depth is observed in the Hellisheidi field, a reversal explained by a lateral, cooler fluid recharge from the south. A partial driving force for the deep recharge is presumed to be a pressure low within the high-enthalpy up-flow zone, at >2 km

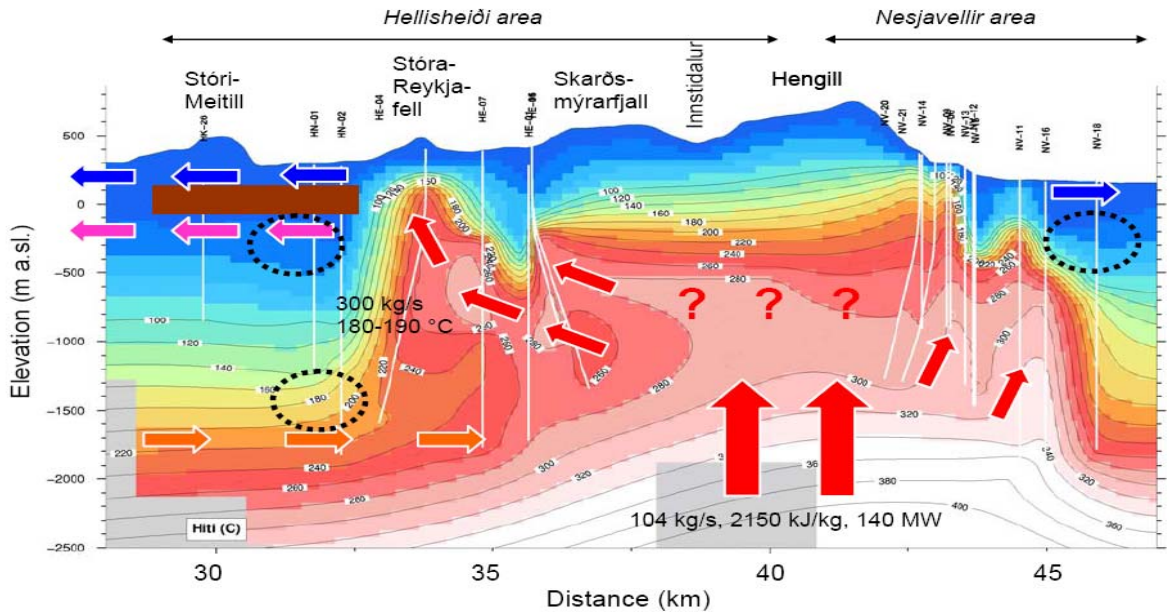

FIGURE 13: S-N temperature cross-section between Hellisheidi and Nesjavellir. Arrows denote direction of flow. Cross-section location is from lower left to upper right corner of Figure 11. Arrows denote direction of proposal flow. Ellipses show re-injection sites (Bjornsson et al. 2006)

depth (Bjornsson et al. 2006). Cold groundwater reservoirs are fed by rain and snowfall on the Hengill topographic high. These discharge tens of cubic meters of cold water into Thingvallavatn Lake in the north and to the coastline in the south. Drilling of re-injection wells south of Hellisheidi has identified a stratified warm outflow zone, most likely resulting from mixing of deep and shallow fluids (Bjornsson et al. 2006). Re-injection from the Hellisheidi Power Plant will take place within this zone and also at greater depths within the active rift zone. The Nesjavellir plant reinjects separated fluids at intermediate depths, but not into the deep resource (Bjornsson et al. 2006).

Geodetic surveys confirmed up to 2 cm/year vertical crustal movements that have been attributed to a minor inflation of a magma chamber in the Ölkelduhals area (Sigmundsson et al., 1997; Feigl et al., 2000). Altogether, the geological and geophysical data discussed above, as well as these seismic data, point towards a highly dynamic large scale geothermal resource.

4. TEMPERATURE AND PRESSURE CONDITIONS

4.1 Logging equipment

There is a great variety of logging tools presently in use for logging of geothermal wells (Stefansson and Steingrimsson, 1990; Stevens, 2000; Grant et al., 1982). In general all logging equipment consists of three parts: a down-hole sonde, a transmission line and a registration unit. Such units vary in sophistication. A down-hole sonde can range from one resistor to a very complicated electronic instrument, and the registration unit can be range from a simple notebook and pencil to a modern day computer. The transmission line is usually a logging cable, a cable with one, four or seven conductors with the supporting unit, which also acts as armour, wound on the outside of the conductors. At the lower end of the cable is the cable head through which different sondes can be connected to the cable. At the surface, the logging cable is connected to a slip ring which makes it possible to get continuous registration while the cable drum rotates and the sonde is moving in the well.

Temperature and pressure logs are the most important in geothermal system as either from the temperature logs the following information can be obtained:

- Temperature gradient (heat flow)
- Location of aquifers
- Formation or fluid temperature
- Physical conditions of the reservoir (boiling/liquid/steam)
- Temperature distribution in the reservoir
- Temporal variations (monitoring and management of geothermal reservoirs)

Or from pressure logs:

- Fluid density
- Physical conditions of the reservoir (boiling/liquid/steam)
- Fluid flow directions
- Permeability (transmissivity), barriers, flow paths
- Pressure distribution
- Variations in time (monitoring and management of geothermal reservoirs)

The main problem with downhole measurements during disturbed conditions is that temperature and pressure in the wellbore do not match those in the reservoir (Stefansson and Steingrimsson, 1990).

Resistivity thermometers are the temperature sensors most frequently used in well logging today. They have the advantage of small size and ease of transmission from the measuring point to a surface recorder. This is generally done through an electrical cable, and the measuring value is obtained either directly by a simple resistivity measurement, or indirectly by connecting the sensor to a resonant circuit. The data information is then fed through the cable as a pulsed signal where the temperature is given by the frequency of the pulses. Pulsed logging is far less sensitive to electrical leaks in cable and cable-head than DC measurements (Stefansson and Steingrimsson, 1990). It is also not affected by the changing resistivity of the cable due to temperature variations. It's the same principle for the pressure sensor.

Mechanical thermometers are also used, mainly in high temperature wells. The data are not transmitted to the surface, but recorded inside the temperature probe on a clock-driven recorder. Several measuring points (20-30) can be recorded during one run. Electrical memory tools are more accurate measure continuously.

As in the temperature gauge the pressure is recorded on a clock-driven recorder inside the measuring probe. The accuracy of the pressure gauges is ± 0.1-1 bar and like the temperature gauge it needs to be recalibrated regularly.

4.2 Well HE-06

4.2.1 General information

Well HE-06 was completed in October 2002. It was drilled to a depth of 2001 m and the casing program of the well is as shown in Figure 14. It is located at co-ordinates X=384632; Y=395257; Z=420 m above sea level.

4.2.2 Interpretation of temperature and pressure logs

In temperature logs during injection, such as during drilling, fluid loss through feed-zones is seen as a slight change in the gradient of the temperature profiles, whereas fluid gain is reflected by a discontinuous jump in temperature (Stefansson and Steingrimsson, 1990).

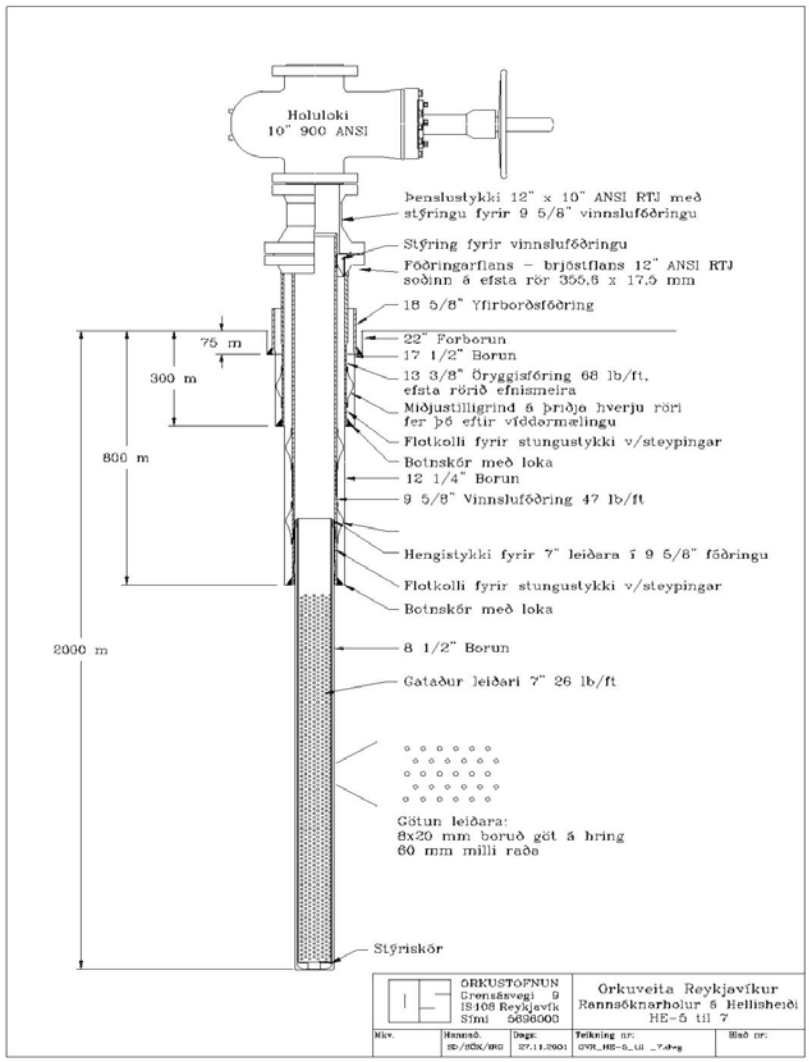

FIGURE 14: Design of well HE-06 in the Heillisheidi field including casing program (Jonsson et al., 2002)

Temperature and pressure logs were measured in HE-06 during drilling, during injection testing, and after completion (during warm-up and discharge testing) (Figure 15). These data were analyzed to estimate the formation temperature and pressure and the location of possible aquifers. Selected logs were also used to simulate the flow pattern of the well. Figure 15 shows down-hole temperatures profiles of the well at different times and conditions.

Some feed zones can be detected. The ones above 770 m are cased off and therefore do not flow into the well. Two main feed zones at 960m and 1250m are evident from the latest temperature monitoring profiles (2004-06-21 and 2006-02-17). Some smaller feed zones are inferred by the injection profiles, (2002-08-03 and 2002-08-05) like at 850, 1500, 1650 and 1990 m depth. The temperature and pressure logs in Figure 12 and 13 show that the boiling level during discharge was at about 1000m depth.

The estimated formation temperature, shown as a black dashed curve (Figure 15), was determined by interpreting the different temperatures profiles during warm-up and monitoring periods. When there is no flow between aquifers, the temperature in the well will usually reach equilibrium with the surrounding rock. However, processes like boiling, accompanied by one-dimensional convection, can disturb the temperature profile in a well. All high-temperature wells tap reservoirs of greater

temperatures than 200°C. Boiling and steam accumulation will, therefore, always be present in these wells during discharge at atmospheric pressure and sometimes even when they are closed. Temperature and pressure profiles measured during warm-up shows a water table at about 240m depth. The reservoir temperature around well HE-06 is about 260°C.

The representative reservoir pressure depth relation is most easily determined by looking at pressure profiles that are regularly measured during the warm-up of a well (Figure 16). These pressure profiles will pivot about a single point at which the pressure is held constant because of the connection of the well to the reservoir (this is because the reservoir controls the pressure in the well at this depth). In a single feed-zone (fracture) well, the feed-zone depth and the pivot point depth will be the same. If the

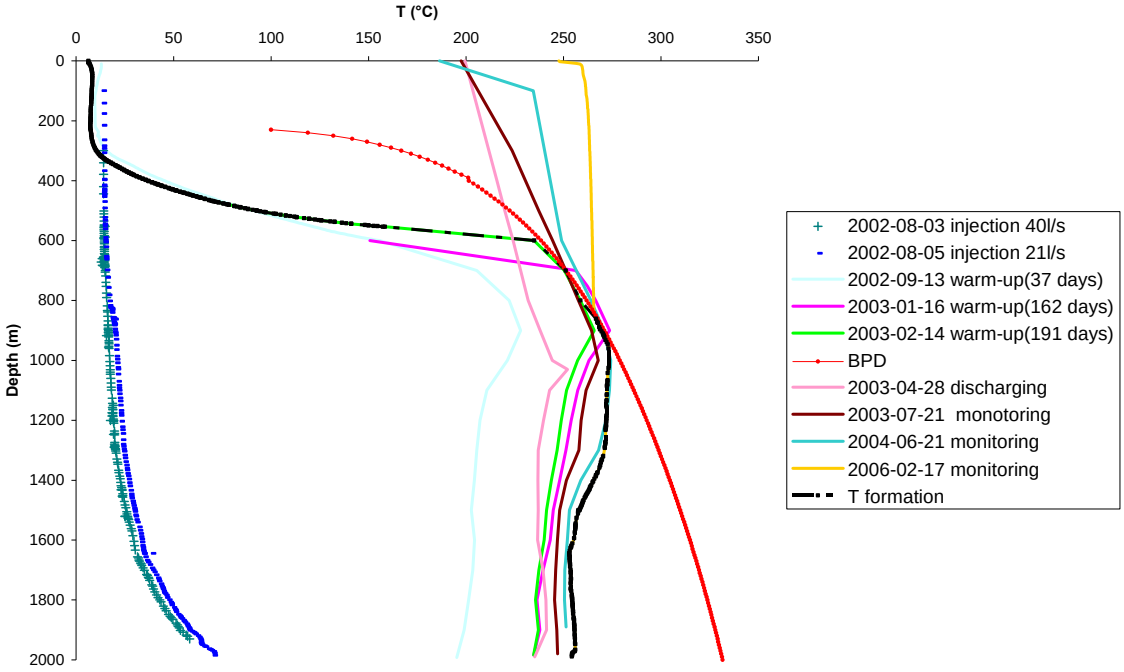

FIGURE 15: Injection, warm-up, and dynamic temperature profiles for well HE-06

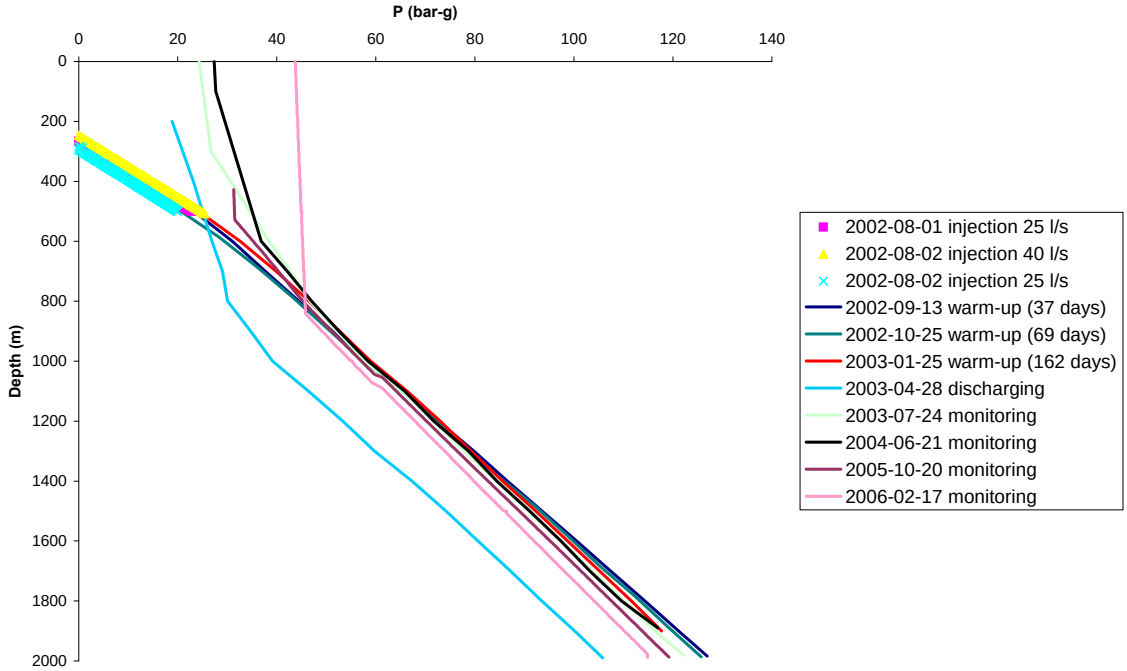

FIGURE 16: Injection, warm-up, and dynamic pressure profiles for well HE-06

well has multiple feed-zones (fractures), the pivot point will be somewhere in-between the top and bottom feed-zone, but its exact location will depend on how well each feed-zone is connected (depends on permeability of feed-zone) to the reservoir. Figure 16 demonstrates that the pivot point is around 1400m depth in well HE-06, with 85 bar-g pressure, as all the pressure profiles measured during the warm-up period intersect at this point.

4.3 Well HE-20

4.3.1 General information

Well HE-20 was completed in December 2005. It was drilled to a depth of 2002m. The casing program for the well is shown in Figure 17. It is located at co-ordinates X=396972.7; Y=390742.5; Z=350m above sea level.

4.3.2 Interpretation of temperature and pressure logs

Figures 18 and 19 present temperature- and pressure logs measured in well HE-20 during injection testing, warm-up and later discharge testing (or dynamic). Temperature and pressure measured during the warm-up period indicate a water table around 300 m depth.

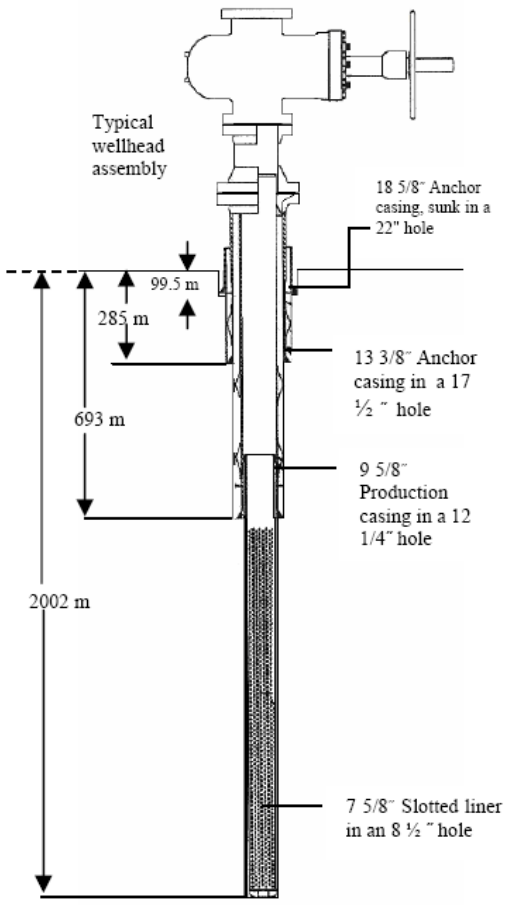

FIGURE 17: Design of well HE-20 in the Hellisheidi field including casing program (Mortensen et al., 2006)

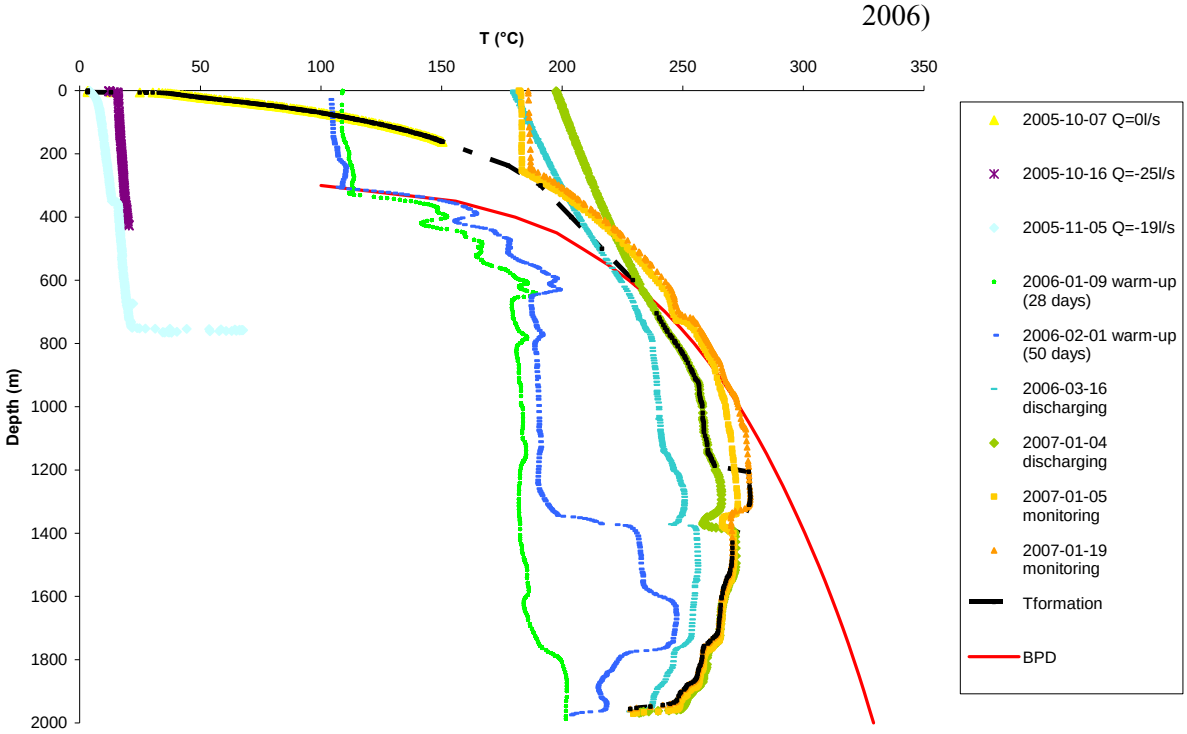

FIGURE 18: Injection, warm-up, and dynamic temperature profiles for well HE-20

The main feed zones of well HE-20 are located around 800, 1375 and 1600 m depth (Figure 18). From both the temperature and pressure profiles during the discharge period, the boiling level appears to be at about 800 m depth.

The pressure pivot point is located between 1400 and 1600 m depth according to the warm-up pressure profiles (Figure 19) and the reservoir pressure at the pivot point is close to 86 bar-g.

According to the temperature logs, the reservoir temperature around well HE-20 is between 250 and 260°C.

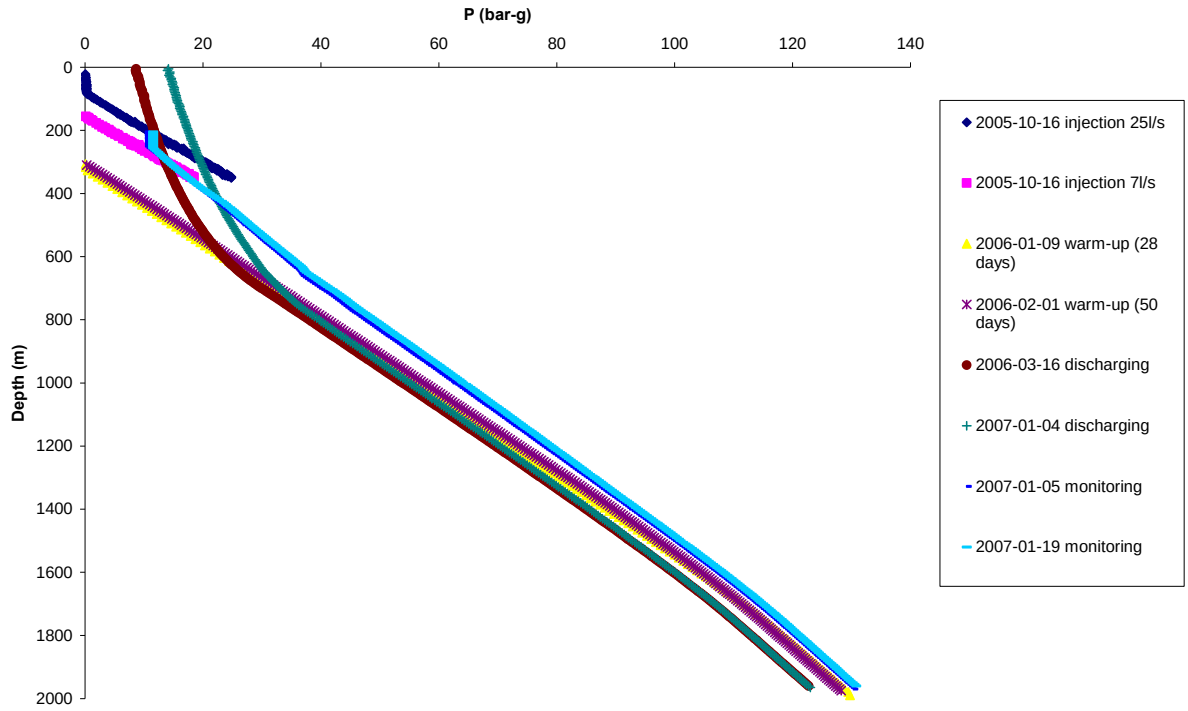

FIGURE 19: Injection, warm-up, and dynamic pressure profiles for well HE-20

5. INJECTION TEST DATA AND INTERPRETATION

5.1 Well HE-06

5.1.1 Multirate injection test

A three-rate step injection test was conducted on 2002-08-07 lasting about 8 hours. The pressure gauge used to monitor the pressure changes in the well was installed at 1400 m depth. The three step injection rates were 35, 50 and 21 l/s, respectively (Figure 20).

The pressure response curves of the three injection steps are presented on a semi-log graph in Figure 21 and a log-log graph in Figure 22. Notice that the effect of the capacity of the borehole is not significant; it appears to be over after a very short period, less than five minutes (Figure 22). There are not fracture effects (no a straight line pressure response with either slope ¼ or ½ at an early time on log $(\Delta P/\Delta Q)$ vs. log (Δt) graph in Figure 22). A short wellbore storage period indicates good hydrodynamic characteristics of the reservoir near the wellbore. The log-log plot for the second step shows a constant pressure boundary effect.

ΔQ is the flow difference between to consecutives flow step rates.

Assuming a reservoir temperature of 260°C the following values for the dynamic viscosity and fluid density were selected for the data interpretation:

$\mu = 1.02\ 10^{-4}$ Pa s $\qquad\qquad$ $\rho = 785$ kg/m^3

In addition a value of $C_w = 1.7\ 10^{-9}$ Pa^{-1} for the compressibility of water at 260°C was used and a typical value for the compressibility of basaltic rock, $C_r = 2\ 10^{-11}$ Pa^{-1}. A porosity φ of 0.14 (Franzson et al., 2001) was used to calculate the skin effect and the total compressibility C_t.

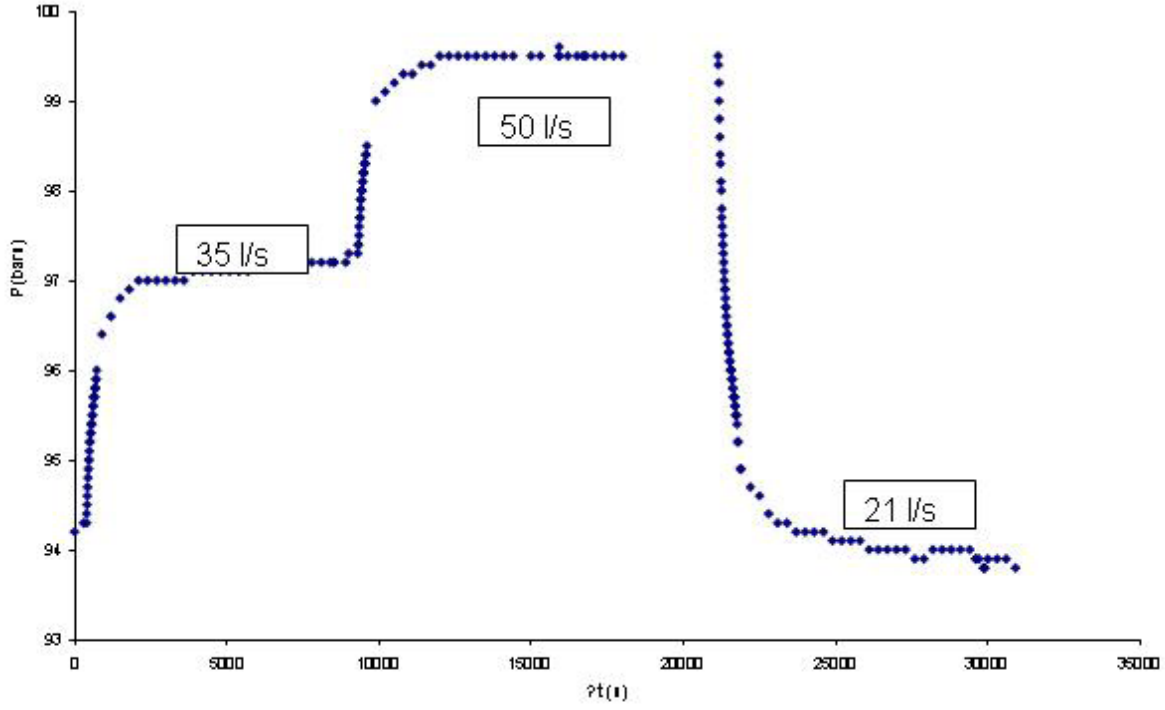

FIGURE 20: Pressures changes at 1400 m depth in well HE-06
during injection testing of the well on 2002-08-07

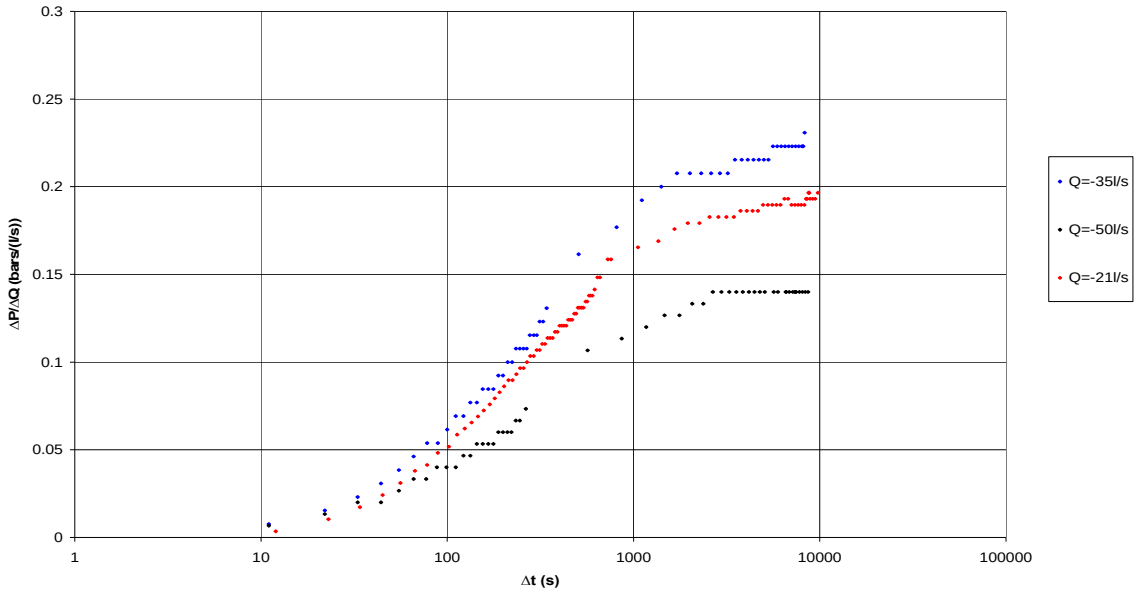

FIGURE 21: Semilog graph of the data in Figure 20. The figure shows the ratio between the pressure changes in each step, ΔP, versus the flow-rate change in the step, ΔQ

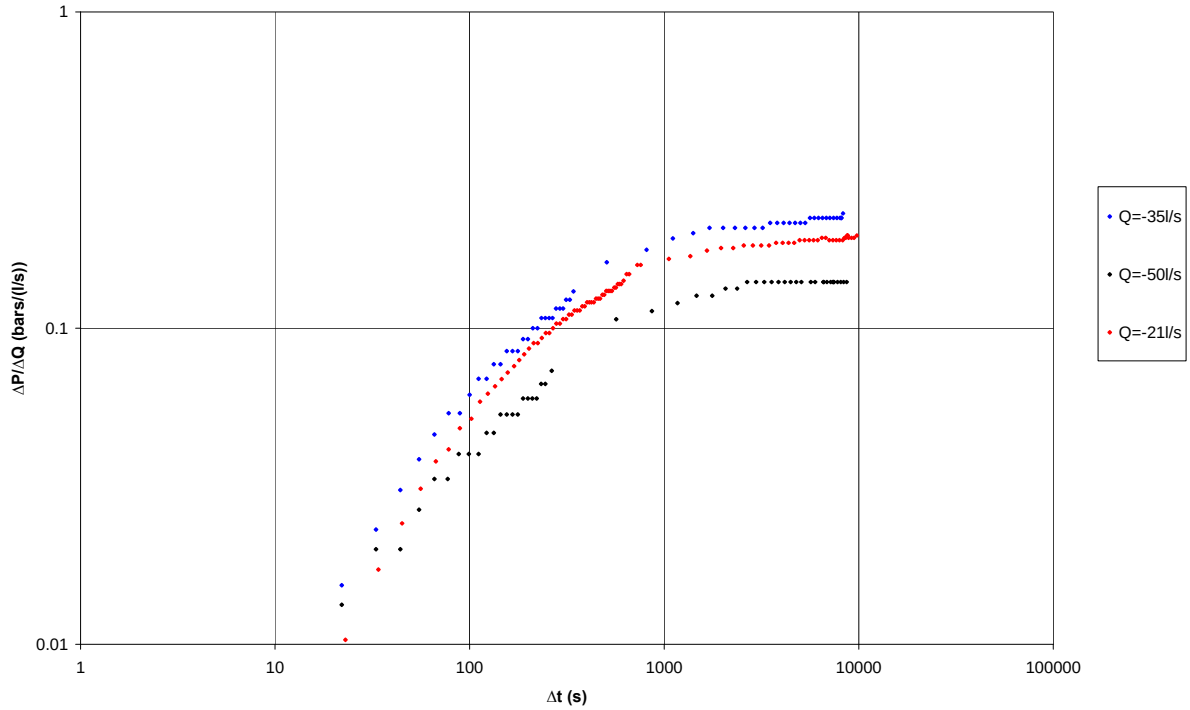

FIGURE 22: Log-log graph of the data in Figure 20. The figure shows the ratio between the pressure changes in each step, ΔP, versus the flow-rate change in the step, ΔQ

The results of interpretation of the HE-6 injection tests (shown in Figure 20) with the semi-log method are presented in Table 1.

TABLE 1: Results of semi-log analysis of 07.08.2002 injection test data from well HE-06

	***q* (l/s)**	**Δq (l/s)**	***m* (bars/(l/s)/log-cycle)**	***kh* (Dm)**	**Skin**
Step1	21 -> 35	14	0.027	7	3.5
Step2	35 -> 50	15	0.02	9.3	2
Step3	50 -> 21	29	0.02	9.3	4.8

According to these results, the permeability-thickness is estimated to be approximately 8.53 Dm. As it doesn't vary much for the different steps, this estimate is considered reliable.

The skin factor for well HE-06 is positive (3.4). It describes an additional pressure change in the near vicinity of the well due to different near-well permeability, during production or injection. The positive factor obtained indicates that the well is not in good communication with the reservoir.

5.1.2 WellTester numerical software modelling

WellTester is computer software that was developed at Iceland GeoSurvey (ÍSOR) to handle data manipulation and analysis of well test data (mainly multi-step injection or production tests). The goal of the WellTester development was to make user friendly software that could speed up the process of analyzing and reporting the results from a given well test. To this end the process was divided into five (or in some cases six) simple steps that range from setting initial conditions to modelling and giving a final report (Juliusson et al., 2007).

The derivative is commonly used to determine the most appropriate type of boundary (Appendix I).

Modelling step 1 for HE-06
According to derivative plot on the right plot in Figure 24 and comparing the trend of the different boundaries case in Appendix I, the well test model selected for step 1 is summarized in Table 2.

TABLE 2: Summary of model selected for step 1 of HE-06 injection testing

Well testing model - Step 1	
Reservoir	Homogeneous
Boundary	No-flow
Well	Constant skin
Wellbore	Wellbore storage

Using this model, nonlinear regression analysis was performed to find the parameters that best fit the data gathered. The results from the regression analysis are shown graphically in Figure 23 and 24.

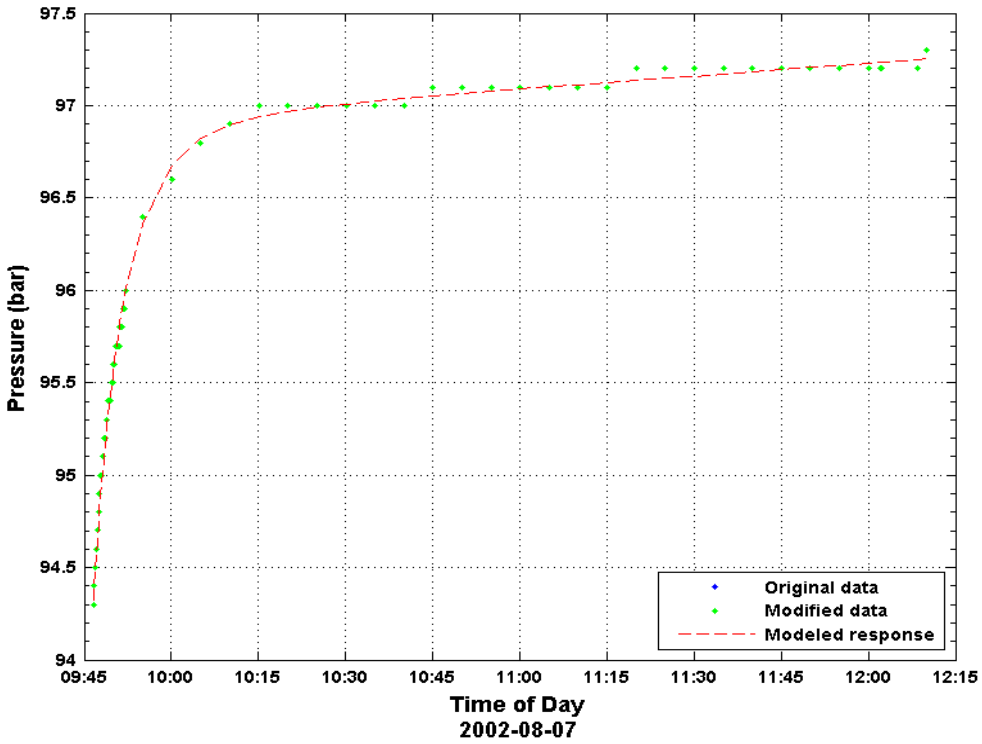

FIGURE 23: Fit between model and collected data for step 1for well HE-06 on 07.08.2002

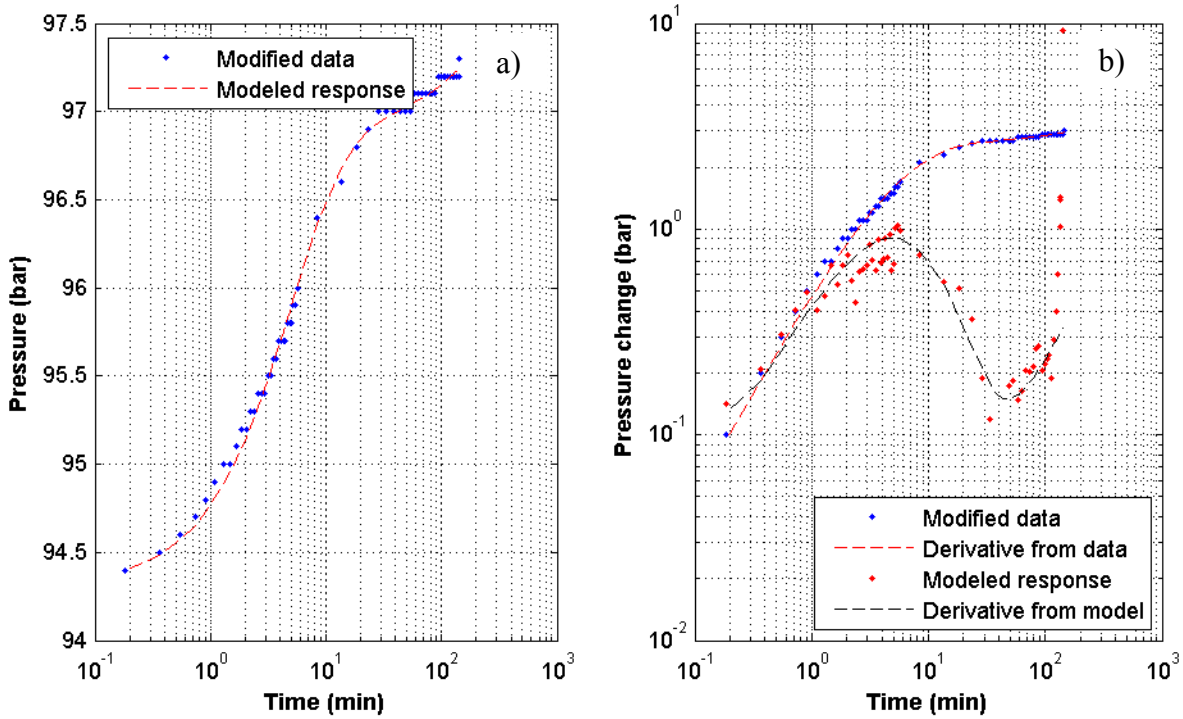

FIGURE 24: Fit between model and selected data: a) on log-linear scale and b) log-log scale

Modelling step 2 for HE-06
The well test model selected for step 2 is summarized in Table 3.

TABLE 3: Summary of model selected for step 2 of HE-06 injection test

Well testing model - Step 2	
Reservoir	Homogeneous
Boundary	Constant pressure
Well	Constant skin
Wellbore	Wellbore storage

The results from the regression analysis are shown graphically in Figure 25.

Figure 26 shows additional plots of the same data on a log-linear scale (left) and log-log scale (right).

Modelling step 3 for HE-06
The well test model selected for step 3 is summarized in Table 4.

TABLE 4: Summary of model selected for step 3 in HE-06 injection testing

Well testing model - Step 3	
Reservoir	Homogeneous
Boundary	Constant pressure
Well	Constant skin
Wellbore	Wellbore storage

The results from the regression analysis are shown graphically in Figure 27.

Figure 28 shows additional plots of the same data on a log-linear scale (left) and log-log scale (right).

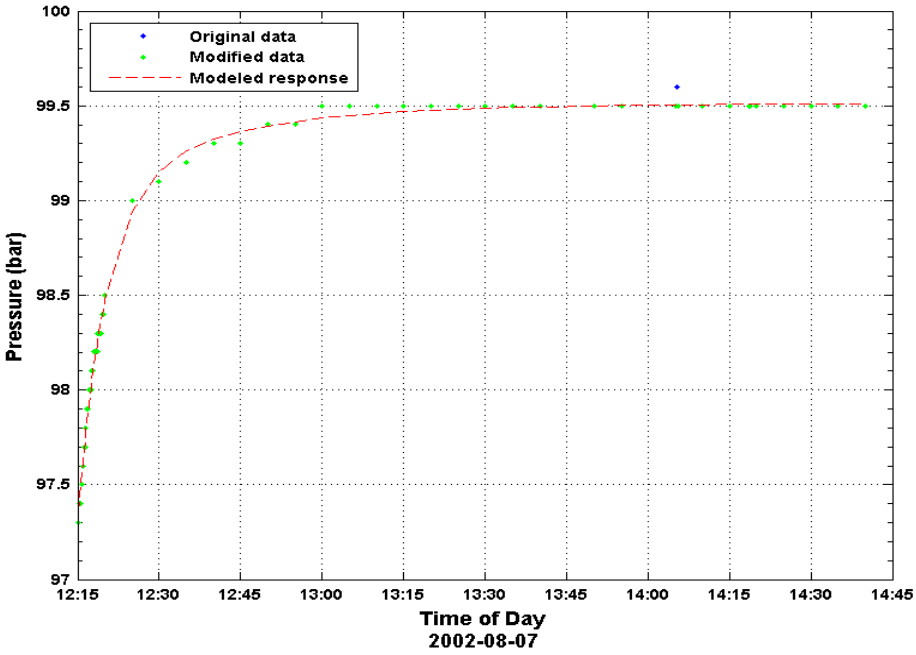

FIGURE 25: Fit between model and collected data for step 2 for well HE-06 at 07.08.2002

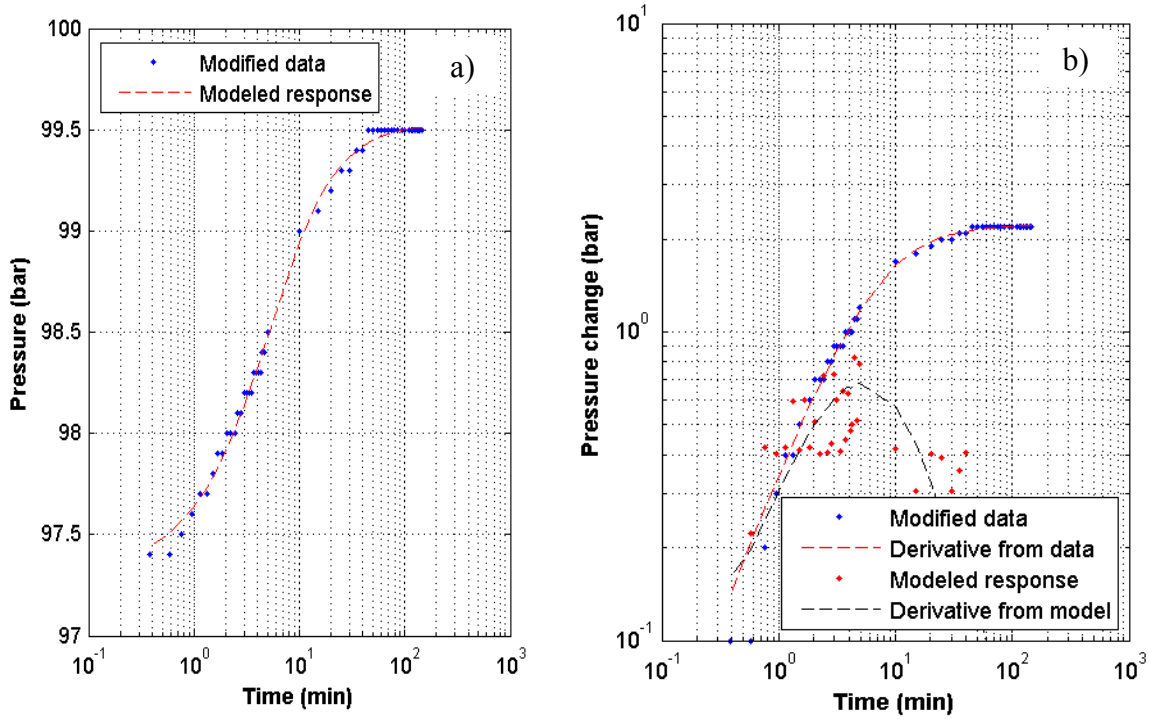

FIGURE 26: Fit between model and selected data: a) on log-linear scale and b) log-log scale

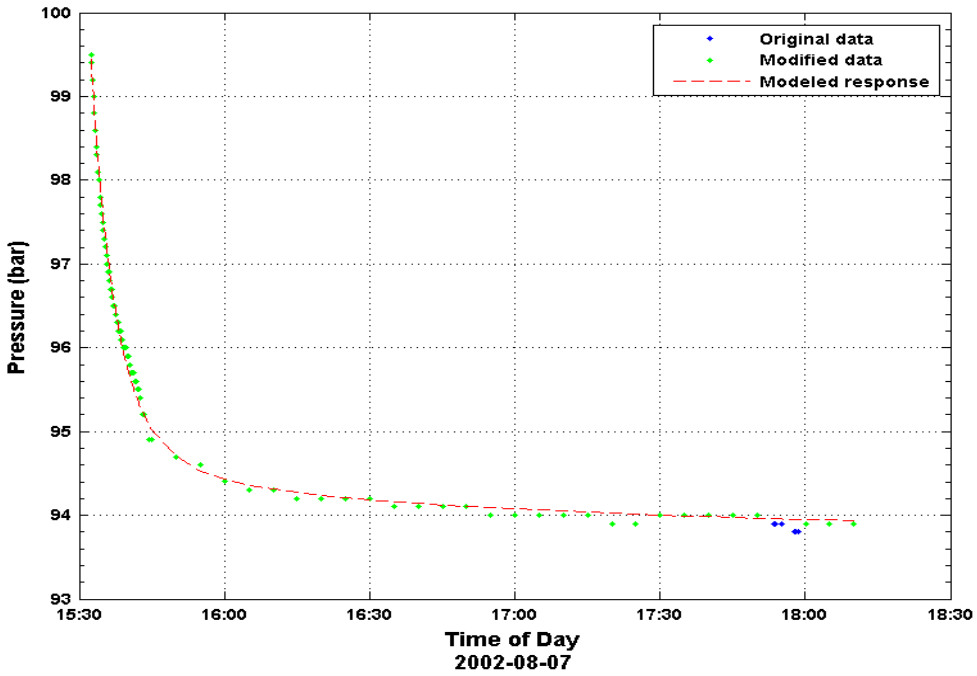

FIGURE 27: Fit between model and collected data for step nr. 3 for well HE-06 at 07.08.2002

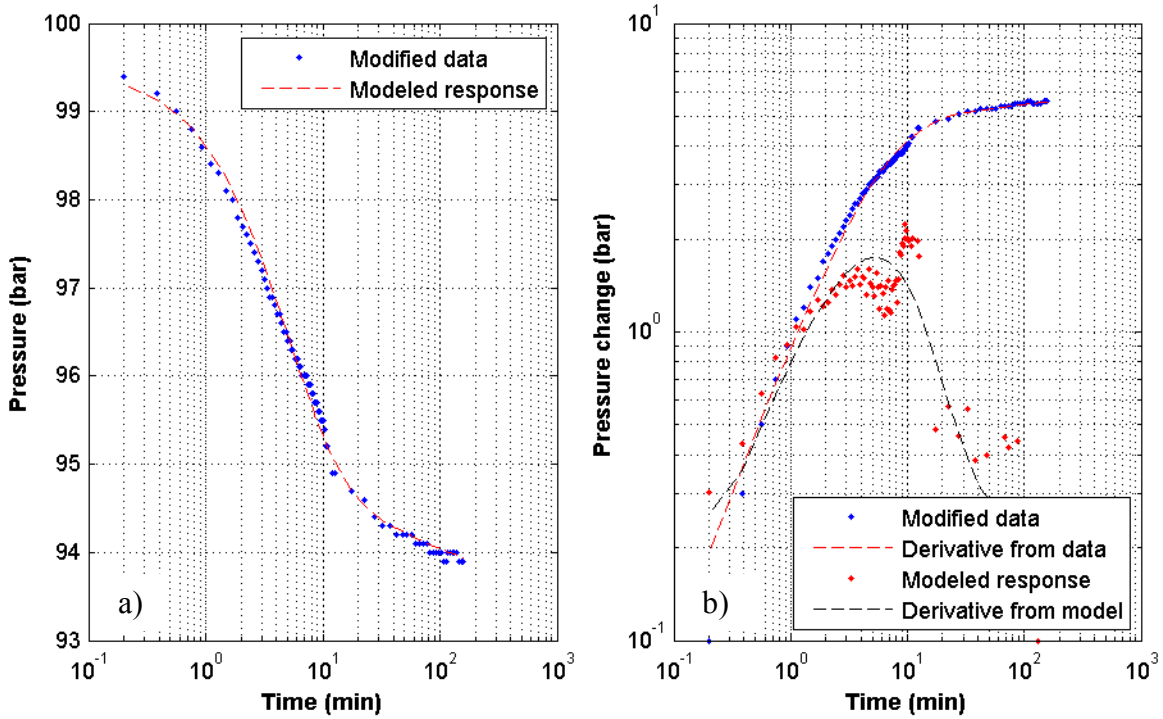

FIGURE 28: Fit between model and selected data: a) on log-linear scale and b) log-log scale

Modelling all steps for HE-06
The well test model selected for modelling all steps at once is listed in Table 5.

TABLE 5: Summary of model selected for all steps at once in HE-06 injection testing

Well testing model - All Steps	
Reservoir	Homogeneous
Boundary	Constant pressure
Well	Constant skin
Wellbore	Wellbore storage

The resulting fit is shown graphically in Figure 29.

The parameter estimates obtained on basis of different steps and models selected (Table 2, 3, 4 and 5) are presented in Table 6.

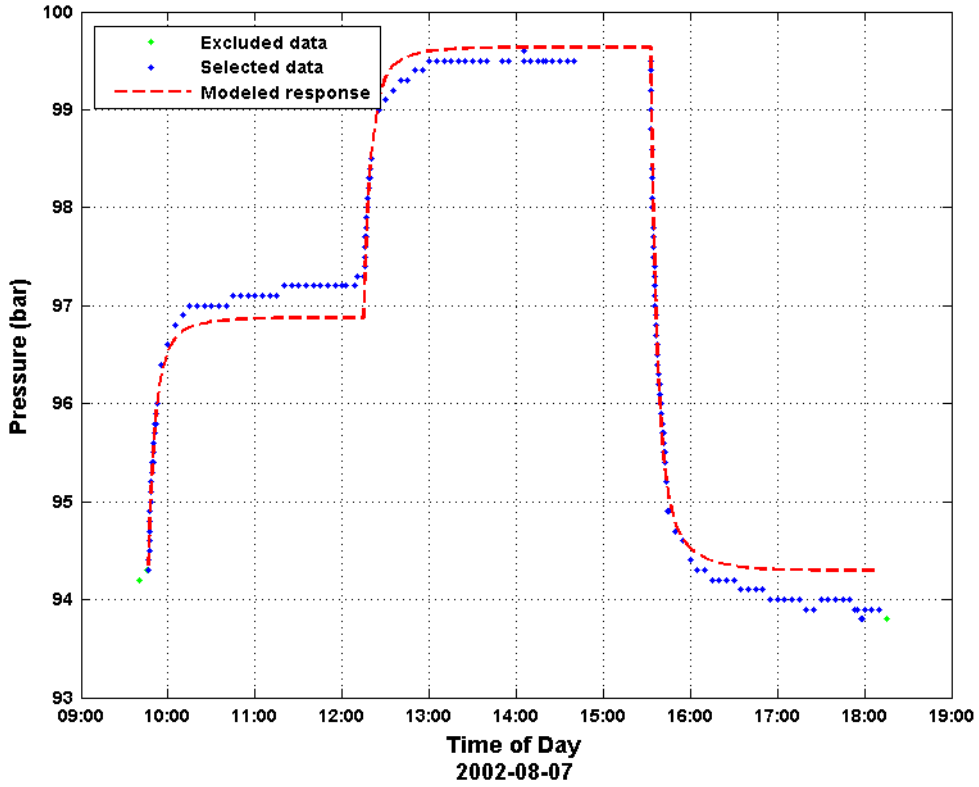

FIGURE 29: Fit between model and collected data for all steps for well HE-06 at 07.08.2002

TABLE 6: Summary of results from nonlinear regression parameter estimate using injection test data from well HE-06 from 07-08-2002

	Transmissivity (m^3/(Pa·s))	**Storage coefficient (m^3/(Pa·m^2))**	***kh*** **(Dm)**	**Skin**	**Injectivity index** ((L/s)/bar)
Step 1	$1.11 \cdot 10^{-7}$	$4.73 \cdot 10^{-8}$	11.2	6.39	4.74
Step 2	$1.07 \cdot 10^{-7}$	$1.81 \cdot 10^{-8}$	10.8	2.00	6.79
Step 3	$1.06 \cdot 10^{-7}$	$6.08 \cdot 10^{-8}$	10.7	5.09	5.21
All steps	$1.06 \cdot 10^{-7}$	$2.31 \cdot 10^{-8}$	10.7	4.67	5.58

Permeability, permeability-thickness and transmissivity can vary by several orders of magnitude in geothermal systems. The permeability-thickness kh value estimate is around 11 Dm. This value is close to the results of the semi-log analysis.

The skin factor obtained by WellTester modelling is positive (4.67) and the same order of magnitude of the one obtained from the semi-log analysis (3.4).

Here the average injectivity index based on pressure changes measured at 1400 m is around 5.58 (l/s)/bar. This value will be compared with productivity index estimates for the same well in chapter 6.1.

5.2 Well HE-20

5.2.1 Multirate injection tests

The two-rate step injection test was made at 2002-12-10 during three and half hours. The pressure gauge was installed at 1350 m depth. The two step injection rate was respectively 40 and 50 l/s (Figure 30).

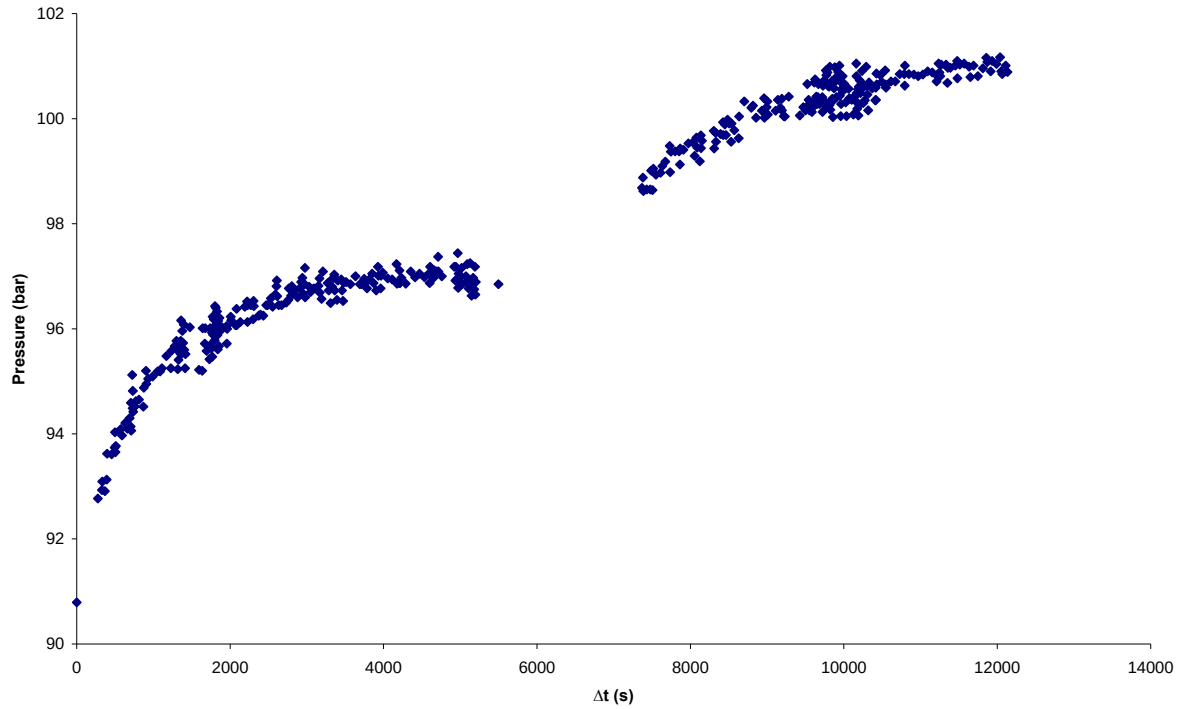

FIGURE 30: Pressures changes at 1350 m depth in well HE-20 during injection testing of the well on 2002-12-10

The curves of two-rate step injection test are presented on a semilog graph in Figure 31.

Notice that the effect of the capacity of the borehole is almost unimportant or seem to be over at very short period, less than three minutes (Figure 32) and there is no effect of fractures seen.

Considering a temperature reservoir (260°C) of the fluid in the reservoir, the following values for the dynamic viscosity and the density of fluid were selected for the interpretations:

$\mu = 1.02\ 10^{-4}$ Pa s $\qquad\qquad$ $\rho = 785$ kg/m^3

Figure 33 shows multirate injection tests using Odeh and Jones´s method (cf 2.1.4). It seen two parallel slopes.

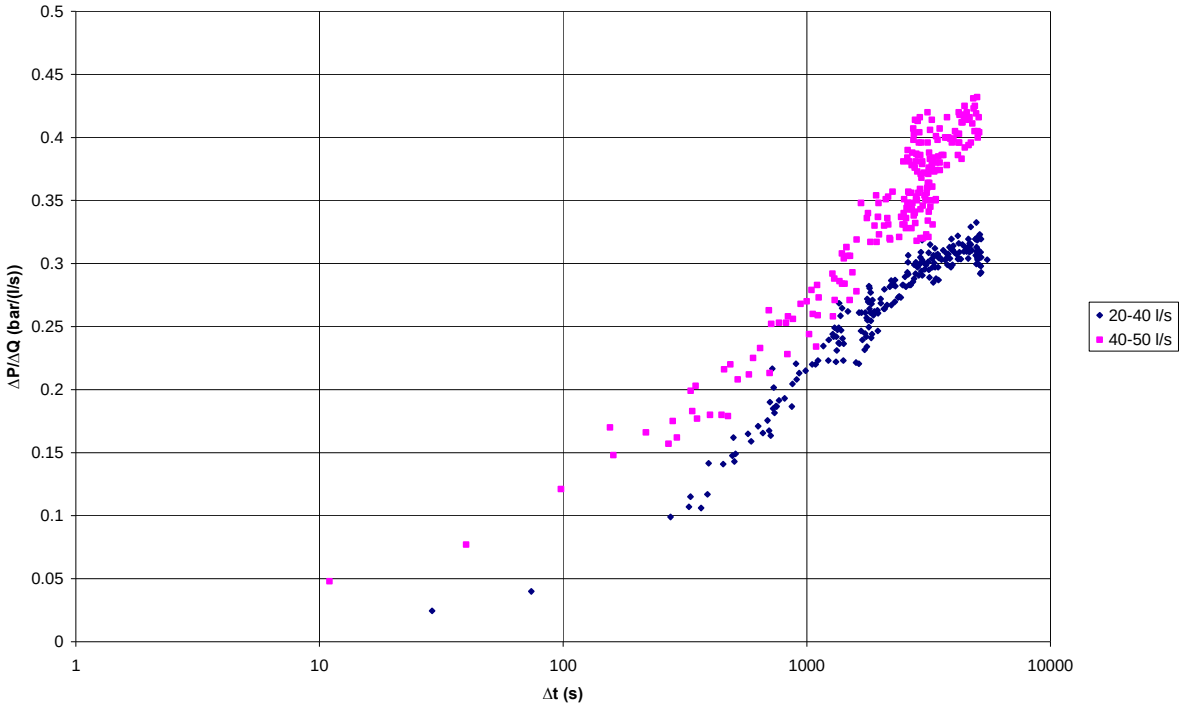

FIGURE 31: Semilog graph of the data in Figure 30. The figure shows the ratio between the pressure changes in each step, ΔP, versus the flow-rate change in the step, ΔQ

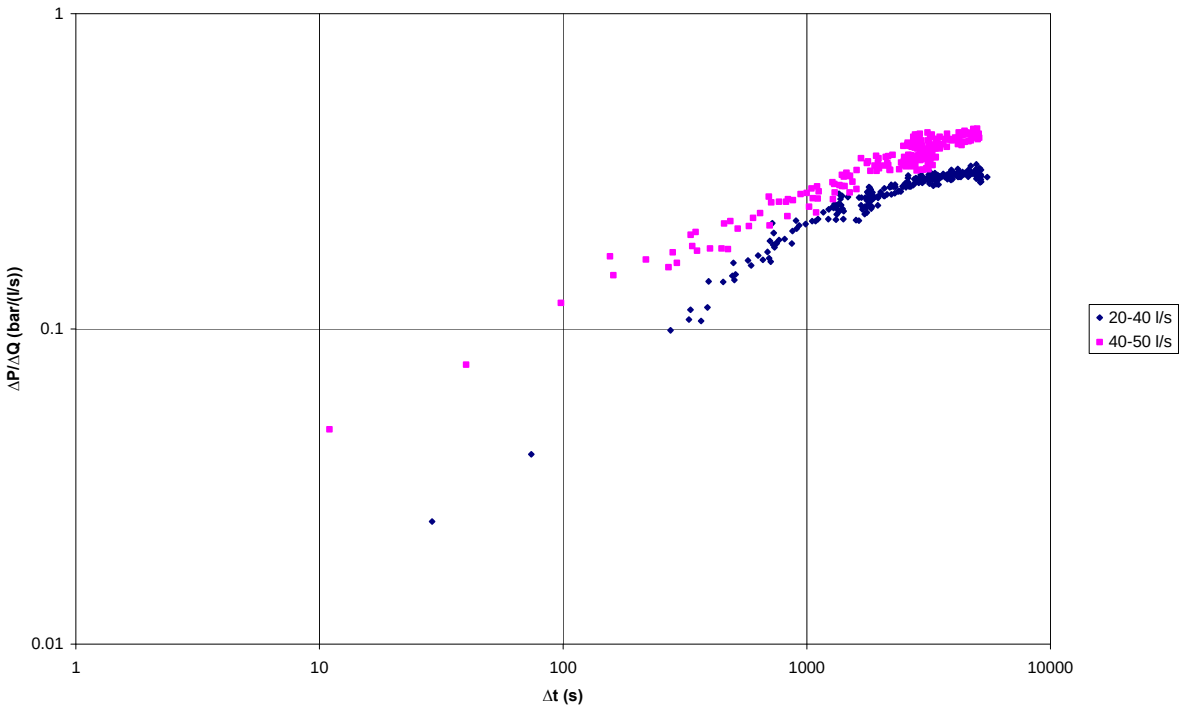

FIGURE 32: Log-log graph of the data in Figure 30. The figure shows the ratio between the pressure changes in each step, ΔP, versus the flow-rate change in the step, ΔQ

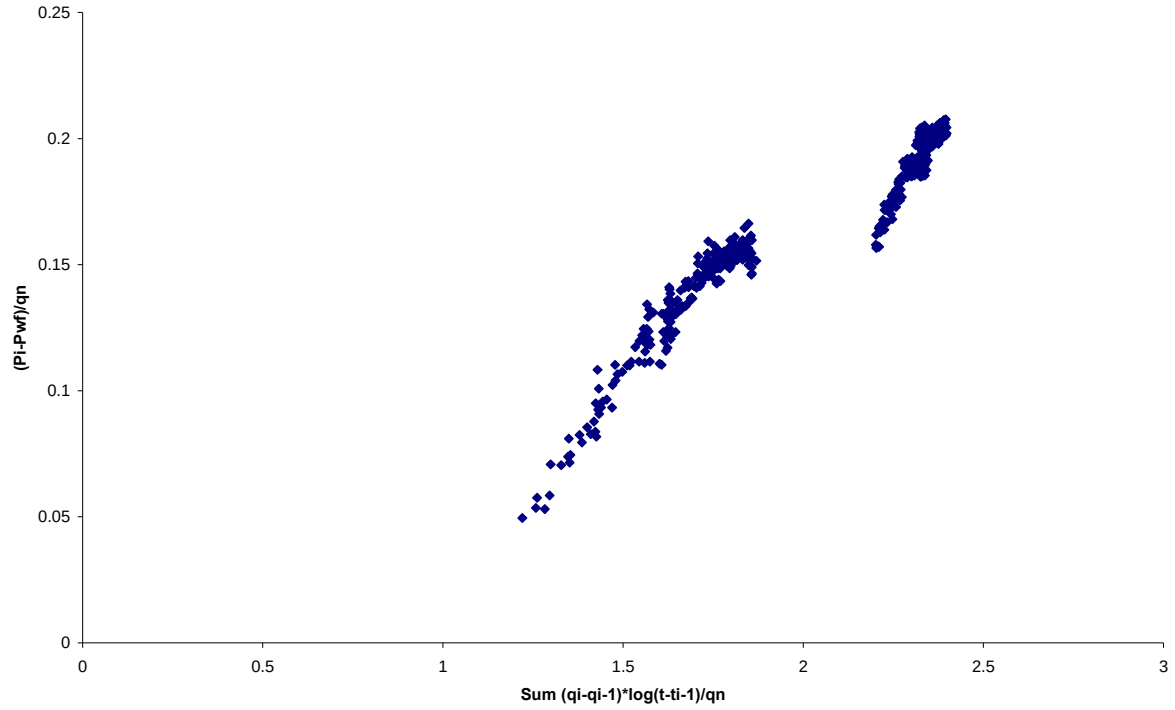

FIGURE 33: Well HE-20 multirates injection test

The results of interpretation of the drawdown tests from the semilog method, the type curve match and for multiflow rates are presented in Table 7.

TABLE 7: Results of semi-log and multirates analysis of 12.10.2002 injection test data from well HE-20

			Semilog		**Match method**	
	***q* (l/s)**	**Δq (l/s)**	**kh (Dm)**	**skin**	$\begin{pmatrix} t_D ; P_D \\ t(s); \Delta P / \Delta q \end{pmatrix}$	***kh* (Dm)**
Step 1	20 -> 40	20	1.86	2	$\begin{pmatrix} 200;1.6 \\ 100;0.1 \end{pmatrix}$	2.9
Step 2	40 -> 50	10	1.69	3	$\begin{pmatrix} 2000;1.2 \\ 1000;0.1 \end{pmatrix}$	1.93
All steps	Multiple		0.93			

The permeability-thickness obtained from all the method show a very low permeability. But as the area is knowing like a permeable, the explanation can be as during injection, we are injected some cold water around 25°C we are cooling the reservoir. This disturbs the real temperature reservoir comparing to during the production test. Then the dynamic viscosity is almost 10 times greater. Looking in the literature (Benson, 1982), this problem is knew and there is no real choice, all is depend about case by case and the history of the well. Here if the value of the dynamic viscosity corresponding to the temperature of the reservoir at the injection time i.e 7.808*1e-4 is taking account then the value of kh will be around 15 Dm.

The injectivity index at 1350 m is about 4 (l/s)/bar. This is calculated as well HE-06 but the difference is just instead to use the model data, it is applied the real pressure data.

5.2.2 Welltester numerical software modelling

Modelling step 1 for HE-20
The well test model selected for step1 is summarized in Table 8.

TABLE 8: Summary of model selected for step 1 of HE-20 injection testing.

Well testing model - Step 1	
Reservoir	Homogeneous
Boundary	Infinite
Well	Constant skin
Wellbore	Wellbore storage

The results from the regression analysis are shown graphically in Figure 34.

Figure 35 shows additional plots of the same data on a log-linear scale (left) and log-log scale (right). The plot on the right also shows the derivative of the pressure response, multiplied with the time passed since the beginning of the step. This trend is commonly used to determine which type of model is most appropriate for the observed data.
.

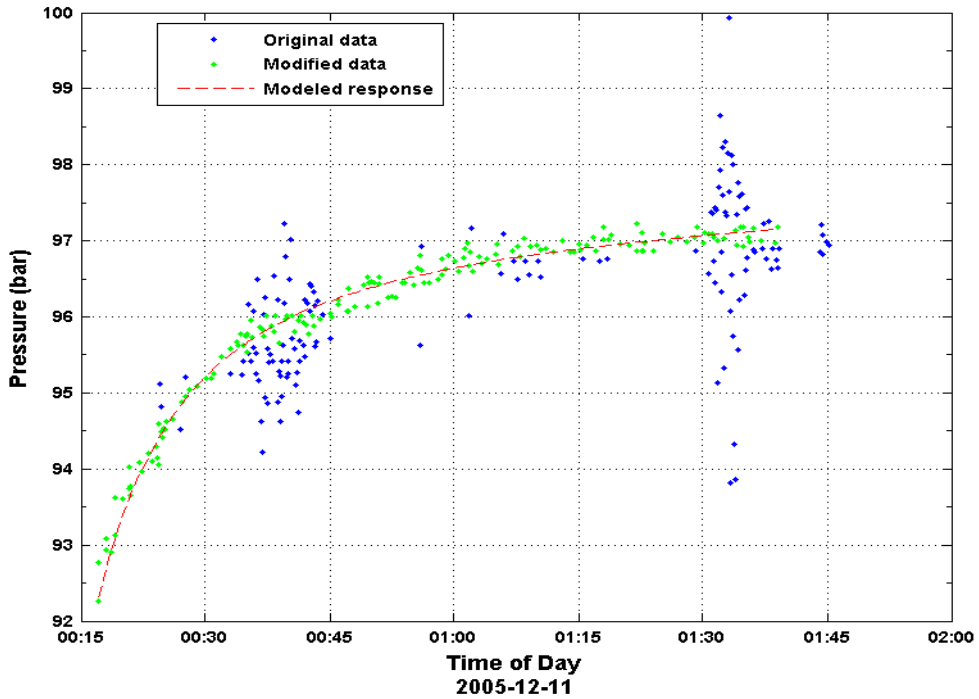

FIGURE 34: Fit between model and collected data for step 1 for well HE-20 at 12.10.2002

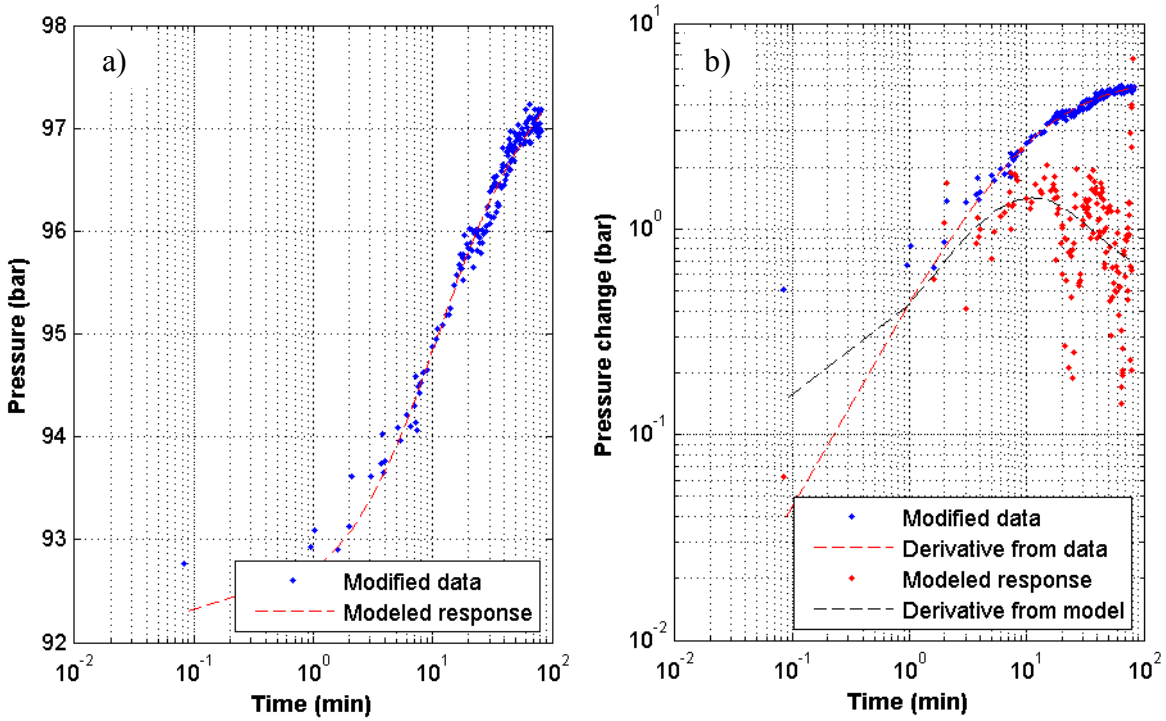

FIGURE 35: Fit between model and selected data: a) on log-linear scale and b) log-log scale

Modelling step 2 for well HE-20
The well test model selected for step 2 is summarized in Table 9.

TABLE 9: Summary of model selected for step 2 of HE-20 injection testing

Well testing model - Step 2	
Reservoir	Homogeneous
Boundary	Infinite
Well	Constant skin
Wellbore	Wellbore storage

The results from the regression analysis are shown graphically in Figure 36.

Figure 37 shows additional plots of the same data on a log-linear scale (left) and log-log scale (right).

Modelling all steps for well HE-20
The well test model selected for modelling all steps at once is listed in Table 10.

TABLE 10: Summary of model selected for all steps at once of HE-20 injection testing

Well testing model - All Steps	
Reservoir	Homogeneous
Boundary	Infinite
Well	Constant skin
Wellbore	Wellbore storage

The resulting fit is shown graphically in Figure 38.

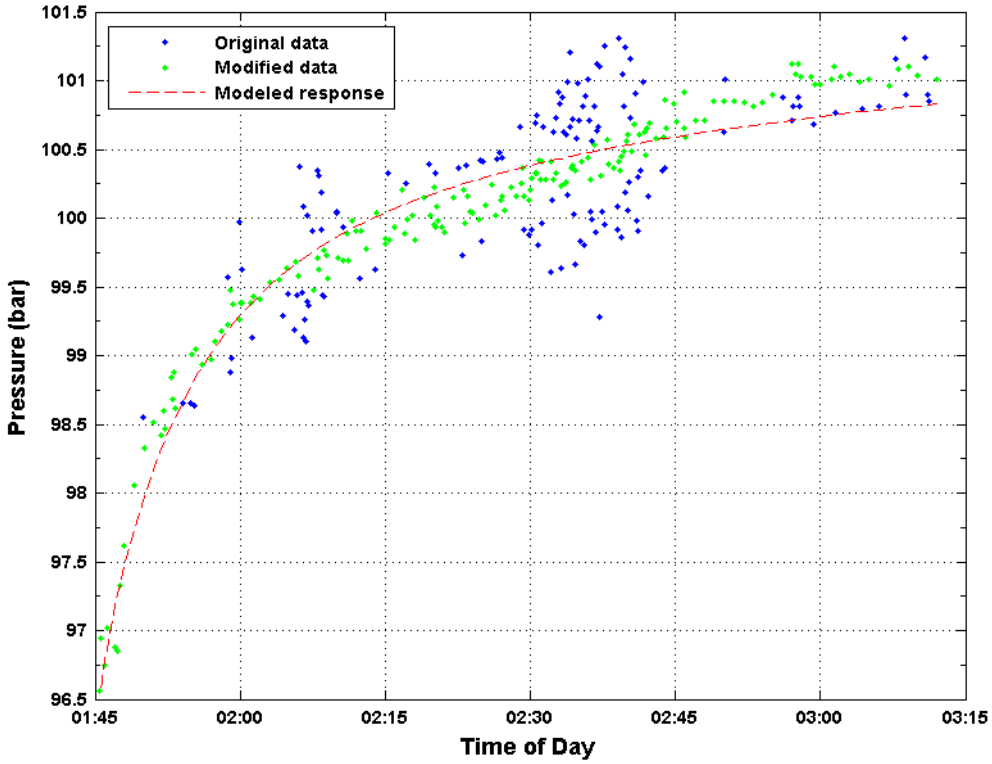

FIGURE 36: Fit between model and collected data for step 2 for well HE-20 at 12.10.2002

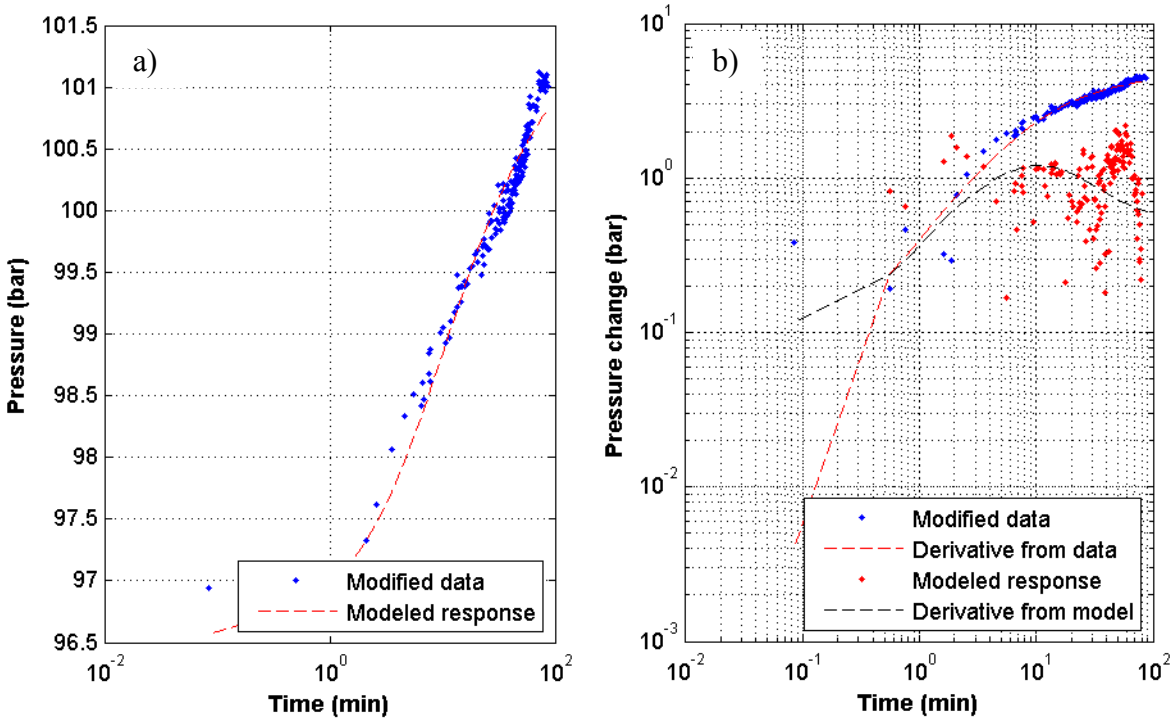

FIGURE 37: Fit between model and selected data: a) on log-linear scale and b) log-log scale

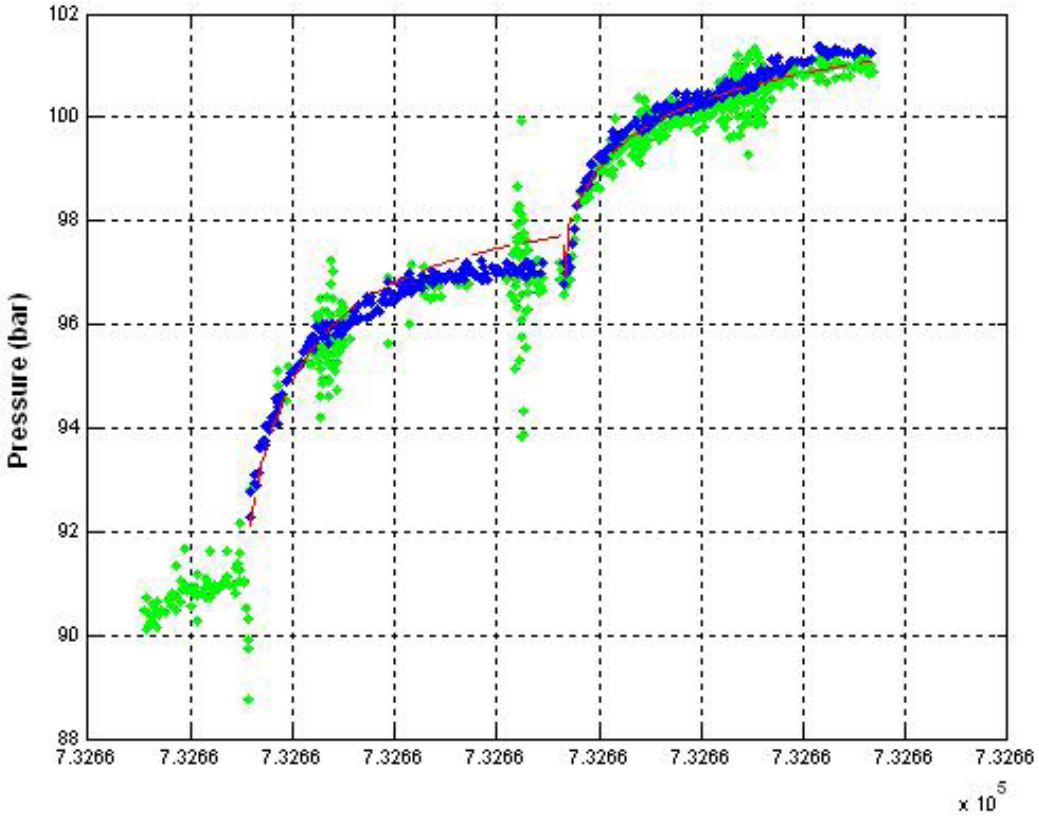

FIGURE 38: Fit between model and collected data for all steps

The parameters relevant to the selected model (Table 8, 9 and 10) are shown in Table 11.

TABLE 11: Summary of results from nonlinear regression parameter estimate using injection test data from well HE-20 from 12-10-2002

	Transmissivity (m^3/(Pa·s))	**Storage coefficient (m^3/(Pa·m^2))**	***kh*** **(Dm)**	**skin**	**Injectivity Index ((l/s)/bar)**
Step 1	$3.00 \cdot 10^{-8}$	$2.75 \cdot 10^{-7}$	3	1.31	4.09
Step 2	$1.64 \cdot 10^{-8}$	$5.51 \cdot 10^{-7}$	1.7	0.92	2.34
All step	$2.59.10^{-8}$	$1.013.10^{-7}$	2.6	1.75	3.21

The permeability-thickness *kh* value is around 2.6 Dm. This value is close to the once obtained from the semilog plot and very low permeability.

The skin factor is positive from the modelling model. This is confirming the result obtained from the semilog method.

Here the average injectivity index at 1400 m is around 3.21 (l/s)/bar. This value will be compared with the productivity index at paragraph 6.2.

6. PRODUCTION TEST DATA AND INTERPRETATION

6.1 Well HE-06

The temperature and pressure profiles measured on April 28, 2003 were selected to be simulated with the HOLA program. After a lengthy process of trial-and-error, and least-squares fitting by HOLA, a successful simulation was achieved. The results are presented in Figure 39 and the simulation parameters presented in Appendix II.

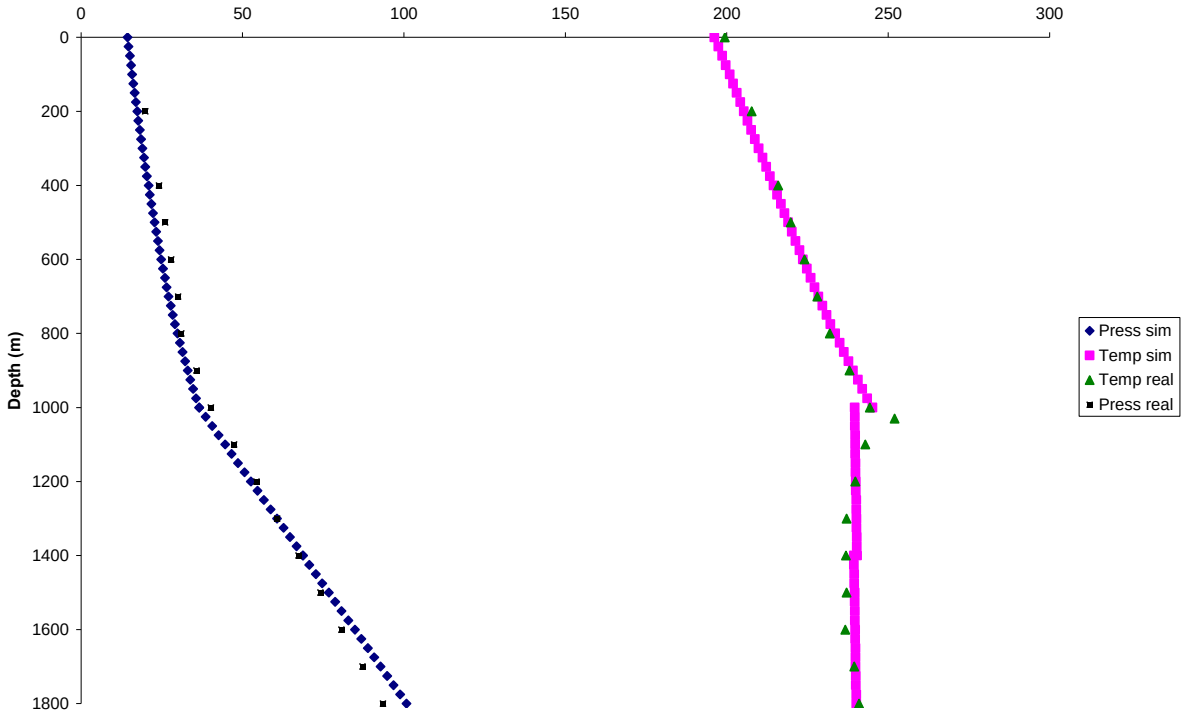

FIGURE 39: Wellbore simulation (HOLA) of pressure- and temperature log-data from well HE-06 logged during discharge testing of the well on 2003-04-28

The modelling results indicated two main feed zone at 1000 and 1400 m depth, each with approximately the same flow rate (18.5 and 13.5 kg/s respectively) and productivity index, *PI*, equalling 10^{-12} m^3 (see Appendix II). The total flow rate simulated was 32.0 kg/s at a well-head pressure of 14.4 bar-g required and the discharge enthalpy is 1020 kJ/kg. These values are very close to the results of discharge measurements by Reykjavik Energy, 33.0 kg/s at 14 bar-g. But there is difference between the values of enthalpy as the enthalpy measured by Reykjavik Energy is around 1350 kJ/kg. This discrepancy could be due to insufficient separation in the silencer where part of the water is carried with the steam leading too low water flow the weir-box during lip pressure measurement. After some it can expected to have higher enthalpy value because of the gain of enthalpy can occurs with the time after the flashing started.

According to the modelling result, the total (combined) *PI* equals to 2.25 (l/s)/bar (Appendix II). If we compare this to the injectivity index, *II*, obtained in section 5.2.2 (5.58 (l/s)/bar), the ratio between *II* and *PI* is 2.5. This difference can come from the model simulation as the data are very sensitive to the variation of *PI*. To be sure to have good value of *PI*, it may be better to use for the discharge measurements a flowmeter in order to be able to measure a good values of flow rate at the feed zones.
The two main feed zones 1000 and 1400 m have a the same maximum temperature of 240 °C (see Appendix II). The corresponding enthalpy of liquid water at this temperature is 1039 kJ/kg. This value is the same at the one at 1400 m. The explanation of the high enthalpy at 1000 m it is because of the

two phase presence and then some gain in enthalpy. And the maximum temperature of about 240°C attained at 1400 m corresponds to an MDP 22 bar-g.

From the simulation, steam-flow at 14.36 bar is 14.6 kg/s. Assuming that the steam flow is converted to electricity at a steam rate of 2 (kg/s)/MW_e, the electrical power potential of the well corresponds to 7.3 MW_e.

6.2 Well HE-20

The temperature and pressure profiles measured on March 16, 2006 were selected to be simulated with the HOLA program. After a lengthy process of trial-and-error, and least-squares fitting by HOLA, a successful simulation was achieved. The results are presented in Figure 40 and the simulation parameters presented in Appendix II.

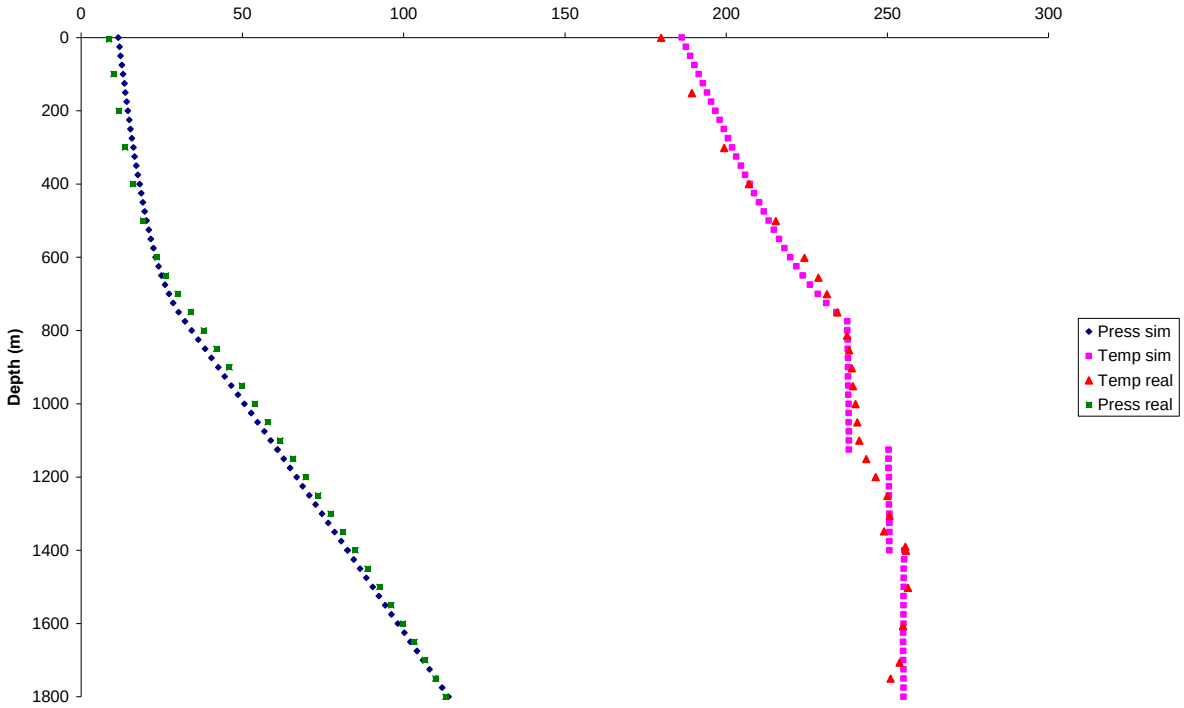

FIGURE 40: Wellbore simulation (HOLA) of pressure- and temperature log-data from well HE-20 logged during discharge testing of the well on on 2006-03-16

The model results indicated three main feed zone at 1125, 1800 and 1400 m (Appendix II). The total flow rate obtained for 10.54 bar-g required is 32.65 kg/s. This value is close to the one obtained during discharge measurements by Reykjavik Energy (35.5 kg/s for 10.1 bar-g). The flow rate at 1125 (21.79 kg/s) is twice higher than the flow rate at 1400 and 1800 m (7.74+3.12 kg/s). The wellhead enthalpy corresponding is 1018 kJ/kg.

From the model result, the *PI* = 4.1 (l/s)/bar (Appendix II). Comparing to the injectivity index *II* value obtained in 5.3 (3.2 (l/s)/bar), the ratio between *II* and *PI* is 0.8.

Downhole simulations indicate two main feed points, the more dominant one at 1125 m. A maximum temperature of about 250°C is attained and the corresponding enthalpy of liquid water is 1085 kJ/kg. Also the corresponding MDP is 25 bar-g. Here also the MDP of well HE-20 was not made. From the simulation, steam at 10.54 bar-g is 11.42 kg/s and then the power electricity expected 5.7 MW_e.

6.3 Comparison between *II* and *PI*

To compare the *PI* and *II* at the high-temperature field, the values of 34 wells from different geothermal high-temperature fields as:

- Three wells from Hellisheidi area in Iceland, wells HE-05 (Rezvani Khalilabad, 2003), HE-06 and HE-20;
- Six wells from Reykjanes in Iceland, wells RN-10, 13, 15, 18, 21 and 22 (Axelsson et al., 2006);
- Seven wells from Oguni in Japan, wells GH-10, 11, 12, 20, IH-2, GH-15 and N2-KW-3 (Garg and Combs, 1997);
- Seven wells from Sumikawa in Japan, S-2i, 2, 4, SA-1, SA-4, SC-1 and SD-1 (Garg and Combs, 1997);
- Eleven wells from Takigami in Japan, NE-4, 5, 6, 11, 11R, TT-2, 7, 8, 8S1, 8S3 and TT-13S (Garg and Combs, 1997).

To summarize all the data are plotted *II* versus *PI* in Figure 41. It appears from Figure 41 that, to first order, the *PI* and *II* for all the boreholes are more or less equal but there is scatter.

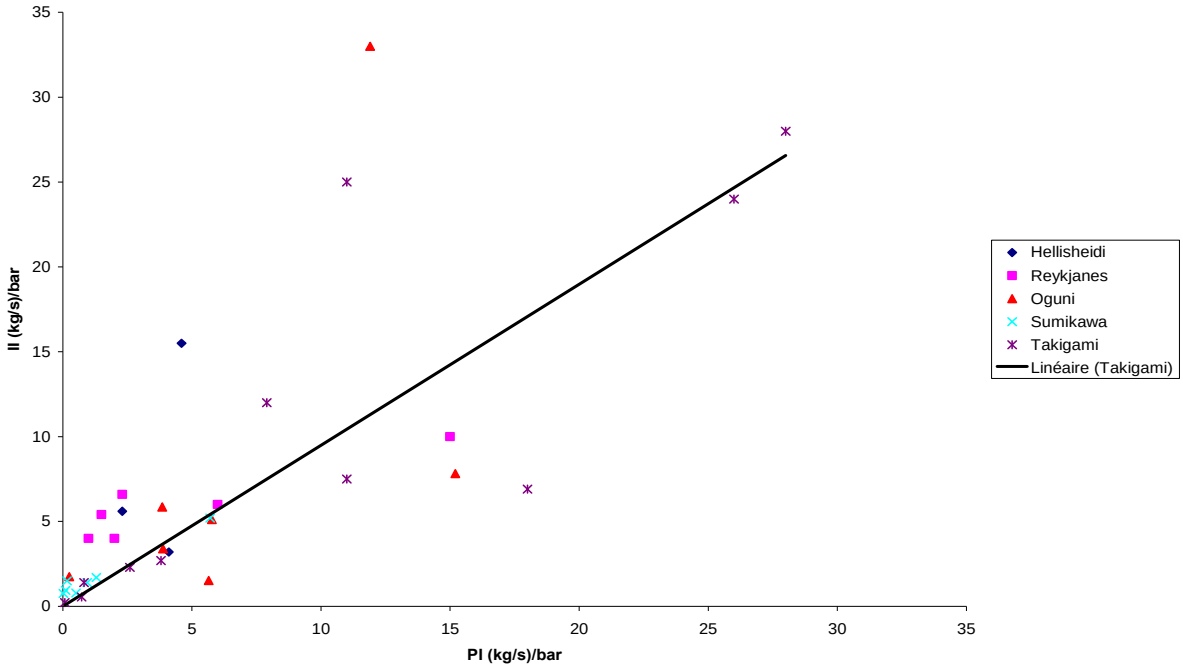

FIGURE 41: Productivity index (PI) vs. injectivity index (II) for Hellisheidi, Reykjanes, Oguni, Sumikawa, and Takigamiwell boreholes with liquid feedzones

7. RESERVOIR ASSESSMENT

Here the pressure decline data (measured as water level) from a centrally located observation well (NJ-15) in the Nesjavellir geothermal field are simulated by open (optimistic) and closed (pessimistic) models using the LPM and CTSM methods. The future pressure decline is also predicted for a 120 MWe production scenario. The Nesjavellir geothermal system is part of the Hengill volcanic system (Figure 6). In2000, before adding 30 MW_e to the 90 MW_e already installed, the mass extraction at Nesjavellir was of the order of 440 kg/s (Axelsson et al., 2005b).

7.1 Simulation and prediction

The main objective of the present reservoir evaluation of the Nesjavellir geothermal reservoir is to estimate the long-term production potential of the reservoir through data from the observation of well NJ-15. The LPM and CTSM methods were used to simulate the observed pressure decline (drawdown) in this well (Figure 42) between 1975 and 2005.

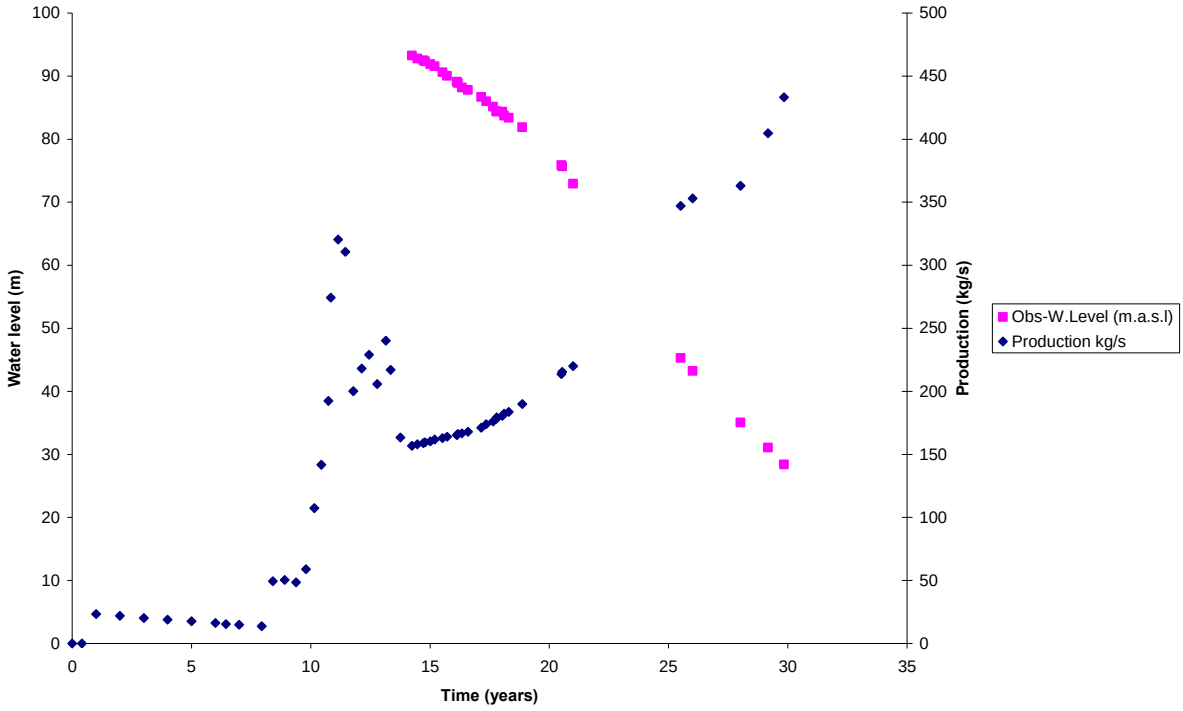

FIGURE 42: Production history of the Nesjavellir field from 1975 to 2005 and the corresponding water level history of well NJ-15

The water level decline was simulated and predicted by two tank open (optimistic), closed (pessimistic) LPM and CTSM methods (Figure 43). Water level data from well NJ-15 was available since 1989. The well was drilled in 1985 and flow tested in 1987. After that the well recovered and was then used as a monitoring well. The data gap in 1996-2000 is due to the fact that the well was used for the power plant during that period.

The CTSM method provides the standard deviation STD of each state of process simulated or predicted. In Figure 43 the ±2*STD of the two tanks CTSM models, both closed and open, is also plotted, showing the 95% confidence interval for the simulation.

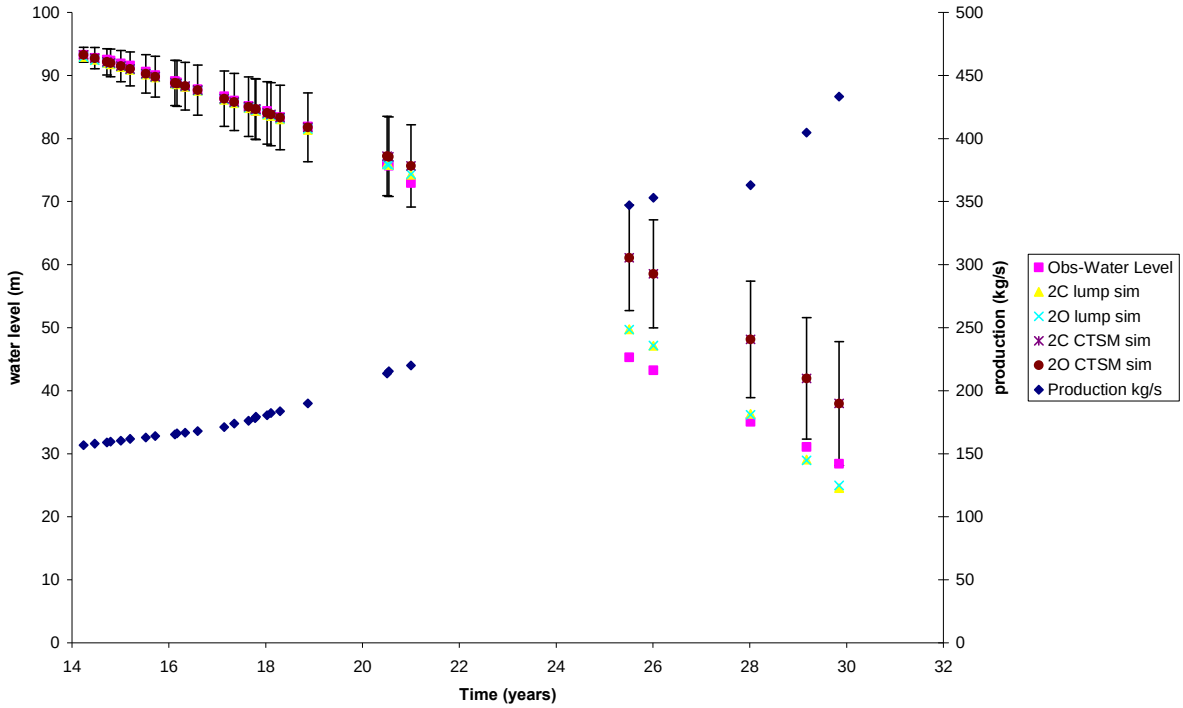

FIGURE 43: Pressure decline data (measured as water level) from an observation well (NJ-15) at Nesjavellir simulated by two tank LPM and CTSM methods, from 1989 (T = 0 corresponds to 1975). Also shown is the total mass extraction from the field

From the Figure 43, the following conclusions can be made:

- There is no significant difference between an open and a closed model for both the LPM and CTSM methods.
- In the open model pressure declines in the same way as in a closed model. This may indicate that the reservoir, or geothermal system, is closed or the outer reservoir for the open model has low permeability.
- From 1989 to 1996, both LPM and CTSM methods fit the data well. As there is a gap in the data between 1996 and 2000, the LPM still fits well after that. But for the CTSM model, the lower interval confidence value fits the data. This is because the LPM model automatically fits the analytical response functions whereas CTSM continuous time models is based on the flow rate is constant between the sample interval times.

Simulation by a CTSM three tanks open and closed models is plotted with a simulation by a two tanks open and closed CTSM model (Figure 44). The fact that both the three tank open and closed model simulations are comparable, resulting in the same standard deviation value, seems to confirm that the Nesjavellir reservoir is either closed, meaning no connection to any type of recharge, or open with a low permeability boundaries of the outer reservoir. The same applies to the two tank simulations. It should be pointed out that the model reflects the whole hydrological system and that the outer tank(s) may be partially simulating colder hydrological systems surrounding the main reservoir. This is supported by chemical data from the production phase of well NJ-15, which indicates mixing with colder fluid (Gunnlaugsson, personal communication).

The parameters estimated for these models are used as input to predict the water level decline for the next 25 years (until 2030) for a 120 MW_e future production scenario (Figure 45). A production of 540 kg/s of fluid is assumed at wellhead pressure providing 240 kg/s of steam.

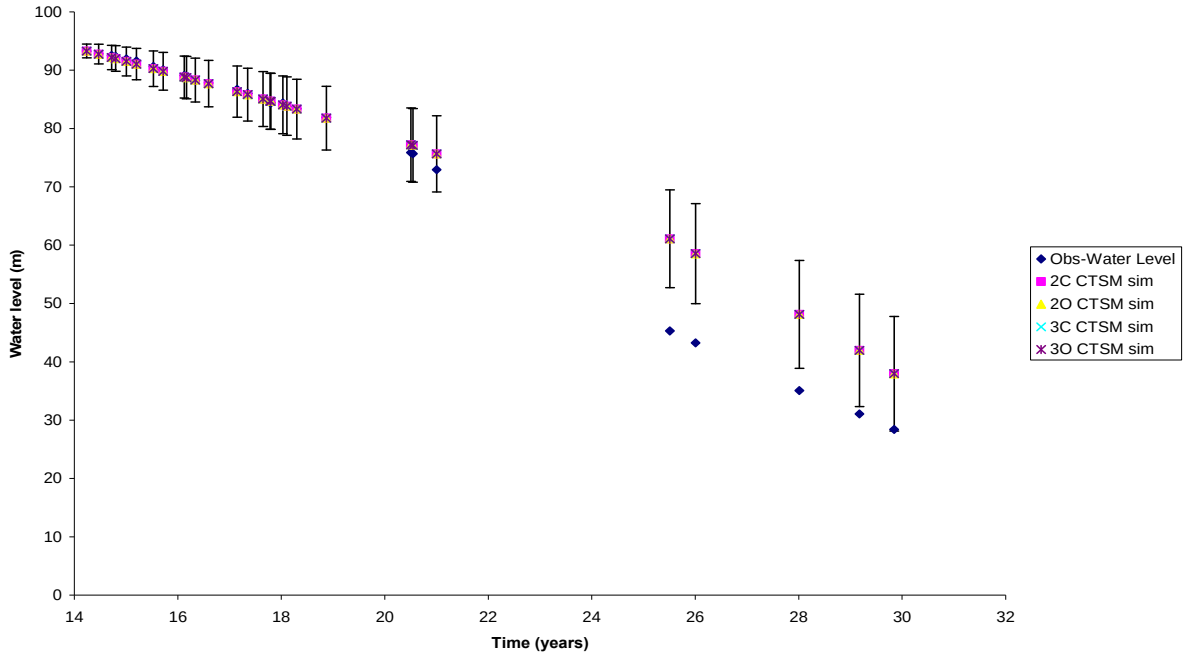

FIGURE 44: Pressure decline data (measured as water level) from an observation well (NJ-15) at Nesjavellir simulated by two and three tank CTSM models.
Data starting in1989 (t = 0 corresponds to 1975)

For the CTSM program the last measured water level value in 2005 is taken as an initial value for the prediction.

Based on the predicted pressure decline in Figures 45 and 46, these remarks can be made:

- From 2005 to 2030 a continuous pressure decline is predicted, both by the LPM and CTSM methods.
- The water level drawdown predicted in the year 2030 in well NJ-15 by the CTSM model will be between -163 and -189 m with 95 % of probability.
- The LPM prediction indicates a pressure decline to about -182 m in well NJ-15. This is considered a good estimation as it is within the confidence interval predicted by CTSM.
- From 1989 to 2030, there is a continuous water level decline between 1.7 and 2 m/year with 95 % of probability.
- This situation has been studied in detail through numerical modelling by Bjornsson and Hjartarson (2003). They predict almost the same pressure draw-down as the lumped parameter model, which indicates that the pressure decline predictions presented are fairly reliable (Figure 46).
- It may be mentioned here that the pressure decline predicted (Figure 45) shows that properly planned reinjection should be beneficial for the operation of the Nesjavellir field.

Having a confidence interval is useful for the management of the reservoir as it indicates the uncertainty in the prediction. It is predicted, for example, that the water level will be -150 m at the 2013 with 97.5 % probability (Figures 45 or 46). This is found by drawing a horizontal line from -150 m until it intersects the first lower value of the confidence interval.

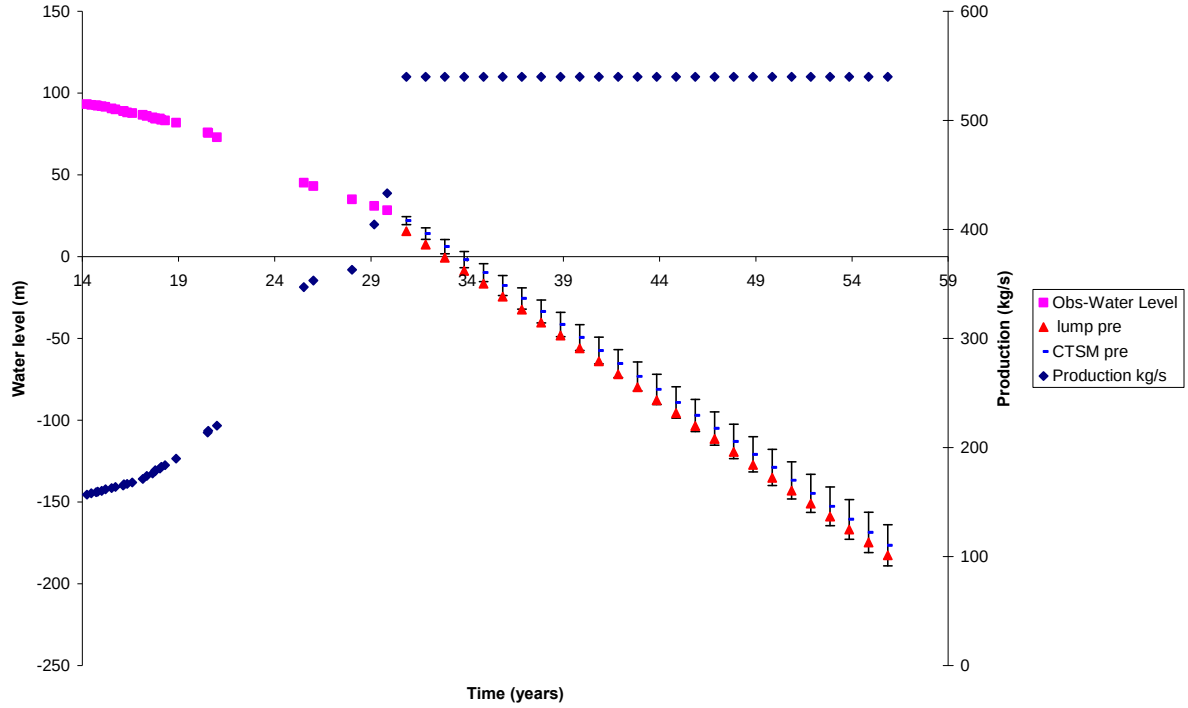

FIGURE 45: Pressure decline (measured as water level) in observation well NJ-15 at Nesjavellir predicted by a LPM and CTSM methods from 2005 to 2030 (starting 30 years after 1975) for a 120 MWe scenario. Also shown is the total mass extraction from the field

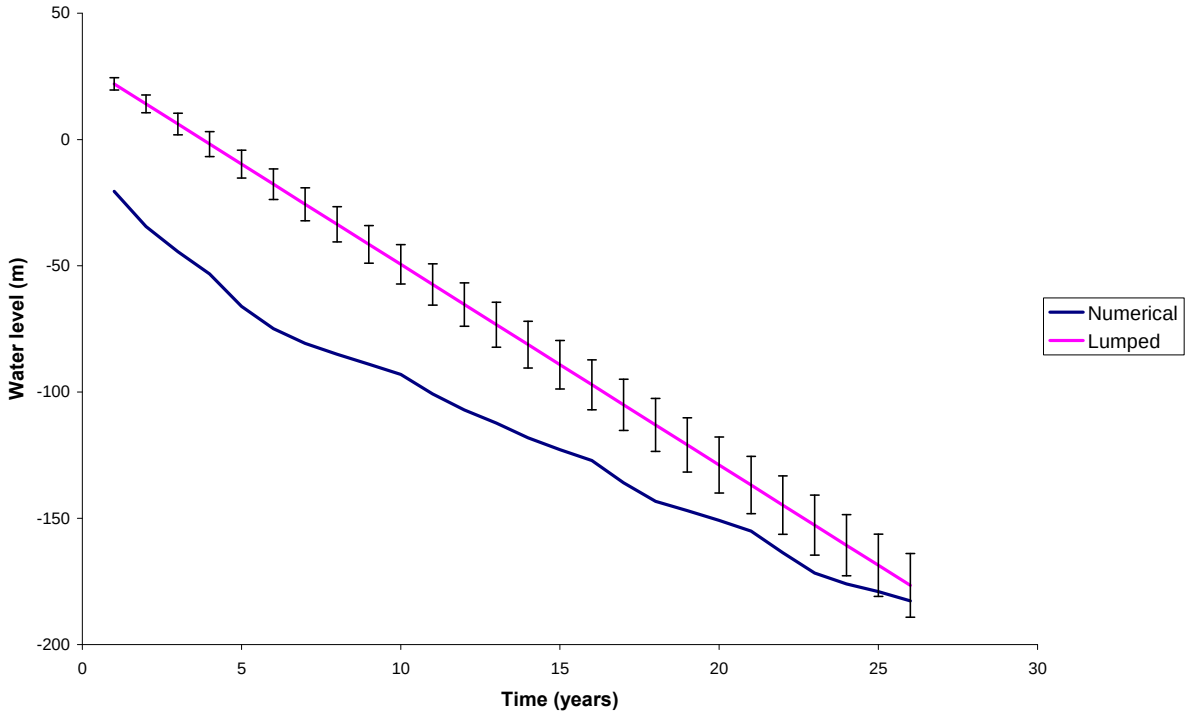

FIGURE 46: Pressure decline (presented as water level) in an observation well (NJ-15) at Nesjavellir from 2005 (30 years after 1975) to 2030 predicted by a lumped parameter model compared with pressure decline predictions calculated by a numerical reservoir model (Björnsson and Hjartarson, 2004; Axelsson et al., 2005b) for a 540 kg/s (120 MWe) total flow rate production plan

7.2 Parameter estimation

From the CTSM program, either for two or three tanks the parameter values obtained are:

$A_1 = 2.7$ km^2
$A_2 = 1$ km^2
$K_1 = 2.5*10^7$ s / m^2
$K_2 = 3.1*10^6$ s / m^2

The flow resistance values are very high. This may signify that the well is not connected to any resource recharge. Therefore, if the production will be stopped the well is not expected to recover. This conclusion contradicts the results of the detailed numerical model set up by Bjornsson and Hjartarson (2003). Their calculated changes in reservoir pressure and temperature at Nesjavellir during the 30-year period of intense production is in good agreement that the results obtained in Chapter 7.1 indicating that a pressure decline of 8 bar-g will expect during this period, but for the following 250 years of recovery (production stopped in 2036) the numerical model recovers because there is some recharge area connected to the reservoir. Based on the nature of the crust of Iceland, and specifically the islands geothermal resources, it is very unlikely that the Nesjavellir system is completely closed. Therefore, the open models with low permeability outer boundaries are much more likely to simulate the nature of the Nesjavellir system. It must emphasized, however, that this work is still in progress and that sustainable management of the Nesjavellir system needs further study.

The parameters estimated by LPM are summarized in Table 12 assuming a thickness of 1000 m and that the volume of the reservoir is equal to the mean of the capacitances divided by storativity as in Eq. (2.32) and (2.33).

TABLE 12: Summary of results LPM parameter estimated

Model type	**Reservoir volume (m^3)**		**Permeability k (m^2)**	
	Confined	**Free surface**	**Confined system**	**Free surface**
			(2-D radial flow)	
2-tank closed	2.28E+12	1.36E+10	2.70E-15	7.29E-14
2-tank open	2.27E+12	1.36E+10	2.21E-14	4.10E-16

From the results summarized in Table 12, these conclusions can be made:

- The volume of the reservoir is between 14 to 2280 km^3. The lower value can corresponds to the main hot reservoir surrounded by a lower temperature geothermal system, thus the hydrological system becomes bigger. This can be related to the pressure decline predictions by concluding that the Nesjavellir reservoir is best simulated by an open model with a low permeability for the outer reservoir.
- The permeability-thickness *kh* is between 2.7 and 22 Dm for a confined system, which is the case for the deep Nesjavellir geothermal system. In the numerical model of Bjornsson and Hjartarson (2003) low *kh* is associated with wells close to the boundary and permeability in the middle of the reservoir is higher.

8. CONCLUSIONS

After a successful program of geothermal well drilling, it is recommended that the following main steps are taken before such wells are connected to a power station, in order to get a good evaluation of reservoir properties:

- Multi-step injection, interference and build-up tests.
- Data analysis data with 'classic' (semilog, log-log, type curves) and 'modern' (derivative plots, well test simulator) methods.
- Close a well for 2-3 months before discharging in order for it to warm-up and reach steady state formation temperature.
- During the whole time pressure and temperature profiles should be measured regularly.
- Discharge testing of the well combined with simulation of its performance and conditions by a wellbore simulation computer program like HOLA.
- Following this the wellhead can be connected to the power station.
- Finally simple reservoir models for matching and predicting changes in one reservoir parameter (such as pressure) caused by the production from the system, such as the lumped parameters or Kalman filter methods.

In summary, the main results of the analysis of data from wells HE-06, HE-20 and NJ-15 are:

- The estimated permeability-thickness for well HE-06 is high, or about 11 Dm. The ratio between the *II* (5.58 (l/s)/bar) and *PI* (2.25 (l/s)/bar) for the well is 2.5. Well HE-06 has two main feed zones around 1000 and 1400 m depth. The EPP estimated is 7.3 MWe.
- The estimated permeability-thickness for well HE-20 is low, or about 2.6 Dm. The ratio between the *II* (3.2 (l/s)/bar) and *PI* (4.1 (l/s)/bar) for the well is 2.5. There are two main feed zones in the well, around 1125 and 1400 m depth. The EPP estimated is 5.7 MWe.
- There is good agreement between all the methods used in analysing the well test data.
- The ratio between *II* and *PI* for Hellisheidi wells, and in other high-temperature liquid dominated reservoirs, seems to indicate a general first order relationship with considerable scatter.
- The LPM and CTSM methods are reliable to simulate and predict the pressure decline caused by production, and can be good tools for reservoir management as well as being much less costly than detailed numerical reservoir modelling.
- On the average the pressure of Nesjavellir geothermal reservoir is predicted to decline at a rate of about1.8 m/year for 120 MWe future generations.
- A comparison of detailed numerical modelling made for Nesjavellir (Bjornsson et al., 2003) with the lumped models and continuous time stochastic modelling, shows that the pressure decline predicted is in a fairly good agreement, and the three methods seem to have a comparable accuracy. The time required for the LPM and CTSM, however, is only a fraction of the time required for more detailed modelling.

Some of recommendations can be made to improve data quality and consequent data interpretation, such as:

- As it was difficulty during this study to get a good data of a total mass output plotted against wellhead pressure from wells HE-06 and HE-20, it shows how it is really important to have correct data in order to get physical parameters estimates close to reality. By the way one important recommendation is to use detailed down-hole flow-meter measurements in order to get an accurate location and amount of loss or gain between well and formation.
- As all the well test analysis give comparable values, it would seem better to use only the Well Tester software, or comparable software, in order to gain time. But here it should be kept in mind that the Well Tester doesn't include the option of having fractures presents. So it'll be

better to check from log-log plot whether the any fracture effects are present or not. If not, then it is useful to make well test interpretation with the Well Tester software.

- As an alternative the Well Tester software can be improved by including a fracture option.
- In order to determine the maximum discharging pressure, the enthalpy and flow rates measurements should be care and it can recommended before connecting the wellhead pressure to the power plant, to run a completely program by taking and analysis carefully the samples from lip pressure. May be it's better to use the chemical tracers even if it is more expensive but more accurate
- The Lumpfit program can be improved by allowing for the introduction of noise (some incertitude) in the pressure decline simulation.

NOMENCLATURE

A = Cross-section area of the lip (cm^2);
C = Wellbore storage coefficient (m^3/Pa);
C_D = Dimensionless wellbore storage coefficient;
C_t = Total compressibility (Pa^{-1});
E_t = Total energy flux in the well (J/s);
g = Gravity (m/s^2);
H = Fluid enthalpy (kJ/kg);
h = Thickness (m);
k = Intrinsic permeability (m^2);
k_r = Relative permeability of the phases;
m = Slope of semilogarithmic straight line;
m = Slope of multi flow rates;
P = Pressure (Pa);
PI = Productivity index of the feed zone (m^3);
P_{lip} = Lip pressure at the end of the pipe (MPa);
P_0 = Well head pressure (Pa);
Q = Ambient heat loss over unit distance (W/m);
q = Flow rate (m^3/s);
r = Radial distance (m);
r_w = Wellbore radius (m);
S = Storage coefficient (m/Pa);
s = Skin factor;
T = Temperature (°C);
T = Transmissivity (m^2/s);
t = Time (s);
t_D = Dimensionless time based on well bore radius;
V = Volume (m^3);
W = Mass flow rate (kg/s);
W_{feed} = Mass flow rate (kg/s);
X = Steam mass fraction ratio;
x = Horizontal coordinate (m);
y = Horizontal coordinate (m);
z = Vertical coordinate (m);
φ = Porosity
μ = Dynamic viscosity (Pa s);
ρ = Density (kg/m^3).

Subscripts

β = Phase liquid or gas;
i = The i'th number of tank;
s = Steam;
t = Total;
w = Water;

REFERENCES

Åström, K.J., 1970: *Introduction to Stochastic Control Theory,* Academic Press, New York.

Arnason, B., Theodorsson, P., Bjornsson, S., and Saemundsson, K., 1967: Hengill, a high-temperature thermal area in Iceland. *Bull. Volcanologique, XXXIII-1*, 245-260.

Arnason, K., Karlsdottir, R., Eysteinsson, H., Flovenz, O.G., and Gudlaugsson, S.Th., 2000: The resistivity structure of high-temperature geothermal systems in Iceland. *Proceedings of the World Geothermal Congress 2000, Kyushu-Tohoku, Japan,* 923-928.

Arnason, K., and Magnusson, I.Th., 2001: *Geothermal activity in the Hengill area. Results from resistivity mapping.* Orkustofnun, Reykjavik, report, OS-2001/091 (in Icelandic with English abstract), 250 pp.

Axelsson, G., 1989: Simulation of pressure response data from geothermal reservoirs by Lumped parameter models, *Proceedings, Fourteenth Workshop on Geothermal Reservoir Engineering Stanford University,* SGP-TR-122.

Axelsson, G., and Arason, P., 1992: *Automated simulation of pressure changes in hydrological reservoirs, user's guide*. Orkustofnun, Reykjavík, report, 17 pp.

Axelsson, G., Bjornsson, G., and Quijano, J.E., 2005a: Reliability of Lumped parameter modelling of pressure changes in geothermal reservoirs. *Proceedings World Geothermal Congress 2005, Antalya, Turkey*.

Axelsson, G., Stefansson, V., Bjornsson, G., and Liu, J, 2005b: Sustainable management of geothermal resources and utilization for 100 – 300 Years. *Proceedings World Geothermal Congress 2005, Antalya, Turkey*.

Axelsson, G., Thorhallsson, S., and Bjornsson, G., 2006: Simulation of geothermal wells in basaltic rock in Iceland. *Enhanced geothermal innovative network for Europe Workshop 3*, Switzerland.

Benson, S., 1982: Interpretation of no isothermal step-rate injection tests. *Proceedings, TOUGH Symposium 2003 Lawrence Berkeley National Laboratory*.

Bjornsson, G., Arason, P., Bodvarsson, G.S., 1993: *The wellbore simulator HOLA. Version 3.1. User's guide.* Orkustofnun, Reykjavík, 36 pp.

Bjornsson, G., Gunnlaugsson, E., and Hjartarson, A., 2006: Lawrence Berkeley National Laboratory, Berkeley, California. *Proceedings, TOUGH Symposium 2006.*

Björnsson, G. and A. Hjartarson, 2003: *Reservoir model for the Hengill geothermal systems and future predictions for 120 MW electrical production at Nesjavellir and Hellisheidi.* Iceland GeoSurvey (ÍSOR), report ÍSOR-2003/009 (in Icelandic), Reykjavík, 150 pp.

Bjornsson, G., Hjartarson, A., Bodvarsson, G.S., and Steingrimsson, B., 2003: Development of a 3-D geothermal reservoir model for the grater Hengill volvano in SW-Iceland. *Proceedings, Eleventh Workshop on Geothermal Reservoir Engineering Stanford University,* SGP-TR-93.

Bjornsson, A., Hersir, G.P., and Bjornsson, G., 1986: The Hengill high-temperature area, SW-Iceland: Regional geophysical survey. *Geoth. Res. Council, Transactions, 10*, 205-210.

Bodvarsson, G.S., Bjornsson, S., Gunnarsson, Á., Gunnlaugsson, E., Sigurdsson, Ó., Stefansson V., and Steingrimsson, B., 1990: The Nesjavellir geothermal field, Iceland. Part 1. Field characteristics and development of a three-dimensional numerical model. *J. Geotherm. Sci. and Tech., 2-3,* 189-228.

Bodvarsson, G.S., and Cox, B.L., 1986: Preliminary studies of two-phase effects on pressure transient data. *Proceedings, Eleventh Workshop on Geothermal Reservoir Engineering Stanford University,* SGP-TR-93.

Bodvarsson, G.S., Pruess, K., and Lippmann, M.J., 1986: Modelling of geothermal systems. *J. Pet. Geotherm. Sci. & Tech., 38-10*, 1007-1021.

Bourdet, D., Ayoub, J.A. and Pirard, Y.M., 1989: Use of pressure derivative in well-test interpretation. *SPE Formation Evaluation, June 1989*, 293-302.

Bourdet, D., Whittle, T.M., Douglas, A.A. and Pirard, Y.M., 1983: A new set of type curves simplifies well test analysis. *World Oil, May 1983,* 95-106.

Eppelbaum, L.V., and Kutasov, I.M., 2008: Designing an interference well test in a geothermal reservoir. *Proceedings, 33rd Workshop on Geothermal Reservoir Engineering, Stanford University, Stanford,* SGP-TR-185.

Earlougher, R.C., Jr. 1977: *Advances in well test analysis*. SPE, New York, Dallas.

Feigl, K.L, Gasperi, J., Sigmundsson, F., and Rigo, A., 2000: Crustal deformation near Hengill volcano, Iceland 1993-1998: Coupling between magmatic activity and faulting inferred from elastic modeling of satellite radar interferograms. *J. Geophys. Res*. *105-25,* 655-670.

Franzson, H., Guðlaugsson, S.Th., and Friðleifsson, G.Ó., 2001: Petrophysical properties of Iceland rocks. *Proceedings of the sixth Nordic symposium on petrophysics, Trondheim, Norway.*

Fridleifsson, G.Ó., Ármannsson, H., Arnason, K., Bjarnason, I.Th., and Gislason, G., 2003: Part I: Geosciences and site selection. In: Fridleifsson, G.Ó. (ed.), *Iceland deep drilling project, feasibility report.* Orkustofnun, Reykjavik, report OS-2003-007, 104 pp.

Garg, S.K., and Combs, J., 1997: Use of slim holes with liquid feedzones for geothermal reservoir assessment. *Geothermics, 26-2,* 153-178.

Gislason, G., and Gunnlaugsson, E., 2003: Preparation for a new power plant in the Hengill geothermal area. *IGA News, 51,* 4-5.

Grant, M.A., Donaldson, I.G., and Bixley, P.F., 1982: *Geothermal reservoir engineering*. Academic Press Ltd., New York, 369 pp.

Gunnlaugsson, E., and Gislason, G., 2005: Preparation for a new power plant in the Hengill geothermal area, Iceland. *Proceedings World Geothermal Congress 2005, Antalya, Turkey*.

Hartanto, D.B., 2005: Borehole geology and alteration mineralogy of the well HE-11, Hellisheidi geothermal field SW-Iceland. Report 8 in: *Geothermal training in Iceland 2005*. UNU-GTP, Iceland, 83-109.

Hersir, G.P., Bjornsson, G., and Bjornsson, A., 1990: *Volcanoes and geothermal systems in the Hengill area, geophysical exploration.* Orkustofnun, Reykjavik, report OS-90031/JHD-06 (in Icelandic), 92 pp.

Horne, R.N, 1995: *Modern well test analysis-a computer-aided approach* (2nd ed). Petroway, Inc, Palo Alto, CA, 257 pp.

James, R., 1962: Steam water critical flow through pipes. *Proceedings of the Institution of Mecanical engineers,* London 176-26, 739-748.

Jones, J.G., 1969: Intraglacial volcanoes of the Laugarvatn region, Southwest-Iceland, I. *Q.J. Geol. Soc. Lond., 124, 197-211.*

Jonsdottir, H., Madsen, H., and Palsson, O.P., 2006: Parameter estimation in stochastic rainfall-runoff models. *Journal of Hydrology, 326,* 379-393.

Jonsson, G., 1990: *Parameter estimation in models of heat exchangers and geothermal reservoirs*, Department of Mathematical Statistics Lund Institute of Technology, chapter F.

Jonsson, G., and Palsson, O.P., 1992: Modelling and parameter estimation of heat exchangers-A statistical approach. *Journal of Dynamic Systems, Measurement and Control, 114,* 673.

Jonsson, S.S., Richter, B., Sigurdsson, O., Steingrimsson, B., Hermannsson, G., Einarsson, E.M., and Skarphedinsson, K., 2002: *Hellisheidi – well HE-6. 3rd part: Drilling of 8½" production part from 813 m to 2013 m depth.* Orkustofnun, Reykjavík, report OS-2002/047 (in Icelandic), 59 pp.

Juliusson, E., Gretarsson, G.J., and Jonsson P., 2007: *Well Tester 1.0b, User's guide*. ISOR, 26 pp.

Mortensen, A.K., Gudmundsson, Á., Egilsson, Th., Bliscke, A., Jónsson, S.S., Gautason, B., Ásmundsson, R.K., Danielsen, P.E., Hjartarson, A., Sigurdsson, G., Bjornsson, G.,Sigurdsson, Ó., and Thorgrímsson, A.K., 2006: *Ölkelduháls – well HE-20. 3rd part: Drilling of 8½" production part from 706 m to 2002 m depth.* ÍSOR, Reykjavík, report ÍSOR-2006/034 (in Icelandic), 178 pp.

Néstor, M.R., and Fernando, S.V., 2001: Advances in the analysis of pressure interference test, *Proceedings, 26th Workshop on Geothermal Reservoir Engineering Stanford University, Stanford,* SGP-TR-162.

Ragnarsson, A., 2000: Geothermal development in Iceland 1995-1999. *Proceedings of the World Geothermal Congress 2000, Kyushu-Tohoku, Japan, 1,* 363-375.

Ragnarsson, A., 2005: Geothermal development in Iceland 2000-2004. *Proceedings of the World Geothermal Congress 2005, Antalya, Turkey*.

Rezvani Khalilabad, M., 2003: Reservoir parameters for well HE-5, Hellisheidi geothermal field, SW-Iceland. Report 18 in: *Geothermal training in Iceland 2003*. UNU-GTP, Iceland, 83-109.

Saemundsson, K., 1967: *Vulkanismus und Tektonik des Hengill-Gebietes in Sudwest-Island*. Acta Nat. Isl., II-7 (in German), 195 pp.

Saemundsson, K., 1979: Outline of the geology of Iceland. *Jökull, 29,* 7-28.

Saemundsson, K., 1995: *Geological map of the Hengill area 1:50,000*. Orkustofnun, Reykjavík.

Sigmundsson, F., Einarsson, P., Rögnvaldsson, S.Th., Foulger, G., Hodkinsson,, K., and Thorbergsson, G., 1997: The 1994-1995 seismicity and deformation at the hengill triple junction, Iceland: Triggering of earthquakes by an inflating magma chamber in a zone of horizontal shear stress. *J. Geophys. Res. 102,* 15151-15161.

Sigurdsson, O., Bodvarsson, G.S., and Stefansson, V., 1983: Nonisothermal injectivity index can infer well productivity and reservoir transmissivity. *Proceedings 9th Workshop on Geothermal Reservoir Engineering, Stanford University, Stanford,* SGP-TR-74.

Stevens, L., 2000: Pressure, temperature and flow logging in geothermal wells. *Proceedings of the World Geothermal Congress 2000, Kyushu-Tohoku, Japan, IV*, 2435-2437.

Stefansson, V., and Steingrimsson, B.S., 1990: *Geothermal logging I, an introduction to techniques and interpretation* (3rd edition). Orkustofnun, Reykjavík, report OS-80017/JHD-09, 117 pp.

Teodoriu, C., and Falcone, G., 2008: Comparison of well completions used in oil/gas production and geothermal operations: a new approach to technology. *Proceedings,33rd Workshop on Geothermal Reservoir Engineering Stanford University, Stanford,* SGP-TR-185.

Welch, G., and Bishop, G., 2006: *An introduction to the Kalman filter.* University of North Carolina, TR 95-041

Wohltz, K., and Heiken, G., 1992: *Volcanology and geothermal energy.* University of California Press, Ca, 432 pp.

APPENDIX I (Horne, 1995)

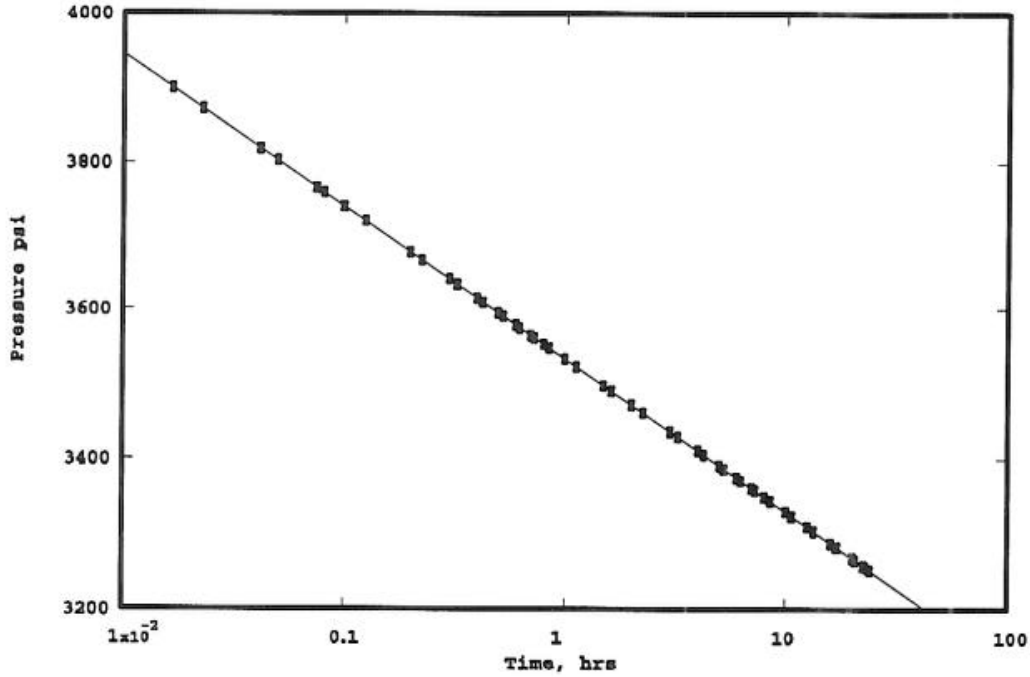

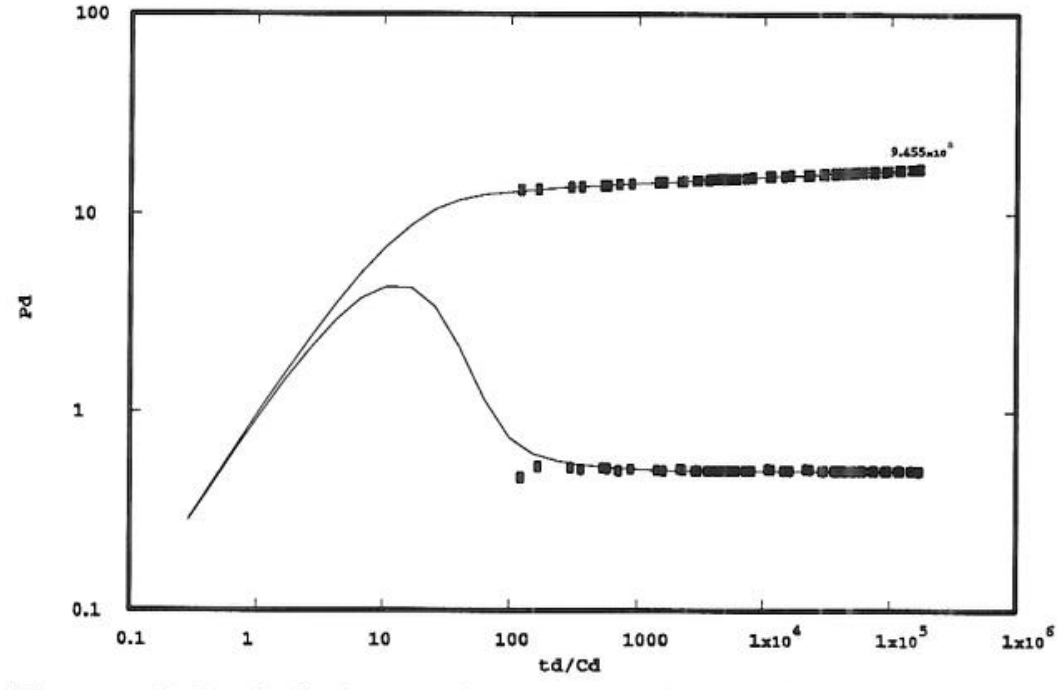

An example from the use of derivative plot, in the Figure above, it represents an infinite acting radial flow shows as semilog straight line on a semilog plot, as a flat region on a derivative plot.

APPENDIX II

HOLA - 4 MODEL RESULTS WELL HE-06

Wellhead	pressure	(bar-a) :	14.36
Wellhead	temperature	(?) :	196.23
Wellhead	dryness (%)	:	14.62
Wellhead	enthalpy	(kJ/kg) :	1120.87
Wellhead	total flow	(kg/s) :	32.04

Feedzone	Depth (m)	Flow (kg/s)	Enthalpy (kJ/kg)	Resv.Press (bar-a)	Saturation (m3/m3)	Prod.Index (kg/s/m3)
1	1000	18.56	1200	60	0	1.00E-12
2	1400	12.68	1040	86	0	1.00E-12
3	1900	0.8	1040	110	0	1.00E-12

Depth (m)	Press (bar-a)	Temp (?)	Dryness (%)	Hw ----(kJ/kg)---	Hs	Ht ----(m/s)----	Vw	Vs --(kg/m3)--	Dw	Ds (mm)	Rad	Reg
0	14.4	196.2	14.6	835	2789	1121	11.28	18.26	869	7.3	110	Sl
25	14.7	197.4	14.4	841	2789	1121	10.89	17.6	867.7	7.5	110	Sl
50	15.1	198.6	14.2	846	2790	1121	10.53	16.98	866.3	7.6	110	Sl
75	15.5	199.7	13.9	851	2791	1122	10.17	16.39	865	7.8	110	Sl
100	15.8	200.9	13.7	856	2791	1122	9.83	15.82	863.7	8	110	Sl
125	16.2	202	13.5	861	2792	1122	9.51	15.27	862.4	8.2	110	Sl
150	16.6	203.1	13.3	866	2793	1123	9.2	14.75	861	8.4	110	Sl
175	17	204.2	13.1	871	2793	1123	8.9	14.24	859.7	8.6	110	Sl
200	17.4	205.3	12.9	876	2794	1123	8.61	13.76	858.4	8.7	110	Sl
225	17.7	206.4	12.6	881	2794	1123	8.33	13.29	857.1	8.9	110	Sl
250	18.2	207.6	12.4	887	2795	1124	8.05	12.82	855.8	9.1	110	Sl
275	18.6	208.7	12.2	892	2796	1124	7.76	12.34	854.3	9.4	110	Sl
300	19	209.9	11.9	897	2796	1124	7.49	11.89	852.9	9.6	110	Sl
325	19.5	211.1	11.7	903	2797	1124	7.23	11.46	851.5	9.8	110	Sl
350	19.9	212.2	11.5	908	2797	1125	6.98	11.04	850.1	10	110	Sl
375	20.4	213.4	11.2	913	2798	1125	6.73	10.64	848.7	10.2	110	Sl
400	20.9	214.5	11	918	2798	1125	6.5	10.25	847.3	10.5	110	Sl
425	21.3	215.6	10.8	924	2798	1125	6.27	9.88	845.9	10.7	110	Sl
450	21.8	216.8	10.5	929	2799	1126	6.05	9.52	844.5	10.9	110	Sl
475	22.3	217.9	10.3	934	2799	1126	5.84	9.17	843	11.2	110	Sl
500	22.8	219	10	939	2800	1126	5.63	8.83	841.6	11.4	110	Sl
525	23.3	220.2	9.8	944	2800	1126	5.43	8.5	840.1	11.7	110	Sl
550	23.8	221.3	9.6	950	2800	1127	5.24	8.18	838.7	11.9	110	Sl
575	24.3	222.5	9.3	955	2801	1127	5.04	7.87	837.2	12.2	110	Sl
600	24.8	223.6	9	960	2801	1127	4.86	7.56	835.7	12.4	110	Sl
625	25.4	224.8	8.8	966	2801	1127	4.67	7.26	834.2	12.7	110	Sl
650	26	226	8.5	971	2801	1127	4.49	6.97	832.7	13	110	Sl
675	26.5	227.2	8.3	977	2802	1128	4.32	6.68	831.1	13.3	110	Sl

700	27.1	228.4	8	983	2802	1128	4.14	6.4	829.5	13.6	110	Sl
725	27.8	229.6	7.7	988	2802	1128	3.97	6.13	827.9	13.9	110	Sl
750	28.4	230.9	7.4	994	2802	1128	3.8	5.86	826.2	14.2	110	Sl
775	29.1	232.1	7.1	1000	2802	1129	3.64	5.59	824.5	14.5	110	Sl
800	29.9	233.6	6.8	1007	2802	1129	7.63	9.46	822.4	15	80	Sl
825	30.6	235	6.5	1014	2802	1129	7.24	8.97	820.6	15.3	80	Sl
850	31.4	236.3	6.1	1020	2802	1129	6.85	8.48	818.7	15.7	80	Sl
875	32.2	237.7	5.8	1027	2802	1130	6.48	8.01	816.8	16.1	80	Sl
900	33	239.1	5.5	1033	2802	1130	6.12	7.55	814.8	16.5	80	Sl
925	33.8	240.6	5.1	1040	2802	1130	5.76	7.1	812.8	16.9	80	Sl
950	34.7	242	4.7	1047	2802	1130	5.4	6.65	810.8	17.4	80	Sl
975	35.6	243.5	4.4	1055	2802	1131	5.05	6.21	808.6	17.8	80	Sl
1000	36.6	245.1	4	1062	2802	1131	4.7	5.77	806.4	18.3	80	Sl
1000	36.6	239.6	0	1036	0	1036	0.82	0	814.5	0	80	1p
1025	38.6	239.7	0	1036	0	1036	0.82	0	814.7	0	80	1p
1050	40.6	239.7	0	1036	0	1036	0.82	0	814.8	0	80	1p
1075	42.6	239.8	0	1037	0	1037	0.82	0	814.9	0	80	1p
1100	44.6	239.8	0	1037	0	1037	0.82	0	815.1	0	80	1p
1125	46.6	239.8	0	1037	0	1037	0.82	0	815.2	0	80	1p
1150	48.6	239.9	0	1037	0	1037	0.82	0	815.4	0	80	1p
1175	50.6	239.9	0	1038	0	1038	0.82	0	815.5	0	80	1p
1200	52.6	240	0	1038	0	1038	0.82	0	815.7	0	80	1p
1225	54.6	240	0	1038	0	1038	0.82	0	815.8	0	80	1p
1250	56.6	240.1	0	1038	0	1038	0.82	0	815.9	0	80	1p
1275	58.7	240.1	0	1038	0	1038	0.82	0	816.1	0	80	1p
1300	60.7	240.2	0	1039	0	1039	0.82	0	816.2	0	80	1p
1325	62.7	240.2	0	1039	0	1039	0.82	0	816.4	0	80	1p
1350	64.7	240.3	0	1039	0	1039	0.82	0	816.5	0	80	1p
1375	66.7	240.3	0	1039	0	1039	0.82	0	816.7	0	80	1p
1400	68.7	240.4	0	1040	0	1040	0.82	0	816.8	0	80	1p
1400	68.7	239.4	0	1035	0	1035	0.05	0	818.2	0	80	1p
1425	70.7	239.4	0	1035	0	1035	0.05	0	818.3	0	80	1p
1450	72.7	239.5	0	1036	0	1036	0.05	0	818.5	0	80	1p
1475	74.7	239.5	0	1036	0	1036	0.05	0	818.6	0	80	1p
1500	76.7	239.6	0	1036	0	1036	0.05	0	818.8	0	80	1p
1525	78.7	239.6	0	1036	0	1036	0.05	0	818.9	0	80	1p
1550	80.7	239.7	0	1037	0	1037	0.05	0	819	0	80	1p
1575	82.8	239.7	0	1037	0	1037	0.05	0	819.2	0	80	1p
1600	84.8	239.8	0	1037	0	1037	0.05	0	819.3	0	80	1p
1625	86.8	239.8	0	1037	0	1037	0.05	0	819.4	0	80	1p
1650	88.8	239.9	0	1038	0	1038	0.05	0	819.6	0	80	1p
1675	90.8	239.9	0	1038	0	1038	0.05	0	819.7	0	80	1p
1700	92.8	239.9	0	1038	0	1038	0.05	0	819.9	0	80	1p
1725	94.8	240	0	1038	0	1038	0.05	0	820	0	80	1p
1750	96.8	240	0	1039	0	1039	0.05	0	820.1	0	80	1p
1775	98.8	240.1	0	1039	0	1039	0.05	0	820.3	0	80	1p
1800	100.8	240.1	0	1039	0	1039	0.05	0	820.4	0	80	1p
1825	102.9	240.2	0	1039	0	1039	0.05	0	820.6	0	80	1p
1850	104.9	240.2	0	1040	0	1040	0.05	0	820.7	0	80	1p
1875	106.9	240.3	0	1040	0	1040	0.05	0	820.8	0	80	1p
1900	108.9	240.3	0	1040	0	1040	0.05	0	821	0	80	1p

HOLA - 7 MODEL RESULTS WELL HE-20

Wellhead	pressure (bar-a)	:	11.54
Wellhead	temperature (iv)	:	186.18
Wellhead	dryness (%)	:	11.42
Wellhead	enthalpy (kJ/kg)	:	1017.87
Wellhead	total flow (kg/s)	:	32.65

Feedzone	Depth (m)	Flow (kg/s)	Enthalpy (kJ/kg)	Resv.Press (bar-a)	Saturation (m3/m3)	Prod.Index (kg/s/m3)
1	1125	21.79	1000	71	0	3.00E-12
2	1400	7.74	1080	86	0	3.00E-12
3	1800	3.12	1110	118	0	1.00E-12

Depth (m)	Press (bar-a)	Temp (iv)	Dryness (%)	Hw ----(kJ/kg)---	Hs	Ht ----(m/s)----	Vw	Vs --(kg/m3)--	Dw	Ds (mm)	Rad	Reg
0	11.5	186.2	11.4	791	2781	1018	11.3	18	880.2	5.9	110	Sl
25	11.9	187.5	11.2	797	2782	1018	10.79	17.16	878.7	6.1	110	Sl
50	12.2	188.9	10.9	803	2783	1018	10.31	16.37	877.3	6.2	110	Sl
75	12.6	190.2	10.6	809	2784	1019	9.85	15.61	875.8	6.4	110	Sl
100	13	191.5	10.4	814	2785	1019	9.41	14.89	874.3	6.6	110	Sl
125	13.4	192.8	10.1	820	2786	1019	9	14.21	872.9	6.8	110	Sl
150	13.7	194.1	9.9	826	2787	1020	8.6	13.55	871.4	7	110	Sl
175	14.1	195.4	9.6	832	2788	1020	8.21	12.93	869.9	7.2	110	Sl
200	14.5	196.7	9.4	838	2789	1020	7.85	12.33	868.5	7.4	110	Sl
225	14.9	198	9.1	843	2790	1020	7.49	11.75	867	7.6	110	Sl
250	15.3	199.3	8.8	849	2791	1021	7.15	11.2	865.5	7.8	110	Sl
275	15.7	200.6	8.6	855	2791	1021	6.82	10.66	864	8	110	Sl
300	16.2	201.9	8.3	861	2792	1021	6.5	10.14	862.4	8.2	110	Sl
325	16.6	203.2	8	867	2793	1021	6.19	9.64	860.9	8.4	110	Sl
350	17.1	204.6	7.7	873	2794	1022	5.88	9.15	859.3	8.6	110	Sl
375	17.6	205.9	7.5	879	2794	1022	5.59	8.68	857.7	8.9	110	Sl
400	18.1	207.3	7.2	885	2795	1022	5.3	8.21	856.1	9.1	110	Sl
425	18.6	208.7	6.9	892	2796	1023	5.01	7.75	854.4	9.4	110	Sl
450	19.1	210.2	6.5	899	2796	1023	4.73	7.3	852.6	9.6	110	Sl
475	19.7	211.7	6.2	905	2797	1023	4.45	6.85	850.8	9.9	110	Sl
500	20.3	213.2	5.9	912	2798	1023	4.17	6.41	848.9	10.2	110	Sl
525	21	214.8	5.5	920	2798	1024	3.9	5.99	846.9	10.5	110	Sl
550	21.6	216.4	5.2	927	2799	1024	3.64	5.56	844.9	10.9	110	Sl
575	22.4	218.1	4.8	935	2799	1024	3.37	5.14	842.8	11.2	110	Sl
600	23.1	219.9	4.4	943	2800	1024	3.1	4.73	840.5	11.6	110	Sl
625	24	221.8	3.9	952	2800	1025	2.84	4.31	838.1	12	110	Sl
650	24.9	223.8	3.5	961	2801	1025	2.56	3.88	835.5	12.5	110	Sl

675	26	226	2.9	971	2801	1025	2.29	3.45	832.7	13	110	Sl
700	27.2	228.4	2.3	983	2802	1025	1.99	3	829.5	13.6	110	Sl
725	28.5	231.1	1.7	995	2802	1026	3.49	4.28	825.9	14.3	80	Sl
750	30.2	234.2	0	1026	0	1026	1.99	0	816.9	0	80	Bu
775	32.2	237.6	0	1026	0	1026	1.99	0	817	0	80	1p
800	34.3	237.6	0	1026	0	1026	1.99	0	817.2	0	80	1p
825	36.3	237.7	0	1027	0	1027	1.99	0	817.3	0	80	1p
850	38.4	237.7	0	1027	0	1027	1.99	0	817.5	0	80	1p
875	40.4	237.8	0	1027	0	1027	1.99	0	817.6	0	80	1p
900	42.5	237.8	0	1027	0	1027	1.99	0	817.8	0	80	1p
925	44.5	237.8	0	1027	0	1027	1.99	0	817.9	0	80	1p
950	46.5	237.9	0	1028	0	1028	1.99	0	818.1	0	80	1p
975	48.6	237.9	0	1028	0	1028	1.98	0	818.2	0	80	1p
1000	50.6	238	0	1028	0	1028	1.98	0	818.4	0	80	1p
1025	52.7	238	0	1028	0	1028	1.98	0	818.5	0	80	1p
1050	54.7	238	0	1029	0	1029	1.98	0	818.7	0	80	1p
1075	56.8	238.1	0	1029	0	1029	1.98	0	818.8	0	80	1p
1100	58.8	238.1	0	1029	0	1029	1.98	0	819	0	80	1p
1125	60.9	238.1	0	1029	0	1029	1.98	0	819.2	0	80	1p
1125	60.9	250.4	0	1088	0	1088	0.67	0	801.1	0	80	1p
1150	62.8	250.4	0	1088	0	1088	0.67	0	801.3	0	80	1p
1175	64.8	250.4	0	1088	0	1088	0.67	0	801.4	0	80	1p
1200	66.8	250.5	0	1088	0	1088	0.67	0	801.6	0	80	1p
1225	68.7	250.5	0	1088	0	1088	0.67	0	801.8	0	80	1p
1250	70.7	250.5	0	1088	0	1088	0.67	0	802	0	80	1p
1275	72.7	250.5	0	1088	0	1088	0.67	0	802.2	0	80	1p
1300	74.7	250.6	0	1088	0	1088	0.67	0	802.4	0	80	1p
1325	76.6	250.6	0	1089	0	1089	0.67	0	802.6	0	80	1p
1350	78.6	250.6	0	1089	0	1089	0.67	0	802.7	0	80	1p
1375	80.6	250.6	0	1089	0	1089	0.67	0	802.9	0	80	1p
1400	82.6	250.6	0	1089	0	1089	0.67	0	803.1	0	80	1p
1400	82.6	255.2	0	1111	0	1111	0.19	0	796.1	0	80	1p
1425	84.5	255.2	0	1111	0	1111	0.19	0	796.4	0	80	1p
1450	86.5	255.1	0	1111	0	1111	0.19	0	796.7	0	80	1p
1475	88.4	255.1	0	1110	0	1110	0.19	0	797	0	80	1p
1500	90.4	255.1	0	1110	0	1110	0.19	0	797.3	0	80	1p
1525	92.3	255	0	1110	0	1110	0.19	0	797.6	0	80	1p
1550	94.3	255	0	1110	0	1110	0.19	0	797.8	0	80	1p
1575	96.2	255	0	1110	0	1110	0.19	0	798.1	0	80	1p
1600	98.2	255	0	1110	0	1110	0.19	0	798.3	0	80	1p
1625	100.2	254.9	0	1110	0	1110	0.19	0	798.6	0	80	1p
1650	102.1	254.9	0	1110	0	1110	0.19	0	798.8	0	80	1p
1675	104.1	254.9	0	1110	0	1110	0.19	0	799.1	0	80	1p
1700	106	254.9	0	1110	0	1110	0.19	0	799.3	0	80	1p
1725	108	255	0	1110	0	1110	0.19	0	799.5	0	80	1p
1750	110	255	0	1110	0	1110	0.19	0	799.7	0	80	1p
1775	111.9	255	0	1110	0	1110	0.19	0	799.9	0	80	1p
1800	113.9	255	0	1110	0	1110	0.19	0	800	0	80	1p

APPENDIX III

CTSM 2.3

Model: C:\CTSM23\documentation\Examples\master\nejva2o.ctsm
Results 8

Value of objective function: -1.023758531884291E+02
Value of penalty function: 5.126827045335438E-04
Negative logarithm of determinant of Hessian: -3.418604041891855E+01

Number of iterations: 50
Number of objective function evaluations: 78

Initial states		Min. value	Initial value	Max. value	Pr. std. dev.	Estimate	Std. dev.	t-score	p(>|t|)	dF/dPar	dPen/dPar
x10	ML	0.0	11.0	15.0	N/A	9.3290E-01	5.8878E-03	158.4468	0.0000	0.0031	0.0000

Parameters		Min. value	Initial value	Max. value	Pr. std. dev.	Estimate	Std. dev.	t-score	p(>|t|)	dF/dPar	dPen/dPar
A1	ML	0.1	1.0	500.0	N/A	2.7158E+02	6.4604E+00	42.0377	0.0000	-0.0012	0.0003
k1	ML	0.1	1.0	10000.0	N/A	7.9418E+03	6.9864E+02	11.3675	0.0000	0.0000	0.0019
sig	ML	0.0	0.1	1.0	N/A	1.2353E-02	1.6764E-03	7.3688	0.0000	0.0000	0.0000
S	ML	0.0	1.0E-10	1.0	N/A	9.9632E-11	1.3659E-11	7.2941	0.0000	0.0001	0.0000

Correlation matrix:

	x10	A1	k1	sig	S
x10	1				
A1	0.0054	1			
k1	-0.0045	-0.0741	1		
sig	-0.0348	-0.0659	0.0095	1	
S	0.0190	0.0182	0.0170	0.0103	1

Data files: C:\CTSM23\documentation\Examples\master\nej1.csv

Varying sample time
Zero order hold interpolation between inputs

Filter settings: Scaling factor for initial covariance: 1.0

Optimisation settings: Maximum number of objective function evaluations: 500
Adjustment factor for initial step length in line search: 1.0E-6
Relative error in calculation of objective function: 1.0E-14

Computational settings: Cut-off value for Huber's psi-function: 3.0
Padé approximation order: 6
Tolerance for singular value decomposistion: 1.0E-12

Advanced optimisation settings: Lagrange multiplier in penalty function: 1.0E-4
Minimum absolute value used for normalizing in penalty function: 1.0E-30